

CHANNEL ESTIMATION ERROR, OSCILLATOR STABILITY
AND WIRELESS POWER TRANSFER IN WIRELESS COMMUNICATION
WITH DISTRIBUTED RECEPTION NETWORKS

by

Sabah Razavi

A Dissertation
Submitted to the Faculty
of the
WORCESTER POLYTECHNIC INSTITUTE
in partial fulfillment of the requirements for the
Degree of Doctor of Philosophy
in
Electrical and Computer Engineering
by

January 2019

APPROVED:

Professor D. Richard Brown III, Major Advisor, WPI

Professor John McNeill, Dean of Engineering, WPI

Professor Andrew G. Klein, Department of Engineering and Design, WWU

Abstract

This dissertation considers three related problems in distributed transmission and reception networks. Generally speaking, these types of networks have a transmit cluster with one or more transmit nodes and a receive cluster with one or more receive nodes. Nodes within a given cluster can communicate with each other using a wired or wireless local area network (LAN/WLAN). The overarching goal in this setting is typically to increase the efficiency of communication between the transmit and receive clusters through techniques such as distributed transmit beamforming, distributed reception, or other distributed versions of multi-input multi-output (MIMO) communication. More recently, the problem of wireless power transfer has also been considered in this setting.

The first problem considered by this dissertation relates to distributed reception in a setting with a single transmit node and multiple receive nodes. Since exchanging lightly quantized versions of in-phase and quadrature samples results in high throughput requirements on the receive LAN/WLAN, previous work has considered an approach where nodes exchange hard decisions, along with channel magnitudes, to facilitate combining similar to an ideal receive beamformer. It has been shown that this approach leads to a small loss in SNR performance, with large reductions in required LAN/WLAN throughput. A shortcoming of this work, however, is that all of the prior work has assumed that each receive node has a perfect estimation of its channel to the transmitter.

To address this shortcoming, the first part of this dissertation investigates the effect of channel estimation error on the SNR performance of distributed reception. Analytical expressions for these effects are obtained for two different modulation schemes, M -PSK and M^2 -QAM. The analysis shows the somewhat surprising result that channel estimation error causes the same amount of performance degradation in ideal beamforming and pseudo-beamforming systems despite the fact that the channel estimation errors manifests themselves quite differently in both systems.

The second problem considered in this dissertation is related to oscillator stability and phase noise modeling. In distributed transmission systems with multiple transmitters in the transmit cluster, synchronization requirements are typically very strict, e.g., on the order of one picosecond, to maintain radio frequency phase alignment across transmitters. Therefore, being able to accurately model the behavior of the oscillators and their phase noise responses is of high importance. Previous approaches have typically relied on a two-state model, but this model is often not sufficiently rich to model low-cost oscillators. This dissertation develops a new three-state oscillator model and a method for estimating the parameters of this model from experimental data. Experimental results show that the proposed model provides up to 3 dB improvement in mean squared error (MSE) performance with respect to a two-state model.

The last part of this work is dedicated to the problem of wireless power transfer in a setting with multiple nodes in the transmit cluster and multiple nodes in the receive cluster. The problem is to align the phases of the transmitters to achieve a certain power distribution across the nodes in the receive cluster. To find optimum transmit phases, we consider an iterative approach, similar to the prior work on one-bit feedback for distributed beamforming, in which each receive node sends a one-bit feedback to the transmit cluster indicating if the received power in that time slot for that node is increased. The transmitters then update their phases based on the feedback. What makes this problem particularly interesting is that, unlike the prior work on one-bit feedback for distributed beamforming, this is a multi-objective optimization problem where not every receive node can receive maximum power from the transmit array. Three different phase update decision rules, each based on the one-bit feedback signals, are analyzed. The effect of array sparsity is also investigated in this setting.

Acknowledgements

First, I would like to sincerely thank my advisor, Professor Rick Brown for all his support and guidance during these years. I am so glad that I had a chance to work with such a great and distinguished professor as my advisor during my Ph.D. study, which helped me to gain valuable insights and explore different research topics. Without his help and support this achievement would not be possible. I also would like to thank the other members of my dissertation committee, Professors John McNeill and Andrew G. Klein for their insightful comments and encouragement, which helped me to improve and expand my research in different perspectives.

My sincere thanks also goes to Professors Kaveh Pahlavan and Hossein Hakim for their continuous support, help and encouragement during all these years of my study.

I want to thank my previous and current fellow labmates, Dr. Radu David, Dr. Rui Wang, Kimberly Chinkidjakarn and Kirty Vedula for all the interesting discussions, research we did together and all the fun moments we had during these past years.

I also would like to thank all my friends who supported me in any way they could and stood by my side during all the ups and downs of my life in these past years. I want to particularly thank Sepanta Yousefian, Dr. Sina Youssefian, Dr. Tannaz MonfaredZadeh, Milad Zabeti, Dr. Siamak Ghorbani Faal and Shadi Tasdighi Kalat.

Last but not least, I would like to thank my father Mohammadhassan, my mother Ferdos and my sister Sara, for all their support and help, and for their great patience and kindness in tolerating and forgiving my absence beside them when they needed me the most during all these years. I also would like to sincerely thank my grandmother Ezzat and my uncle Fariborz for all the warm wishes and support.

Contents

List of Figures	vii
List of Tables	ix
1 Introduction	1
1.1 Motivation	1
1.2 Problem Statement	5
1.3 Dissertation Organization	5
2 Channel Estimation Error Effect	7
2.1 Background	7
2.2 Unquantized channel outputs	10
2.3 Quantized channel outputs	10
2.4 Combining Techniques	11
2.4.1 Optimal Beamforming	11
2.4.2 Ideal Receive Beamforming	13
2.4.3 Pseudo-Beamforming	13
2.5 Process of Combining Quantized Signals	13
2.6 M -PSK Modulated Transmission	14
2.6.1 System Model	15
2.6.2 Channel Estimation	16
2.6.3 Asymptotic SNR Analysis	17
2.6.3.1 Ideal Receive Beamforming: Perfect Channel Estimation	18
2.6.3.2 Ideal Receive Beamforming: Noisy Channel Estimation	20
2.6.3.3 Pseudo-Beamforming: Perfect Channel Estimation	23
2.6.3.4 Pseudo-Beamforming: Noisy Channel Estimation	25
2.6.4 Numerical Results	32
2.6.5 Conclusion	33
2.7 M^2 -QAM Modulated Transmission	35
2.7.1 System Model	36

2.7.2	Channel Estimation	36
2.7.3	Asymptotic SNR Analysis	37
2.7.3.1	Ideal Receive Beamforming: Perfect Channel Estimation	37
2.7.3.2	Ideal Receive Beamforming: Noisy Channel Estimation	38
2.7.3.3	Pseudo-Beamforming: Perfect Channel Estimation	41
2.7.3.4	Pseudo-Beamforming: Noisy Channel Estimation	44
2.7.4	Numerical Results	50
2.7.5	Conclusion	51
3	Oscillator Modeling For Improved Phase Synchronization	54
3.1	Introduction	54
3.2	Background	55
3.2.1	Cooperative communication	55
3.2.2	SDR output phase noise	57
3.3	Oscillator Noise Modeling	59
3.3.1	Two-state oscillator phase noise model	59
3.3.2	Role of oscillator model in phase prediction	63
3.4	Three-state Oscillator Model	64
3.4.1	Survey of crystal oscillators	64
3.4.2	Development of three-state model	65
3.4.3	Determining PLL parameters	67
3.5	Measurement and Simulation results	68
3.6	Conclusion	71
4	Wireless Power Transfer With Simultaneous Distributed Beamforming Using One-bit Feedback	72
4.1	Introduction	73
4.2	System Model	75
4.3	Problem Setup	76
4.4	Problem Solution	78
4.5	Proposed Decision Making Methods	85
4.5.1	Unanimous Rule	86
4.5.2	Majority Rule	86
4.5.3	Summation Rule	86
4.6	Phase Update Procedure	87
4.7	Simulation results	88
4.7.1	Unanimous Rule Results	89
4.7.2	Majority Rule Results	89
4.7.3	Summation Rule Results	90
4.7.4	Effect Of Scaling Factor α On Convergence	91
4.7.5	Effect Of Sparsity On Convergence	92

4.8	Conclusion	93
5	Summary and Future Work	100
5.1	Conclusions	100
5.2	Future Work	101
	Bibliography	102

List of Figures

2.1	Timeline of distributed reception protocol	9
2.2	Comparison of the SNRs between ideal receive beamforming and pseudo-beamforming with and without channel estimation error in QPSK modulation. The dotted lines are the calculated SNRs for large N in each scenario.	33
2.3	Comparison of the penalties between the ideal and pseudo beamformer in QPSK modulation.	34
2.4	Mean and variance of the hard decisions when there is channel estimation error in QPSK modulation.	35
2.5	Comparison of the SNRs between ideal receive beamforming and pseudo-beamforming with and without channel estimation error in 16-QAM modulation. The dotted lines are the calculated SNRs for large N in each scenario.	51
2.6	Comparison of the penalties between the ideal and pseudo beamformer in 16-QAM modulation.	52
2.7	Mean and variance of the hard decisions when there is channel estimation error in 16-QAM modulation.	53
3.1	Conceptual beamforming.	56
3.2	Need for clock resynchronization.	57
3.3	SDR simplified block diagram.	58
3.4	Measured phase noise of USRP carrier output.	59
3.5	2-state clock noise model.	61
3.6	Measured phase noise for oscillator CS4 with 2-state model fit.	62
3.7	Summary of phase noise measurements.	65
3.8	Three-state model for phase noise of source with PLL synthesizer.	66
3.9	Measured phase noise for oscillator CS8 with 3-state model fit.	68
3.10	Prediction for oscillator CS8 with 2- and 3-state model fits.	69
3.11	Relative performance, 2-state vs. 3-state model fit.	70

4.1	A wireless transmission system with multiple receivers and one-bit feedback	73
4.2	First and second derivative with respect to Δ_3 when $\Delta_2 = 0$	84
4.3	First and second derivative with respect to Δ_2 when $\Delta_3 = 0$	84
4.4	Contour plots of received weighted sum power vs Δ_3 and Δ_2	85
4.5	Received power at each node in Unanimous rule over iterations.	90
4.6	Contour plot of the received power in Unanimous rule over all transmitters phase difference iterations.	91
4.7	Received power at each node in Majority rule over iterations.	92
4.8	Contour plot of the received power in Majority rule over all transmitters phase difference iterations.	93
4.9	Received power at each node in Summation rule over iterations.	94
4.10	Contour plot of the received power in Summation rule over all transmitters phase difference iterations.	95
4.11	The effect of different scaling factors in received power for one of the receivers in Summation rule.	96
4.12	Contour of received power in Unanimous rule with sparse array.	97
4.13	Contour of received power in Majority rule with sparse array.	98
4.14	Contour of received power in Summation rule with sparse array.	99

List of Tables

3.1 Clock sources evaluated in this work 63

Chapter 1

Introduction

In this chapter an introduction and a general definition of distributed reception is given and the problems that are addressed in this dissertation are discussed.

1.1 Motivation

In recent years the need for having advanced networks with distributed transmission or reception has increased rapidly [1]. These types of networks have wide variety of applications especially in wireless networks and signal processing applications. As an example of these applications we can refer to wireless sensor networks (WSNs), cellular communication systems, detection of a target position in radar systems with multiple antennas and communication systems in military. In cellular networks like the ones utilizing 3GPP standard [2], the use of coordinated multi point (CoMP) [3, 4] makes cooperation of multiple base stations possible in order to help the users that are on the border between those stations. Techniques that are usually used in those base stations which facilitates the cooperation between them are joint transmission (JT) [5, 6] or coordinated scheduling/coordinated beamforming (CS/CB) [7, 8]. Another distributed transmission/reception technique that is developed to increase the performance of cellular communications is the distributed

antenna systems (DAS) [9–11] in which for each base station there are multiple antenna ports and each port is connected to multiple micro-diversity antennas. Another example of distributed reception is the radar systems in which there are multiple receiving antennas that are geographically separated from each other and they receive the reflected signal from the target. Then the obtained information from these signals are combined to make a better decision about the target properties like position or velocity [12–14]. Due to special requirement of sensors in a wireless sensor network, like low power consumption and low processing speed which limits them to perform simple tasks, a more effective and efficient transmission and reception technique is necessary [15–18]. In battlefields and military applications, the squad units that are in charge of radio and communication can be considered as distributed array which both transmit and receive signals and they can form a distributed transmission/reception system with multiple antennas [19, 20].

As technology advances and new smart devices emerge each year, the use of Internet enabled machines and gadgets like TVs, smart appliances, cars, phones and tablets, sensors, etc. grows rapidly. Introduction of these smart devices has opened a new concept in communication systems named as Internet of Things (IoT) [21]. Since usually most of the IoT devices, especially at home or buildings, communicate with a single server or router on the same network, they could be considered as nodes in a distributed transmit or receive scenario. These configuration, makes the implementation of massive distributed multi-input multi-output (MIMO) possible. As an example, at homes with multiple IoT devices like the sensors used in appliances such as TVs, light bulbs, refrigerator, locks, etc. for control and monitor purposes, they can be used to enhance and improve data transmission and reception by other devices like smartphones and computers [22]. Using distributed reception in wireless communication networks increases the performance of the networks by providing a reliable communication between transmitter and fusion center in a receive cluster with geographically separated receive nodes [23]. In these types of network,

the wireless channel between the transmitter and the receive nodes are assumed to be independent which results in increased diversity gain at receive cluster. The fusion center then processes the received information from receivers and tries to estimate the transmitted data [22]. Distributed reception for wireless sensor networks (WSNs) uses almost the same techniques as the one for wireless communication systems. The difference between them is their application. In WSNs the aim is to do environment classification and monitoring while in wireless communication networks the goal is data transfer and communication. There has been many studies and research around WSNs such as these references [16–18, 24–31].

Distributed reception is referred to a network with multiple receivers where those receivers are fully connected to each other and are known as receive cluster. The received messages by these receive nodes are exchanged among all other nodes in the receive cluster to increase diversity and power gain and, consequently, improve the probability of successful decoding noisy transmission [32]. The receivers inside the cluster are assumed to be connected together via a reliable wired or wireless LAN with no or very small noise effect that can be ignored.

Distributed reception has been in use for a long time and in different types of applications, e.g., it has been used in aperture synthesis for radio astronomy where there are multiple radio telescopes that receive signals from outer space and then these signals from the telescopes are mixed to generate images with the same spatial resolution just like if we used a large telescope with the size of all the ones inside this cluster. Another application of distributed reception is in sensor fusion where the received data from a number of sensors in a network is fused or combined together to obtain the information that was not able to achieve by only using just one sensor, like calculating the position or orientation of an object in a three-dimensional space.

One of the latest applications of distributed reception is in wireless networks that have limited backhaul capabilities. As a simple example of distributed reception in these types of network we can refer to the soft handoff which has been developed

and used in cellular systems since 1990s [32]. The soft handoff technique is employed where a mobile user is moving from one base station coverage area or cell to another base station coverage area and during this transition it transmits and receives from both base stations at the same time. In a cellular systems with spread spectrum CDMA which uses universal frequency reuse and with receivers that have a Rake receiver inside, these two signals can be separated and their time and phase can be synchronized to support each other on the forward link [33]. In recent studies using information theory [26, 34–36] it has been shown that more advanced distributed reception techniques have the abilities to increase diversity, enhance capacity and improve interference rejection even with limited backhaul constraints. There has been several techniques that have been introduced which could reach to these mentioned goals [37–45], but there are two major issues with these techniques, the first one is that all of them use iterative transmission and decoding which means that the requirements for backhaul are not fixed and can change and if the number of iterations is large it could cause delay in decoding. The other problem with these techniques is that they are mostly focused on improving diversity gains rather than SNR gains while the later one is making more sense in distributed receiver beamforming.

One of the main problem in distributed reception is limited backhaul/LAN available throughput. If all the receivers in the cluster have to exchange their unquantized observations it may easily passes the throughput limitation and causes large latency in the network. The solution to this problem is to use quantized observations in exchange of information between nodes in the receive cluster. This method gives us a less complicated but efficient approach for fully distributed reception with no iterative transmission over a backhaul with limited capacity. There are two techniques using this method, ideal receive beamforming and pseudo-beamforming. In the first one a high order quantization level is used while in the second one instead of fine quantization, hard decisions are used. These two techniques are discussed in more details in section 2.4.

1.2 Problem Statement

There are a couple of issues and areas in distributed reception that need to be addressed and improved. In this dissertation we are focusing on three problems.

- The first problem that is going to be addressed is the problem of having channel estimation error at the receivers inside receive cluster. We have to find out what would be the performance degradation with and without channel estimation error and what would be the effect of modulation scheme on the performance of the network in presence of channel estimation error.
- The second problem that is going to be discussed is the problem of oscillator modeling and phase noise characteristic prediction for oscillators that are used in both transmitters and receivers. In here, we try to come up with new methods to better model the behavior and performance of oscillators to predict their phase noise characteristics.
- The third problem is about wireless power transfer to receive cluster using one-bit feedback signals and how we can achieve the fastest convergence to maximum transferable power in the networks while deploying one-bit feedback.

The answers and results for the above mentioned problems are stated in the rest of the chapters in this dissertation.

1.3 Dissertation Organization

The rest of this dissertation would be as follow. In Chapter 2 the problem of having channel estimation error using two different combining methods for two different modulation schemes (M -PSK and M^2 -QAM) is investigated. In Chapter 3, we introduce a new modeling method for oscillators and we compare the new proposed model to the previously used one in terms of phase noise error prediction. In Chapter

4, we propose three different methods of decision making on one-bit feedback received signal for transmitter phase update and maximum power transfer. And at the end in Chapter 5 the overall conclusion is given and the possible future works are discussed.

Chapter 2

Channel Estimation Error Effect

In real world applications there is no such thing as ideal estimators and there are always some errors in estimation process. So, in this chapter the same distributed reception network with hard decision exchanges as described in the previous chapter is assumed. The only difference here is that, channel estimations at the receivers are assumed to be not perfect and there are some channel estimation errors present in the decoding process. These effects of channel estimation error are then characterized for both ideal receive beamforming and pseudo-beamforming techniques for two different modulation schemes.

2.1 Background

As described in [32], in the distributed reception networks with large number of receivers and under the condition that the received SNR at receivers are low, it is hard for each individual receivers to completely decode the received messages sent from a far away transmitter. Therefore, during the reception of a block, every receiver inside the cluster demodulates the transmitted signal locally and for each one of the coded bits in the resent block produces log likelihood ratios (LLRs). The generated LLRs are not used instantly for decoding, instead, all or a subset of the nodes, which

have a higher SNR compared to others, in the receive cluster, quantize the output signal of their soft demodulators and send all of these quantized values together with quantized estimate of the SNR over the backhaul LAN network to all other nodes in the receive cluster. Then, these received information at each receiver are mixed with local unquantized LLRs and the results are fed to each node's local decoder for doing the decoding processes. If the original transmitted message is successfully decoded at any of the receivers, that node transmits the decoded signal to all other nodes in the receive cluster over the backhaul LAN. Here, the backhaul LAN is supposed to have a mechanism for contention resolution, in case if more than one receiver is able to decode the message and all of them intend to transmit the signal over the LAN.

As mentioned in the previous section, the main limitation in the backhaul LAN is the limited available throughput. If the LAN did not have this limitation, the nodes inside the receive cluster could have send their unquantized observations over the LAN to other nodes instead of transmitting a quantized version of that. In this case each node could easily add up all the LLRs and make a perfect ideal receive beamformer.

To visually show this process for a LAN with limited capacity, we can use the given figure for the distributed reception timeline in [32]. This timeline is shown in Figure 2.1.

After each node receives and locally demodulates a block, the receive cluster performs the following steps over the backhaul LAN:

- In the first step, all the N nodes inside the cluster share their estimates of channel magnitudes or the SNRs they have received.
- In the second step, those nodes that have higher channel magnitudes or have the strongest SNRs will participate in the message exchange over the LAN by transmitting their quantized observations to all other nodes in the cluster. When these messages are received by each node in the cluster, having the knowledge

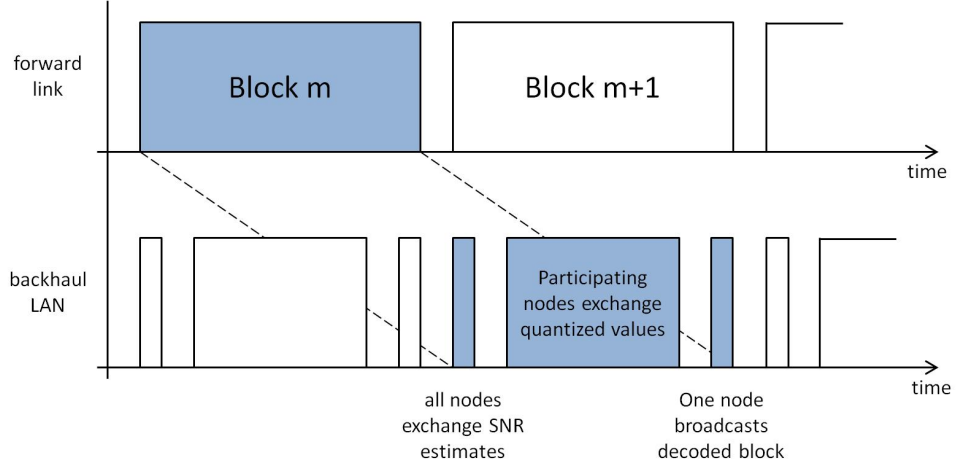


Figure 2.1: Timeline of distributed reception protocol

of previously transmitted channel magnitudes, they scale the received quantized information and combine it with their own locally unquantized LLRs.

- After the scaling and combination is done in each node, if any one of them is successful in decoding the message correctly it would transmit the decoded signal to the rest of the node in the receive cluster.

In the second step the number of participating nodes M is chosen so that it satisfies the backhaul throughput limitation. The number of participating nodes M can be obtained using the equation given in [32]. Here we assume that the number of quantization bits for each coded bit is a constant number and is denoted by b . The ratio of LAN bits per forward link information bits gives the normalized throughput for the LAN and can be expressed as

$$\eta_{LAN} = \frac{No_1 + Mbn + k + o_2}{k} \approx \frac{Mb}{r} + 1 \leq C_{LAN} \quad (2.1)$$

where No_1 is the overhead for determining the participating node and exchanging the SNRs. o_2 is contention overhead in disseminating the successfully decoded block. Since the messages are assumed to be (n,k) block coded at the transmitter, n and

k are block length and message length, both in bits, respectively and it is assumed they are sufficiently large so the overhead can be ignored. r is the block code rate and C_{LAN} is the maximum normalized LAN throughput. Equation 2.1 results that $M \leq \min\{N, r(C_{LAN} - 1)/b\}$ if r , b and C_{LAN} are given.

2.2 Unquantized channel outputs

In an ideal situation when there is no LAN throughput limitation the nodes inside receive cluster can exchange their unquantized received signals to achieve an ideal beamforming. In this case if no quantization is done at the receivers, the exchanged signal for the i^{th} node would

$$Z_i = Y_i = \sqrt{\rho_i}X + W_i \quad (2.2)$$

Where the $\rho_i = 2|h_i|^2\mathcal{E}_s/N_0$ is defined as the SNR of the received signal, h_i is the forward link complex channel, \mathcal{E}_s is the energy per coded forward link bit and $N_0/2$ is the noise power spectral density.

2.3 Quantized channel outputs

Most of the time, receivers, due to limited LAN capacity, quantize their received signals so the message exchange over LAN requires less throughput. This quantization process which is done on the soft demodulator outputs makes the channel look like a discrete memory-less channel from the distant transmitter to that receiver. In this case each node's continuous observation is mapped to a codebook index. The continuous observations and the codebook index are defined as follow,

$$Y_i = \sqrt{\rho_i}X + W_i \rightarrow Z_i \in \{0, \dots, K_i - 1\} \quad (2.3)$$

where K_i is the number of partitions based on the precision of quantization.

2.4 Combining Techniques

There are two main techniques that are used for combining the transmitted observations inside the receive cluster as described in [46]. The first technique is ideal receive beamforming or optimal combining. In this method a mixture of both continuous and discrete vector of observation is used to calculate for the posterior likelihoods of each symbol. The other technique is called pseudo-beamforming which computes the posterior likelihoods of each symbol using Gaussian approximation by linearly combining the hard decisions and generating a scalar statistic. The common thing between these two techniques is that both of them use exchanged channel magnitudes at beginning of the distributed reception protocol. Pseudo-beamforming compared to ideal receive beamforming results in less computations but the main cause for using this technique is that, asymptotic analysis of its loss of performance in comparison with ideal receive beamforming is easily manageable in the regime with low per-node SNR and a large number of receivers in the receive cluster. Due to limited performance of pseudo-beamforming compared to ideal receive beamforming, this analysis can be used to determine the maximum penalty that has been caused by using hard decisions instead of unquantized observations in this asymptotic analysis.

2.4.1 Optimal Beamforming

In optimal combining a mixture of continuous and discrete vector of observation is used to calculate the posterior probabilities for each of the symbols. This vector contains all the information received by the receivers. These posterior probabilities are then used to generate the log-likelihood ratios which is used by the soft-input decoder.

To compute posterior probabilities, we assume receive node j is the node of interest for doing all the combining processes and we consider optimal combining of hard decisions $V_i \in \mathcal{X}$ for $i \in \mathcal{P} \setminus j$ with the local unquantized observation $V_j = U_j$.

Now we can calculate for the probability of symbol $X = x_m \in \mathcal{X}$ given the vector observation \mathbf{V} as

$$\begin{aligned} \text{Prob}(X = x_m | \mathbf{V} = \mathbf{v}) &= \frac{p_{\mathbf{V}|X}(\mathbf{v}|X = x_m)\text{Prob}(X = x_m)}{p_{\mathbf{V}}(\mathbf{v})} \\ &= \frac{p_{V_j|X}(v_j|X = x_m) \prod_{i \in \mathcal{P} \setminus j} p_{V_i|X}(v_i|X = x_m)}{\sum_{\ell=1}^M p_{V_j|X}(v_j|X = x_\ell) \prod_{i \in \mathcal{P} \setminus j} p_{V_i|X}(v_i|X = x_\ell)} \end{aligned} \quad (2.4)$$

the above result is based on the assumption that symbols are equiprobable and the elements in \mathbf{V} are all conditionally independent. In order to obtain posterior probabilities, at each receive node using the local unquantized observation the $p_{V_j|X}(v_j|X = x_\ell)$ and using the hard decisions received from other nodes the $p_{V_i|X}(v_i|X = x_\ell)$ is calculated where $\ell = 1, \dots, M$. Since the channel magnitudes $|h_k|_{k=1, \dots, N}$ are known to each node in the cluster, above computations are possible. At receive node j the local observation is unquantized so $v_j = u_j$ and the posterior probability for the complex alphabet would be

$$p_{V_j|X}(v_j|X = x_\ell) = \frac{1}{\pi N_0} \exp\left(-\frac{|v_j - |h_j|x_\ell|^2}{N_0}\right) \quad (2.5)$$

and for real alphabet would be

$$p_{V_j|X}(v_j|X = x_\ell) = \frac{1}{\sqrt{\pi N_0}} \exp\left(-\frac{(v_j - |h_j|x_\ell)^2}{N_0/2}\right) \quad (2.6)$$

Hard decisions at node i create a discrete memory-less channel (DMC) with channel transition probabilities of $p_{V_i|X}(v_i|X = x_\ell)$ for $i \in \mathcal{P} \setminus j$.

Generating hard decisions at each node in the receive cluster will create a DMC with M inputs and M outputs where transition probabilities for most of the common modulation techniques like BPSK, QPSK, M -PAM and M^2 -QAM can be determined exactly using standard analysis techniques. For M -PSK modulation with $M > 4$ and with the use of hard decisions, the transition probabilities cannot be calculated exactly and need approximations or numerical methods.

In the process of decoding, the transition probabilities $\text{Prob}(X = x_m | \mathbf{V} = \mathbf{v})$ are used and since the local unquantized observations are combined with the hard

decisions at each node, these probabilities are not the same, which will result in some nodes not be able to decode the message correctly while the others can. If any of the nodes can successfully decode the message it will transmit the message to all other nodes in the receive cluster but if none of the nodes are able to decode the message, the transmitted block is considered unsuccessfully received.

2.4.2 Ideal Receive Beamforming

For creating an ideal receive beamformer, the continuous phase-corrected channel outputs U_j are scaled by their corresponding channel magnitudes and then summed together which can be stated as

$$Y_{bf} \equiv Y_i = \sum_{j \in \mathcal{P}} \sqrt{\rho_i} U_j = \alpha \sum_{j \in \mathcal{P}} |h_j| U_j \quad (2.7)$$

where $\rho_i = \frac{|h_i|^2 \mathcal{E}_s}{N_0}$ and $\alpha = \sqrt{\frac{\mathcal{E}_s}{N_0}}$.

2.4.3 Pseudo-Beamforming

For obtaining the pseudo-beamformer output, instead of using unquantized continuous phase-corrected channel outputs U_j , the quantized version of the received signal, V_j , is used.

$$Y_{bf} \equiv Y_i = \sum_{j \in \mathcal{P}} \sqrt{\rho_i} V_j = \alpha \sum_{j \in \mathcal{P}} |h_j| V_j \quad (2.8)$$

The quantized signals are obtained from performing the demodulation on the continuous received signal and it is based on the modulation scheme selected at the transmitter side.

2.5 Process of Combining Quantized Signals

In a distributed reception network with quantized observation, each node receives quantized signals from all other nodes. Then, as mentioned before, these quantized

signals are scaled and combined with each other and also with the local unquantized LLRs and generate an overall LLR which is then used by the local block decoder. In the process of generating an overall LLR the only information that is needed to be known by the corresponding node is the SNRs of participating nodes which have shared their unquantized observations with other nodes, and the related partitions for the current quantization level of interest. These generated overall LLRs in each node inside the receive cluster are different from each other, since the quantized signals received at each receiver would not be the same for all. If the node of interest is not among the participating nodes it would have an extra quantized observation to process in the sum compared to the case where itself is a part of participating nodes, since in this case it should not include its own quantized observation. So, in a distributed reception system which uses quantized version of observations during exchanges, the decision statistics are different at each node compared to ideal receive beamforming where all the decision statistics are the same. Due to this difference, some nodes are able to decode the transmitted messages while others cannot.

2.6 M -PSK Modulated Transmission

In this section we investigate the effect of channel estimation error on hard decision exchanges in distributed reception when the modulation scheme used in forward link is M -PSK. These computations are done for a low-per node SNR regime and for large number of receive nodes in receive cluster. We first describe the system model that is going to be used for transmitting node and the receive cluster along with the channel notations and possible M -PSK transmission symbols. Then, channel estimation process along with channel estimation error statistics are introduced. After computing the channel estimation the asymptotic SNR analysis of the received signals in four different scenarios, ideal receive beamforming and pseudo-beamforming each with and without channel estimation error, are calculated.

2.6.1 System Model

We assume a block transmission scenario with blocks of length n as in [46] and let N denote the number of receive nodes in the cluster. The complex forward link channel to receive node i in block m is denoted as $h_i[m]$ for $i = 1, \dots, N$ and the vector channel for block m is denoted as $\mathbf{h}[m] = [h_1[m], \dots, h_N[m]]^\top$. Over each block, the forward link channels are assumed to be constant but may change block to block.

For clarity of exposition and to explore the effects of channel phase and magnitude errors on distributed reception, we assume M -PSK modulation in the forward link. The ℓ^{th} symbol in block m is denoted as $X[m, \ell]$ for $\ell = 1, \dots, n$ and is assumed to be drawn equiprobably from the PSK alphabet $\mathcal{X} = \{x_1, \dots, x_M\} = \{a, ae^{j2\pi/M}, ae^{j4\pi/M}, \dots, ae^{j(M-1)2\pi/M}\}$. The average energy per transmitted symbol is denoted as

$$\mathcal{E}_s = \text{E}[|X[m, \ell]|^2] = \frac{1}{M} \sum_{m=1}^M |x_i|^2 = a^2 \quad (2.9)$$

Given an additive white Gaussian noise channel (AWGN) with power spectral density $N_0/2$ in the real and imaginary dimensions, the complex baseband signal received at the i^{th} receive node for the ℓ^{th} symbol of block m can be written as

$$U_i[m, \ell] = h_i[m]X[m, \ell] + W_i[m, \ell] \quad (2.10)$$

for $i = 1, \dots, N$ and $\ell = 1, \dots, n$ where $W_i[m, \ell] \sim \mathcal{CN}(0, N_0)$ is spatially and temporally independent and identically distributed (i.i.d.) proper complex Gaussian baseband noise. We assume the noise variance is identical at each receive node. The quantity $\rho_i[m] = \frac{|h_i[m]|^2 \mathcal{E}_s}{N_0}$ corresponds to the signal-to-noise ratio (SNR) at receive node i for symbols received in block m where $|h_i[m]|^2 \mathcal{E}_s$ corresponds to the average received energy per transmitted forward link symbol at receive node i .

To facilitate distributed reception, it is assumed that the receive cluster has an established LAN backhaul, either ad-hoc or through infrastructure such as an access

point, and that LAN transmissions are reliable. The LAN is also assumed to support broadcast transmission in which any single node can send a message to all other nodes simultaneously. To prevent any interruption in transmission over forward link, it is assumed that LAN and forward link operating frequencies differ from each other which enables the receive cluster to send and receive over the LAN, and also receive signals from transmitter at the same time. The LAN is also assumed to support a sufficient throughput for the exchange of hard decisions among all nodes in the receive cluster.

2.6.2 Channel Estimation

Unlike the prior work in [32, 46, 47], we do not assume $h_i[m]$ is known perfectly here. To facilitate estimation of $h_i[m]$ at receiver i , we assume some of the symbols in each transmitted block are known. Suppose $X[m, 1], \dots, X[m, P]$ are known, where $P \leq n$. Then node i can estimate $h_i[m]$ by computing a least squares solution to

$$\begin{bmatrix} U_i[m, 1] \\ \vdots \\ U_i[m, P] \end{bmatrix} = \begin{bmatrix} X[m, 1] \\ \vdots \\ X[m, P] \end{bmatrix} h_i[m] \quad (2.11)$$

$$\mathbf{U}_i[m] = \mathbf{X}[m]h_i[m] \quad (2.12)$$

such that

$$\hat{h}_i[m] = \frac{\mathbf{X}^H[m]\mathbf{U}_i[m]}{\mathbf{X}^H[m]\mathbf{X}[m]} \quad (2.13)$$

Substituting $\mathbf{U}_i[m] = h_i[m]\mathbf{X}[m] + \mathbf{W}_i[m]$, we can write

$$\begin{aligned} \hat{h}_i[m] &= \frac{h_i[m]\mathbf{X}^H[m]\mathbf{X}[m] + \mathbf{X}^H[m]\mathbf{W}_i[m]}{\mathbf{X}^H[m]\mathbf{X}[m]} \\ &= h_i[m] + \frac{\mathbf{X}^H[m]\mathbf{W}_i[m]}{\mathbf{X}^H[m]\mathbf{X}[m]} \\ &= h_i[m] + \tilde{h}_i[m] \end{aligned} \quad (2.14)$$

where $\tilde{h}_i[m] \sim \mathcal{CN}(0, 2\delta)$ is a proper complex Gaussian random variable with variance δ in the real and imaginary dimensions. Since the training sequence $\mathbf{X}[m]$ is known, we can determine 2δ by computing

$$\text{var}[\tilde{h}_i[m]] = \text{E}[\tilde{h}_i[m]]^2 - \text{E}[\tilde{h}_i[m]]^2 \quad (2.15)$$

but we know that $\text{E}[\tilde{h}_i[m]] = 0$. So we get

$$\begin{aligned} \text{var}[\tilde{h}_i[m]] &= \text{E} \left[\left(\frac{\mathbf{X}^H[m] \mathbf{W}_i[m, \ell]}{\mathbf{X}^H[m] \mathbf{X}[m]} \right)^2 \middle| \mathbf{X}[m] \right] \\ &= \text{E} \left[\frac{\mathbf{X}^H[m] \mathbf{W}_i[m, \ell] \mathbf{W}_i^H[m, \ell] \mathbf{X}[m]}{\mathbf{X}^H[m] \mathbf{X}[m] \mathbf{X}^H[m] \mathbf{X}[m]} \middle| \mathbf{X}[m] \right] \\ &= \frac{\mathbf{X}^H[m]}{\mathbf{X}^H[m] \mathbf{X}[m]} \text{E} [\mathbf{W}_i[m, \ell] \mathbf{W}_i^H[m, \ell] | \mathbf{X}[m]] \frac{\mathbf{X}[m]}{\mathbf{X}^H[m] \mathbf{X}[m]} \\ &= \frac{\mathbf{X}^H[m]}{\mathbf{X}^H[m] \mathbf{X}[m]} (\mathbf{I} N_0) \frac{\mathbf{X}[m]}{\mathbf{X}^H[m] \mathbf{X}[m]} \\ &= \frac{N_0}{\mathbf{X}^H[m] \mathbf{X}[m]} \\ &= \frac{N_0}{P \mathcal{E}_s} \end{aligned} \quad (2.16)$$

where the last result follows from our M -PSK assumption and the fact that the length of $\mathbf{X}[m]$ is P .

2.6.3 Asymptotic SNR Analysis

In this section, we consider the case where $N \rightarrow \infty$ and the per-node SNR goes to zero at a rate of $\frac{1}{N}$ so that the SNR of an ideal receive beamformer combiner is finite and bounded away from zero. We can suppress the block/symbol indices and consider the scalar observation at receive node i as

$$U_i = h_i X + W_i \quad (2.17)$$

where X is drawn from an M -PSK constellation with $|X|^2 = \mathcal{E}_s$. For our asymptotic analysis, we will assume signal energy $\mathcal{E}_s = \mathcal{E}_s^{(1)}/N$, i.e., the transmit power scales as

$1/N$, where $\mathcal{E}_s^{(1)}$ is the per-symbol transmit energy with one receiver. We also assume $P = NP^{(1)}$, i.e., the training signal length scales with N , where $P^{(1)}$ is the training signal length with one receiver. Under this assumption, note that $P\mathcal{E}_s$ is a constant. Since N_0 is also fixed, the variance of the channel estimation errors is constant.

The following subsections analyze the performance of ideal distributed receive beamforming and a suboptimal combining technique called “pseudo-beamforming” with and without channel estimation error.

2.6.3.1 Ideal Receive Beamforming: Perfect Channel Estimation

The output of ideal receive beamformer at node i is realized by using unquantized observations U_j and is defined as

$$Y_{bf} \equiv Y_i = \sum_{j \in \mathcal{P}} \sqrt{\rho_i} U_j = \alpha \sum_{j \in \mathcal{P}} |h_j| U_j \quad (2.18)$$

Where $\rho_i = \frac{|h_i|^2 \mathcal{E}_s}{N_0}$ and $\alpha = \sqrt{\frac{\mathcal{E}_s}{N_0}}$. Also, \mathcal{P} denotes the set of nodes that are participating in hard decision exchanges in receive cluster, since not all the receiving nodes participate in exchange due to poor received signal. For the ideal receive beamformer, we have the vector observation

$$\mathbf{U} = \mathbf{h}X + \mathbf{W}. \quad (2.19)$$

Assuming no channel estimation error, the ideal receive beamformer output is given as

$$Y_{bf} = \mathbf{h}^H \mathbf{U} = \mathbf{h}^H \mathbf{h}X + \mathbf{h}^H \mathbf{W}. \quad (2.20)$$

The SNR of ideal receive beamforming (conditioned on the channel realizations) can be computed as

$$\begin{aligned}
\text{SNR}_{bf} &= \frac{(\text{E}[Y_{bf} | X])^2}{\text{var}[Y_{bf} | X]} \\
&= \frac{(\text{E}[\mathbf{h}^H \mathbf{h} X + \mathbf{h}^H \mathbf{W} | X])^2}{\text{var}[\mathbf{h}^H \mathbf{h} X + \mathbf{h}^H \mathbf{W} | X]} \\
&= \frac{(\text{E}[\mathbf{h}^H \mathbf{h} X | X])^2 + 2\text{E}[\mathbf{h}^H \mathbf{h} X | X] \text{E}[\mathbf{h}^H \mathbf{W} | X] + (\text{E}[\mathbf{h}^H \mathbf{W} | X])^2}{\text{var}[\mathbf{h}^H \mathbf{h} X + \mathbf{h}^H \mathbf{W} | X]}
\end{aligned} \tag{2.21}$$

since the channel \mathbf{h} and noise \mathbf{W} are independent of each other and the mean of the noise is assumed zero, therefore $\text{E}[\mathbf{h}^H \mathbf{W} | X] = 0$ and we would have

$$\text{SNR}_{bf} = \frac{(\text{E}[\mathbf{h}^H \mathbf{h} X | X])^2}{\text{var}[\mathbf{h}^H \mathbf{h} X + \mathbf{h}^H \mathbf{W} | X]} \tag{2.22}$$

using the fact that X is given and in the current block the channel \mathbf{h} is constant we would have

$$\text{E}[\mathbf{h}^H \mathbf{h} X | X] = \mathbf{h}^H \mathbf{h} X = \|\mathbf{h}\|^2 X \tag{2.23}$$

Therefore

$$\text{E}[Y_{bf} | X] = \|\mathbf{h}\|^2 X \tag{2.24}$$

Also, since transmitted symbol X , channel \mathbf{h} and noise \mathbf{W} are independent of each other we can write

$$\begin{aligned}
\text{var}[\mathbf{h}^H \mathbf{h} X + \mathbf{h}^H \mathbf{W} | X] &= \text{var}[\mathbf{h}^H \mathbf{h} X | X] + \text{var}[\mathbf{h}^H \mathbf{W} | X] \\
&= \text{var}[\mathbf{h}^H \mathbf{W} | X]
\end{aligned} \tag{2.25}$$

The first term in variance is zero due to given X and constant channel. The above obtained variance can be calculated as

$$\begin{aligned}
\text{var} [\mathbf{h}^H \mathbf{W} | X] &= \text{E} [\mathbf{h}^H \mathbf{W} | X]^2 - \text{E} [(\mathbf{h}^H \mathbf{W})^2 | X] \\
&= \text{E} [(\mathbf{h}^H \mathbf{W})^2 | X] = \text{E} [\mathbf{h}^H \mathbf{W} \mathbf{W}^H \mathbf{h} | X] \\
&= \mathbf{h}^H \text{E} [\mathbf{W} \mathbf{W}^H | X] \mathbf{h} \\
&= \|\mathbf{h}\|^2 N_0
\end{aligned} \tag{2.26}$$

So therefore we would have

$$\text{var} [Y_{bf} | X] = \|\mathbf{h}\|^2 N_0 \tag{2.27}$$

where we used the fact that $\text{E}[\mathbf{W} \mathbf{W}^H | X] = \text{var}[\mathbf{W}] = N_0$. Also, by knowing that $|X|^2 = \mathcal{E}_s$ and putting the results from (2.24) and (2.27) back into the SNR equation (2.22), we get

$$\text{SNR}_{bf} = \frac{\|\mathbf{h}\|^4 \mathcal{E}_s}{\|\mathbf{h}\|^2 N_0} = \frac{\|\mathbf{h}\|^2 \mathcal{E}_s}{N_0}. \tag{2.28}$$

If we further assume an i.i.d. Rayleigh fading channel such that $h_i \sim \mathcal{CN}(0, 2\lambda)$, then asymptotically we have $\lim_{N \rightarrow \infty} \frac{\|\mathbf{h}\|^2}{N} = 2\lambda$, since $\text{E}[\mathbf{h}^H \mathbf{h}] = 2\lambda$. The asymptotic SNR is then

$$\text{SNR}_{bf} \rightarrow \frac{2N\lambda \mathcal{E}_s}{N_0} = \frac{2\lambda \mathcal{E}_s^{(1)}}{N_0}. \tag{2.29}$$

2.6.3.2 Ideal Receive Beamforming: Noisy Channel Estimation

Now we consider ideal receive beamforming with channel estimates of the form

$$\hat{\mathbf{h}} = \mathbf{h} + \tilde{\mathbf{h}} \tag{2.30}$$

Where $\tilde{\mathbf{h}} \sim \mathcal{CN}(0, 2\delta\mathbf{I})$. The ideal receive beamformer output with channel estimation error is given as

$$\begin{aligned}
Y_{bfe} &= \hat{\mathbf{h}}^H \mathbf{U} = \hat{\mathbf{h}}^H (\mathbf{h}X + \mathbf{W}) \\
&= (\mathbf{h} + \tilde{\mathbf{h}})^H (\mathbf{h}X + \mathbf{W}) \\
&= \mathbf{h}^H (\mathbf{h}X + \mathbf{W}) + \tilde{\mathbf{h}}^H (\mathbf{h}X + \mathbf{W}) \\
&= Y_{bf} + \tilde{Y}_{bf}
\end{aligned} \tag{2.31}$$

Then, the SNR of ideal receive beamforming with channel estimation error (conditioned on the channel realizations) can be computed as

$$\text{SNR}_{bfe} = \frac{(\mathbb{E}[Y_{bfe} | X])^2}{\text{var}[Y_{bfe} | X]} = \frac{(\mathbb{E}[Y_{bf} + \tilde{\mathbf{h}}^H (\mathbf{h}X + \mathbf{W}) | X])^2}{\text{var}[Y_{bf} + \tilde{\mathbf{h}}^H (\mathbf{h}X + \mathbf{W}) | X]} \tag{2.32}$$

Note that $\tilde{\mathbf{h}}$ is independent of \mathbf{h} and X and is also independent of \mathbf{W} . That is because, the channel estimates were generated from different observations than the ones used in the SNR calculations. Hence,

$$\begin{aligned}
\mathbb{E}[Y_{bf} + \tilde{\mathbf{h}}^H (\mathbf{h}X + \mathbf{W}) | X] &= \mathbb{E}[Y_{bf} | X] \\
&= \|\mathbf{h}\|^2 \sqrt{\mathcal{E}_s}
\end{aligned} \tag{2.33}$$

Therefore we get

$$\mathbb{E}[Y_{bfe} | X] = \|\mathbf{h}\|^2 \sqrt{\mathcal{E}_s} \tag{2.34}$$

As can be seen from the result above, the numerator of SNR_{bfe} is not changed from the case with no channel estimation error. As for the denominator, since Y_{bf} and \tilde{Y}_{bf} are independent, by using the result from (2.27), we would have

$$\begin{aligned}
\text{var}[Y_{bf} + \tilde{Y}_{bf} | X] &= \text{var}[Y_{bf} | X] + \text{var}[\tilde{\mathbf{h}}^H (\mathbf{h}X + \mathbf{W}) | X] \\
&= \|\mathbf{h}\|^2 N_0 + \text{var}[\tilde{\mathbf{h}}^H (\mathbf{h}X + \mathbf{W}) | X]
\end{aligned} \tag{2.35}$$

We can compute the second term as

$$\begin{aligned}\text{var} \left[\tilde{\mathbf{h}}^H (\mathbf{h}X + \mathbf{W}) | X \right] &= \text{E} \left[\left(\tilde{\mathbf{h}}^H (\mathbf{h}X + \mathbf{W}) \right)^2 | X \right] - \left(\text{E} \left[\tilde{\mathbf{h}}^H (\mathbf{h}X + \mathbf{W}) | X \right] \right)^2 \\ &= \text{E} \left[\tilde{\mathbf{h}}^H (\mathbf{h}X + \mathbf{W}) \times (\mathbf{h}X + \mathbf{W})^H \tilde{\mathbf{h}} | X \right]\end{aligned}\quad (2.36)$$

Where the second equality follows from the fact that $\tilde{\mathbf{h}}$ is zero mean and independent of the other terms in the expectation. We can further compute

$$\begin{aligned}\text{var} \left[\tilde{\mathbf{h}}^H (\mathbf{h}X + \mathbf{W}) | X \right] &= \text{E} \left[\tilde{\mathbf{h}}^H (\mathbf{h}X X^H \mathbf{h}^H + \mathbf{W} \mathbf{W}^H + \mathbf{h}X \mathbf{W}^H + \mathbf{W} X^H \mathbf{h}^H) \tilde{\mathbf{h}} | X \right] \\ &= \text{E} \left[(\tilde{\mathbf{h}}^H \mathbf{h}X X^H \mathbf{h}^H \tilde{\mathbf{h}} + \tilde{\mathbf{h}}^H \mathbf{W} \mathbf{W}^H \tilde{\mathbf{h}}) | X \right] \\ &= \mathcal{E}_s \text{E} \left[\tilde{\mathbf{h}}^H \mathbf{h} \mathbf{h}^H \tilde{\mathbf{h}} | X \right] + \text{E} \left[\tilde{\mathbf{h}}^H \mathbf{W} \mathbf{W}^H \tilde{\mathbf{h}} | X \right] \\ &= \mathcal{E}_s \mathbf{h}^H \text{E} \left[\tilde{\mathbf{h}} \tilde{\mathbf{h}}^H | X \right] \mathbf{h} + \text{E} \left[\tilde{\mathbf{h}}^H \mathbf{W} \mathbf{W}^H \tilde{\mathbf{h}} | X \right] \\ &= \mathcal{E}_s \|\mathbf{h}\|^2 2\rho + \text{E} \left[\tilde{\mathbf{h}}^H \mathbf{W} \mathbf{W}^H \tilde{\mathbf{h}} | X \right] \\ &= \frac{\|\mathbf{h}\|^2 N_0}{P} + \text{E} \left[\tilde{\mathbf{h}}^H \mathbf{W} \mathbf{W}^H \tilde{\mathbf{h}} | X \right]\end{aligned}\quad (2.37)$$

The final expectation can be solved with iterated expectations since $\tilde{\mathbf{h}}$ and \mathbf{W} are independent. We can write

$$\begin{aligned}\text{E} \left[\tilde{\mathbf{h}}^H \mathbf{W} \mathbf{W}^H \tilde{\mathbf{h}} | X \right] &= \text{E} \left[\tilde{\mathbf{h}}^H \text{E} \left[\mathbf{W} \mathbf{W}^H | X, \tilde{\mathbf{h}} \right] \tilde{\mathbf{h}} | X \right] \\ &= \text{E} \left[\tilde{\mathbf{h}}^H (N_0 \mathbf{I}) \tilde{\mathbf{h}} | X \right] \\ &= N_0 \text{E} \left[\tilde{\mathbf{h}}^H \tilde{\mathbf{h}} | X \right] = N_0 N 2\rho \\ &= \frac{N_0^2 N}{P \mathcal{E}_s}.\end{aligned}\quad (2.38)$$

Putting it all together, we have

$$\begin{aligned}\text{var} [Y_{bfe} | X] &= \text{var} \left[Y_{bf} + \tilde{\mathbf{h}}^H (\mathbf{h}X + \mathbf{W}) | X \right] \\ &= \|\mathbf{h}\|^2 N_0 + \frac{\|\mathbf{h}\|^2 N_0}{P} + \frac{N_0^2 N}{P \mathcal{E}_s}\end{aligned}\quad (2.39)$$

Therefore, we can calculate the SNR_{bfe} as

$$\begin{aligned}\text{SNR}_{bfe} &= \frac{(\|\mathbf{h}\|^2 \sqrt{\mathcal{E}_s})^2}{\|\mathbf{h}\|^2 N_0 + \frac{\|\mathbf{h}\|^2 N_0}{P} + \frac{N_0^2 N}{P \mathcal{E}_s}} \\ &= \frac{\|\mathbf{h}\|^2 \mathcal{E}_s}{N_0 + \frac{N_0}{P} + \frac{N_0^2 N}{\|\mathbf{h}\|^2 P \mathcal{E}_s}}\end{aligned}\quad (2.40)$$

Asymptotically, since P grows proportionally with N and $P \mathcal{E}_s$ is fixed, the middle term in the denominator vanishes. So for large N with vanishing per-node SNR we can write

$$\text{SNR}_{bfe} \rightarrow \frac{\|\mathbf{h}\|^2 \mathcal{E}_s}{N_0 + \frac{N_0^2 N}{\|\mathbf{h}\|^2 P \mathcal{E}_s}}.\quad (2.41)$$

Moreover, since $\lim_{N \rightarrow \infty} \frac{\|\mathbf{h}\|^2}{N} = 2\lambda$, $\mathcal{E}_s = \frac{\mathcal{E}_s^{(1)}}{N}$, and $P = NP^{(1)}$, it can be easily obtained that

$$\text{SNR}_{bfe} \rightarrow \frac{2\lambda \mathcal{E}_s^{(1)}}{N_0 \left(1 + \frac{N_0}{2\lambda P^{(1)} \mathcal{E}_s^{(1)}}\right)}.\quad (2.42)$$

The results in (2.29) and (2.42) allow us to compute the penalty of channel estimation error in an ideal receive beamformer as $N \rightarrow \infty$ as

$$\mathcal{P}_{bf} = \frac{\text{SNR}_{bf}}{\text{SNR}_{bfe}} \rightarrow 1 + \frac{N_0}{2\lambda P^{(1)} \mathcal{E}_s^{(1)}}.\quad (2.43)$$

2.6.3.3 Pseudo-Beamforming: Perfect Channel Estimation

Pseudo-beamforming is a simple but sub-optimal combining technique where (2.18) is performed on the *hard decisions* from each node. Specifically, the pseudo-beamformer combiner output is

$$Y_{pbf} \equiv Y_i = \sum_{j \in \mathcal{P}} \sqrt{\rho_i} V_j = \alpha \sum_{j \in \mathcal{P}} |h_j| V_j\quad (2.44)$$

Where $V_j \in \mathcal{X}$ for all j and are conditionally independent given the transmitted symbol. In order to find the SNR of pseudo-beamforming, like the previous steps, we

first have to calculate the mean and variance of the pseudo-beamformer output which itself requires calculation of the mean and variance of hard decisions V_j . Therefore, to obtain these statistics, we use the asymptotic SNR of pseudo-beamforming for M -PSK modulation that was already computed in [46]. The main results are summarized here. First, the conditional mean of M -PSK hard decisions has been calculated as

$$\mathbb{E}[V_j|X = x_\ell] = \left(\frac{M\rho_j \sin\left(\frac{\pi}{M}\right)}{2\sqrt{\pi}} \right) x_\ell \quad (2.45)$$

Second, the conditional variance of with M -PSK hard decisions in the low per-node SNR regime were calculated as

$$\text{var}[V_j|X = x_\ell] \approx a^2 \quad (2.46)$$

These results allow us to compute the conditional mean and variance of the pseudo-beamformer output with M -PSK hard decisions. Therefore, the conditional mean has been computed as

$$\mathbb{E}[Y_{pbf}|X = x_\ell] = \alpha \frac{aM \sin\left(\frac{\pi}{M}\right)}{2\sqrt{N_0\pi}} \|\mathbf{h}\|^2 x_\ell \quad (2.47)$$

Similarly, the conditional variance of the pseudo-beamformer output with M -PSK hard decisions in the low per-node SNR regime were computed as

$$\text{var}[Y_{pbf}|X = x_\ell] = \alpha^2 a^2 \|\mathbf{h}\|^2 \quad (2.48)$$

Where we used the facts that $\rho_j = \frac{|h_j|a}{\sqrt{N_0}}$ and $\sum_j |h_j|^2 = \|\mathbf{h}\|^2$. Using the results from (2.47) and (2.48) we can compute the SNR of pseudo-beamforming as

$$\begin{aligned} \text{SNR}_{pbf} &= \frac{(\mathbb{E}[Y_{pbf}|X = x_\ell])^2}{\text{var}[Y_{pbf}|X = x_\ell]} \\ &= \frac{M^2 \sin^2\left(\frac{\pi}{M}\right) \|\mathbf{h}\|^2 \mathcal{E}_s}{4N_0\pi} \end{aligned} \quad (2.49)$$

$$= \frac{M^2 \sin^2\left(\frac{\pi}{M}\right)}{4\pi} \text{SNR}_{bf}. \quad (2.50)$$

With QPSK, we have $M = 4$ and $\frac{M^2 \sin^2(\frac{\pi}{M})}{4\pi} = \frac{2}{\pi}$. This then implies

$$\text{SNR}_{pbf}^{\text{QPSK}} \approx \frac{2}{\pi} \text{SNR}_{bf}. \quad (2.51)$$

For large M , we can use small angle approximation which means we can say $\sin(\frac{\pi}{M}) = \frac{\pi}{M}$ and it results in $\frac{M^2 \sin^2(\frac{\pi}{M})}{4\pi} \rightarrow \frac{\pi}{4}$. Hence

$$\lim_{M \rightarrow \infty} \text{SNR}_{pbf}^{M\text{-PSK}} \approx \frac{\pi}{4} \text{SNR}_{bf}. \quad (2.52)$$

2.6.3.4 Pseudo-Beamforming: Noisy Channel Estimation

The effect of channel estimation error on pseudo-beamforming has two effects: (i) channel *phase* errors cause increased likelihood of hard decision errors and (ii) channel *magnitude* errors cause combining errors. To model the effect of channel estimation error on the decision variable at an individual receiver, we first define the perfect and noisy channel estimate, respectively, as

$$h_j = |h_j| e^{j\theta} \quad (2.53)$$

$$\hat{h}_j = |\hat{h}_j| e^{j\hat{\theta}} \quad (2.54)$$

Lemma 1 provides expressions for the conditional mean and variance of hard decisions at an individual receiver with low per-node SNR in presence of channel estimation error.

Lemma 1. *For a forward link with M – PSK modulation with $M \geq 4$ and even, at low per-node SNR we have*

$$\text{E}[V_j | X = x_l] = \left(\frac{M \rho_j |h| \sin(\frac{\pi}{M})}{2\sqrt{\pi} \text{E}[|\hat{h}|]} \right) x_l \quad (2.55)$$

and the variance is

$$\text{var}[V_j | X = x_l] \approx a^2. \quad (2.56)$$

The proof for this lemma is given below.

Proof. To be able to find the mean and variance of hard decisions, the distribution of decision variable phase at the receiver should be calculated. The decision variable with no estimation error would be

$$\bar{U}_j = e^{-j\theta} h_j X + e^{-j\theta} W_j \quad (2.57)$$

and with estimation error would be

$$\bar{U}_{j_e} = e^{-j\hat{\theta}} h_j X + e^{-j\hat{\theta}} W_j \quad (2.58)$$

if we define $\theta_e = \theta - \hat{\theta}$ and replace the h_j with its polar format defined in (2.53) we get

$$\bar{U}_{j_e} = (|h_j|X + e^{-j\theta} W_j) e^{j\theta_e} = \bar{U}_j \times e^{j\theta_e} \quad (2.59)$$

If we replace the decision variables with their polar formats we get

$$\theta_{\bar{U}_{j_e}} = \theta_{\bar{U}_j} + \theta_e \quad (2.60)$$

Since we already have the distribution of $\theta_{\bar{U}_j}$ from (11) in [48], we can derive the distribution of $\theta_{\bar{U}_{j_e}}$ by convolving the distributions of $\theta_{\bar{U}_j}$ and θ_e . So,

$$\begin{aligned} f(\theta_{\bar{U}_{j_e}} | X = x_1) &= f(\theta_{\bar{U}_j} | X = x_1) * f(\theta_e) \\ &= \int_{-\infty}^{\infty} \left(\frac{1}{2\pi} e^{-\rho_j^2} + \frac{\rho_j}{\sqrt{\pi}} \cos(\theta_{\bar{U}_{j_e}} - \theta_e) e^{-\rho_j^2 \sin^2(\theta_{\bar{U}_{j_e}} - \theta_e)} \right. \\ &\quad \left. \left(1 - Q(\sqrt{2\rho_j^2 \cos^2(\theta_{\bar{U}_{j_e}} - \theta_e)}) \right) \right) \times f(\theta_e) d\theta_e \end{aligned} \quad (2.61)$$

where $f(\theta_e)$ is the distribution of θ_e and could have any distribution.

Using $\theta_{\bar{U}_{j_e}}$ distribution, transition probability or the probability of deciding $V_j = x_m$ given $X = x_1$, can be expressed as

$$p_{m,1} = \int_{\frac{(2m-3)\pi}{M}}^{\frac{(2m-1)\pi}{M}} f(\theta_{\bar{U}_{j_e}} | X = x_1) d\theta_{\bar{U}_{j_e}} \quad (2.62)$$

In a low per-node SNR regime, we can calculate a first-order Taylor series expansion of $p_{m,1}$ at $\rho_j = 0$ by computing

$$\begin{aligned}
p_{m,1}|_{\rho_j=0} &= \int_{\frac{(2m-3)\pi}{M}}^{\frac{(2m-1)\pi}{M}} f(\theta_{\bar{U}_{j_e}} | X = x_1) \Big|_{\rho_j=0} d\theta_{\bar{U}_{j_e}} \\
&= \int_{\frac{(2m-3)\pi}{M}}^{\frac{(2m-1)\pi}{M}} \frac{1}{2\pi} \left[\int_{-\infty}^{\infty} f(\theta_e) d\theta_e \right] d\theta_{\bar{U}_{j_e}} \\
&= \frac{1}{M}
\end{aligned} \tag{2.63}$$

The expression in the brackets is equal to 1 since it is the integral of a distribution. For the second term we have

$$\begin{aligned}
\frac{\partial}{\partial \rho_j} p_{m,1}|_{\rho_j=0} &= \int_{\frac{(2m-3)\pi}{M}}^{\frac{(2m-1)\pi}{M}} \frac{\partial}{\partial \rho_j} f(\theta_{\bar{U}_{j_e}} | X = x_1) \Big|_{\rho_j=0} d\theta_{\bar{U}_{j_e}} \\
&= \int_{\frac{(2m-3)\pi}{M}}^{\frac{(2m-1)\pi}{M}} \int_{-\infty}^{\infty} \frac{\cos(\theta_{\bar{U}_{j_e}} - \theta_e)}{2\sqrt{\pi}} f(\theta_e) d\theta_e d\theta_{\bar{U}_{j_e}} \\
&= \int_{\frac{(2m-3)\pi}{M}}^{\frac{(2m-1)\pi}{M}} \left[\frac{1}{2\sqrt{\pi}} \left(\cos(\theta_{\bar{U}_{j_e}}) \mathbb{E}[\cos(\theta_e)] \right. \right. \\
&\quad \left. \left. + \sin(\theta_{\bar{U}_{j_e}}) \mathbb{E}[\sin(\theta_e)] \right) \right] d\theta_{\bar{U}_{j_e}}
\end{aligned} \tag{2.64}$$

Channel estimation \hat{h} in polar format can be written as $|\hat{h}|e^{j\hat{\theta}} = |h|e^{j\theta} + \tilde{h}|e^{j\hat{\theta}}$. Also, h is given and $\tilde{h} \sim \mathcal{CN}(0, 2\rho)$. Then, from expectation of real and imaginary part of \hat{h} , respectively, we have

$$\mathbb{E}[\cos(\hat{\theta})] = \frac{|h| \cos(\theta)}{\mathbb{E}[|\hat{h}|]} \tag{2.65}$$

$$\mathbb{E}[\sin(\hat{\theta})] = \frac{|h| \sin(\theta)}{\mathbb{E}[|\hat{h}|]} \tag{2.66}$$

Using $\theta_e = \theta - \hat{\theta}$ and getting the expectation of $\cos(\theta_e)$, we would have

$$\mathbb{E}[\cos(\theta_e)] = \frac{|h|}{\mathbb{E}[|\hat{h}|]} \tag{2.67}$$

$$\mathbb{E}[\sin(\theta_e)] = 0 \tag{2.68}$$

Now if we substitute these result into equation (2.64) we would have

$$\begin{aligned} \frac{\partial}{\partial \rho_j} p_{m,1} |_{\rho_j=0} &= \int_{(2m-3)\pi/M}^{(2m-1)\pi/M} \left[\frac{1}{2\sqrt{\pi}} \cos(\theta_{\bar{U}_{j_e}}) \frac{|h|}{\mathbb{E}[|\hat{h}|]} \right] d\theta_{\bar{U}_{j_e}} \\ &= \frac{|h| \sin\left(\frac{\pi}{M}\right)}{\sqrt{\pi} \mathbb{E}[|\hat{h}|]} \left[\cos\left(\frac{2\pi(m-1)}{M}\right) \right] \end{aligned} \quad (2.69)$$

So, in a low pre-node SNR regime with ρ_j small, we have

$$p_{m,1} \approx \frac{1}{M} + \frac{|h| \sin\left(\frac{\pi}{M}\right)}{\sqrt{\pi} \mathbb{E}[|\hat{h}|]} \left[\cos\left(\frac{2\pi(m-1)}{M}\right) \right] \rho_j \quad (2.70)$$

Under the assumption that $M \geq 4$ is even, we can compute the conditional expectation as follow

$$\begin{aligned} \mathbb{E}[V_j | X = x_1] &= \sum_{m=1}^M x_m p_{m,1} \\ &\approx \sum_{m=1}^M a e^{j2\pi(m-1)/M} \left\{ \frac{1}{M} + \frac{|h| \sin\left(\frac{\pi}{M}\right)}{\sqrt{\pi} \mathbb{E}[|\hat{h}|]} \right. \\ &\quad \left. \times \left[\cos\left(\frac{2\pi(m-1)}{M}\right) \right] \rho_j \right\} \\ &= \frac{2a \rho_j |h| \sin\left(\frac{\pi}{M}\right)}{\sqrt{\pi} \mathbb{E}[|\hat{h}|]} \\ &\quad \times \left[\sum_{m=1}^{M/2} \cos^2\left(\frac{2\pi(m-1)}{M}\right) \right] \\ &= \left(\frac{M \rho_j |h| \sin\left(\frac{\pi}{M}\right)}{2\sqrt{\pi} \mathbb{E}[|\hat{h}|]} \right) x_1 \end{aligned} \quad (2.71)$$

The conditional variance can be computed similarly as

$$\begin{aligned} \text{var}[V_j | X = x_1] &= \mathbb{E}[|V_j|^2 | X = x_1] - |\mathbb{E}[V_j | X = x_1]|^2 \\ &\approx a^2 - \left(\frac{M \rho_j |h| \sin\left(\frac{\pi}{M}\right)}{2\sqrt{\pi} \mathbb{E}[|\hat{h}|]} \right)^2 a^2 \end{aligned} \quad (2.72)$$

Since ρ_j is small under low per-node SNR assumption, we can discard the term with ρ_j^2 , so we get

$$\text{var}[V_j | X = x_1] \approx a^2 \quad (2.73)$$

□

As it can be seen from the proof, the calculation of mean and variance of hard decisions do not depend on any specific phase error distribution, since in the proof process, we have assumed the distribution function in its general term which is not specific to any distribution, and we only calculate the integral over this probability distribution function to obtain the basic statistics. Also, this phase error distribution could be deterministic which will result in all the expectation values of the other variables that are dependent on it to be deterministic as well.

In a low per-node SNR regime and for a large N , since ρ_j becomes very small, it is expected that the mean goes to zero. Also, the variance given in (2.56) serves as an upper bound for the variance of hard decisions as N gets large.

The next step is to find the mean and variance of the pseudo-beamformer output in order to be able to calculate its SNR performance. The pseudo-beamformer output with imperfect channel estimates is given as

$$Y_{pbfe} = \alpha \sum_{j \in N} |\hat{h}_j| V_j. \quad (2.74)$$

Corollary 1 uses the results obtained from lemma 1 to provide expressions for the conditional mean and variance of the pseudo-beamformer output.

Corollary 1. *Given the channel information h_j and input symbol $X = x_l$, the mean and variance of pseudo-beamformer output can be computed as*

$$\mathbb{E}[Y_{pbfe}|X = x_l] = \alpha \frac{aM \sin\left(\frac{\pi}{M}\right)}{2\sqrt{\pi N_0}} \|\mathbf{h}\|^2 x_l \quad (2.75)$$

and the variance is

$$\text{var}[Y_{pbfe}|X = x_l] = \alpha^2 a^2 \left(\|\mathbf{h}\|^2 + \frac{N_0 N}{P \mathcal{E}_s} \right) \quad (2.76)$$

The proof for this corollary is

Proof. By having the mean and variance of hard decision we can now calculate the mean and variance of pseudo-beamformer output. The pseudo-beamformer uses the estimated channel magnitudes to compute the combiner output

$$Y_{pbfe} = \alpha \sum_{j \in N} |\hat{h}_j| V_j \quad (2.77)$$

Therefore the mean of the pseudo-beamformer output is

$$\begin{aligned} \mathbb{E}[Y_{pbfe}|X = x_l] &= \alpha \sum_{j \in N} \mathbb{E}[|\hat{h}_j| | X = x_l] \mathbb{E}[V_j | X = x_l] \\ &= \alpha \frac{M \sin\left(\frac{\pi}{M}\right)}{2\sqrt{\pi}} \sum_{j \in N} (\rho_j |h_j|) x_l \end{aligned} \quad (2.78)$$

by replacing $\rho_j := \frac{|h_j|a}{\sqrt{N_0}}$ and setting $\sum_{j \in N} |h_j|^2 = \|\mathbf{h}\|^2$ we would have

$$\mathbb{E}[Y_{pbfe}|X = x_l] = \alpha \frac{aM \sin\left(\frac{\pi}{M}\right)}{2\sqrt{\pi N_0}} \|\mathbf{h}\|^2 x_l \quad (2.79)$$

Also, the variance of the pseudo-beamformer output can calculate as follow

$$\begin{aligned} \text{var}[Y_{pbfe}|X = x_l] &= \alpha^2 \sum_{j \in N} \text{var}[|\hat{h}_j| V_j | X = x_l] \\ &= \alpha^2 \sum_{j \in N} \left(\mathbb{E}[|\hat{h}_j|^2] \mathbb{E}[V_j^2 | X = x_l] - \mathbb{E}[|\hat{h}_j|]^2 \mathbb{E}[V_j | X = x_l]^2 \right) \end{aligned} \quad (2.80)$$

the second term can be set equal to zero since in a low per-node SNR regime $\mathbb{E}[V_j | X = x_l]^2 \approx 0$. Then we would have

$$\text{var}[Y_{pbfe}|X = x_l] = \alpha^2 a^2 \sum_{j \in N} \mathbb{E}[|\hat{h}_j|^2] \quad (2.81)$$

To obtain $\mathbb{E}[|\hat{h}_j|^2]$ we have to use the fact that

$$|\hat{h}_j|^2 = \left(|h_j| \cos(\theta_j) + |\tilde{h}_j| \cos(\tilde{\theta}_j) \right)^2 \quad (2.82)$$

$$+ \left(|h_j| \sin(\theta_j) + |\tilde{h}_j| \sin(\tilde{\theta}_j) \right)^2 \quad (2.83)$$

After simplifying the above equation and getting the expectation of both side, we have

$$\mathbb{E}[|\hat{h}_j|^2] = |h_j|^2 + \mathbb{E}[|\tilde{h}_j|^2] = |h_j|^2 + \frac{N_0}{P\mathcal{E}_s} \quad (2.84)$$

by replacing it back in the equation (2.81) the variance of pseudo-beamformer output is obtained.

$$\text{var}[Y_{pbfe}|X = x_l] = \alpha^2 a^2 \left(\|\mathbf{h}\|^2 + \frac{N_0 N}{P\mathcal{E}_s} \right) \quad (2.85)$$

□

With the results of Corollary 1, we now can compute the SNR of pseudo-beamforming with channel estimation error as

$$\begin{aligned} \text{SNR}_{pbfe} &= \frac{|\mathbb{E}[Y_{pbfe}|X = x_l]|^2}{\text{var}[Y_{pbfe}|X = x_l]} \\ &= \frac{\alpha^2 a^2 M^2 \sin^2\left(\frac{\pi}{M}\right) \|\mathbf{h}\|^4 x_l^2}{4\pi N_0} \\ &= \frac{\alpha^2 a^2 \left(\|\mathbf{h}\|^2 + \frac{N_0 N}{P\mathcal{E}_s} \right)}{4\pi} \\ &= \frac{M^2 \sin^2\left(\frac{\pi}{M}\right)}{4\pi} \frac{\|\mathbf{h}\|^2 \mathcal{E}_s}{N_0 + \frac{N_0^2 N}{\|\mathbf{h}\|^2 P\mathcal{E}_s}} \end{aligned} \quad (2.86)$$

$$\rightarrow \frac{M^2 \sin^2\left(\frac{\pi}{M}\right)}{4\pi} \frac{2\lambda \mathcal{E}_s^{(1)}}{N_0 \left(1 + \frac{N_0}{2\lambda P^{(1)} \mathcal{E}_s^{(1)}}\right)} \quad (2.87)$$

where the final result assumes $N \rightarrow \infty$ with correspondingly vanishing per-node SNR.

In light of (2.42), we can write

$$\text{SNR}_{pbfe} = \frac{M^2 \sin^2\left(\frac{\pi}{M}\right)}{4\pi} \text{SNR}_{bfe}. \quad (2.88)$$

Hence, the SNR gaps between pseudo-beamforming with channel estimation error and ideal receive beamforming with channel estimation error are identical to the cases without channel estimation error.

Using (2.49) and (2.87), the SNR penalty of channel estimation error with pseudo-beamforming can be expressed as

$$\mathcal{P}_{pbf} = \frac{\text{SNR}_{pbf}}{\text{SNR}_{pbfe}} = 1 + \frac{N_0}{2\lambda P^{(1)} \mathcal{E}_s^{(1)}} \quad (2.89)$$

which is identical to (2.43). This shows the somewhat surprising result that the SNR ratio between ideal receive beamforming and pseudo-beamforming does not depend on the amount of channel estimation error. In other words, the SNR ratio with channel estimation error is identical to the SNR ratio without channel estimation error, as derived in [46].

2.6.4 Numerical Results

In this section the results from the simulation are presented. In this simulation a QPSK modulation is chosen for the forward link between single transmitter and the receive cluster. The number of receive nodes inside the cluster are $N = [10 \ 20 \ 40 \ 80 \ 160 \ 320 \ 640 \ 1280 \ 2560 \ 5120 \ 7680]$. The number of iterations for each channel/noise realization is chosen to be 1000 and the per-symbol transmit energy with one receiver $\mathcal{E}_s^{(1)} = 10$ and training signal length with one receiver $P^{(1)} = 1$. The magnitude of each symbol is $a = \sqrt{2}$ and the number of payload symbols per block is $Q = 100$. The total noise power $N_0 = 15$ and channel variance in real and imaginary dimension is $\lambda = 2$.

Figure 2.2 shows the comparison of the SNRs between ideal receive beamforming and pseudo-beamforming each with and without channel estimation error.

The results from Figure 2.2 confirms our proofs that the ratio of the SNRs between ideal receive beamforming and pseudo-beamforming in both case of perfect and noisy channel estimation are equal to $\frac{2}{\pi}$ and the SNR in each case converges to the calculated limit for large N.

Figure 2.3 shows the comparison of the penalties between the ideal and pseudo beamformer. It can be seen that, the penalty term in both cases converges to the same number since the SNR ratios in each case, as shown in equation (2.43) for an ideal beamformer and (2.89) for a pseudo beamformer are the same.

Figure 2.4 shows the mean and variance of the hard decisions when there is channel estimation error. The results from the figure show that, the calculated mean of the

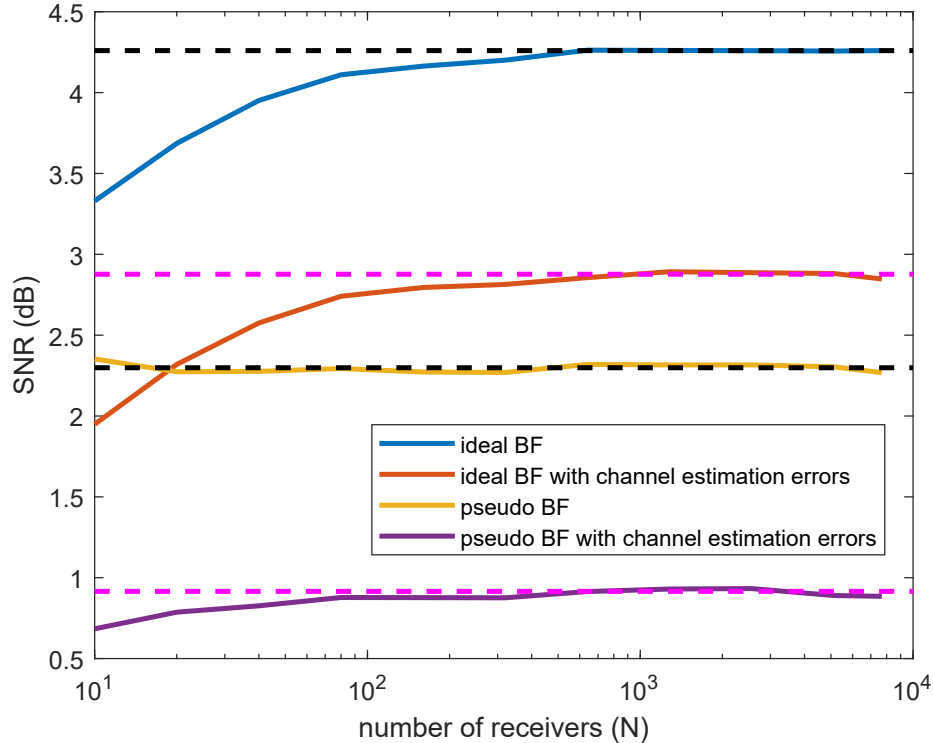


Figure 2.2: Comparison of the SNRs between ideal receive beamforming and pseudo-beamforming with and without channel estimation error in QPSK modulation. The dotted lines are the calculated SNRs for large N in each scenario.

hard decisions closely follows the numerical results. Also, the variance of the hard decisions approaches to the upper bound obtained from the theoretical results.

2.6.5 Conclusion

In this section we used theoretical calculations, asymptotic analysis and numerical results from simulation, to obtain and characterize the effect of imperfect channel estimation in a distributed reception system with M -PSK modulation. As mentioned in this section, channel estimation error had two effects, channel phase error and channel magnitude error, which our analysis had accounted for both of these effects in the channel estimation process at the receiver. In our analysis, phase error did not have a

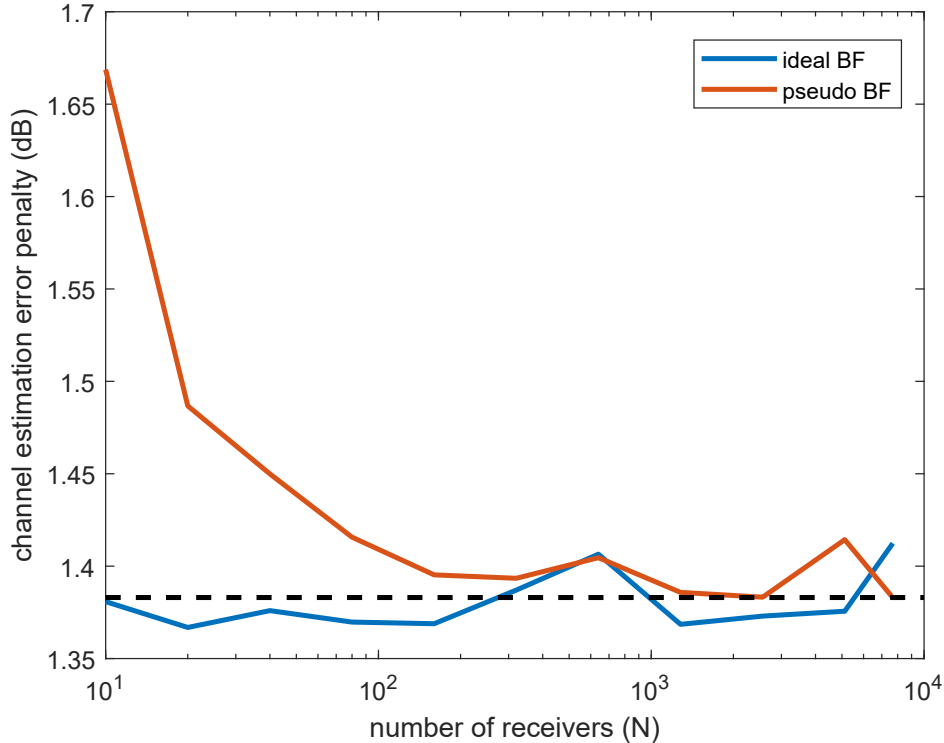


Figure 2.3: Comparison of the penalties between the ideal and pseudo beamformer in QPSK modulation.

specific distribution and our results are valid for any phase error distribution. Using theoretical computations, we derived closed-form expressions for the SNR of both ideal receive beamforming and pseudo-beamforming. As it was expected, the results of our analysis show that in QPSK modulation, channel estimation error degrades the performance of distributed reception with both ideal and pseudo-beamforming techniques by almost 1.38 dB . The interesting outcome of our analysis was that, the SNR ratio between ideal receive beamforming and pseudo-beamforming does not depend on the amount of channel estimation error and are identical to the SNR ratios with no channel estimation error. So, our analysis shows, channel estimation error causes the same amounts of performance degradation in ideal beamforming and pseudo-beamforming systems despite the fact that the channel estimation errors manifests

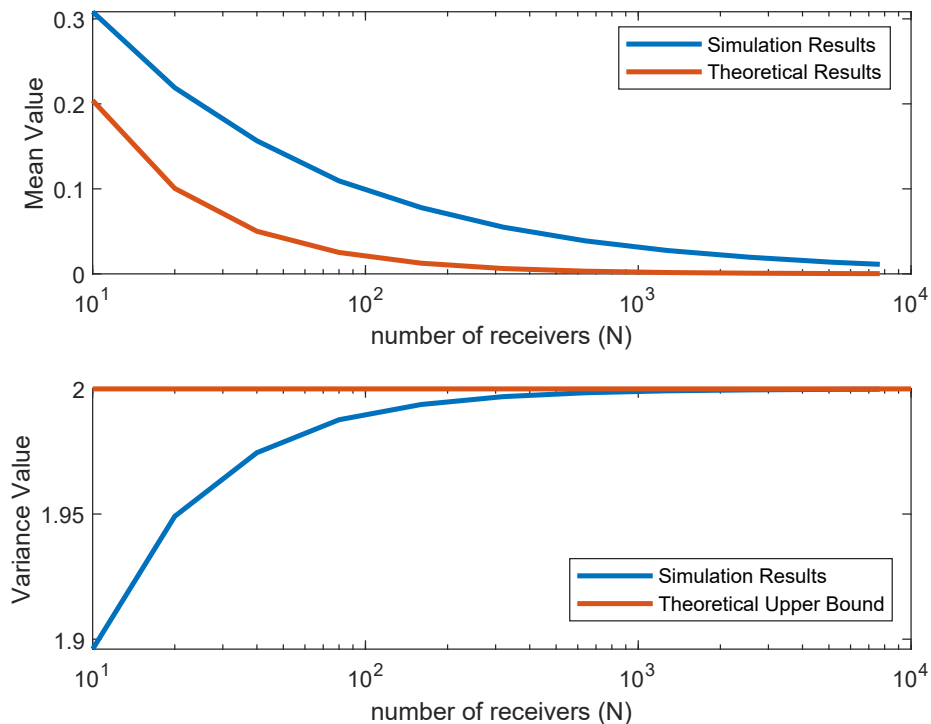


Figure 2.4: Mean and variance of the hard decisions when there is channel estimation error in QPSK modulation.

themselves quite differently in both systems. Also, simulation results confirmed our calculations for the mean and variance of hard decisions with channel estimation error and also, our results for the penalty term in both ideal and pseudo-beamforming systems.

2.7 M^2 -QAM Modulated Transmission

Previously the effect of channel estimation error on distributed reception with hard decision exchange using M -QPSK modulation has been investigated [49]. In this work we investigate the case where M^2 -QAM is used as the modulation technique.

2.7.1 System Model

We assume a block transmission scenario with blocks of length n as in [49]. Here we assume M^2 -QAM modulation in forward link. The ℓ^{th} symbol in block m for each of the in-phase or quadrature component is denoted as $X_{I/Q}[m, \ell]$ for $\ell = 1, \dots, n$ and is assumed to be drawn equiprobably from the QAM alphabet $\mathcal{X}_{I/Q} = \{x_1, \dots, x_M\} = \{-(M-1)a, \dots, -a, a, \dots, (M-1)a\}$. The average energy per transmitted symbol for each of the in-phase or quadrature component is denoted as $\mathcal{E}_s = \text{E}[|X_{I/Q}[m, \ell]|^2]$. Given an additive white Gaussian noise channel (AWGN) with power spectral density $N_0/2$ in the real and imaginary dimensions, the complex baseband signal received at the i^{th} receive node for the ℓ^{th} symbol of block m can be written as

$$U_i[m, \ell] = h_i[m]X[m, \ell] + W_i[m, \ell] \quad (2.90)$$

for $i = 1, \dots, N$ and $\ell = 1, \dots, n$ where $X[m, \ell] = X_I[m, \ell] + \text{j}X_Q[m, \ell]$ and $W_i[m, \ell] \sim \mathcal{CN}(0, N_0)$ is spatially and temporally independent and identically distributed (i.i.d.) proper complex Gaussian baseband noise. We assume the noise variance is identical at each receive node. The quantity $\rho_i[m] = \frac{|h_i[m]|^2 \mathcal{E}_s}{N_0}$ corresponds to the signal-to-noise ratio (SNR) at receive node i for symbols received in block m .

2.7.2 Channel Estimation

Channel estimation is just like [49], so we have

$$\hat{h}_i[m] = h_i[m] + \tilde{h}_i[m] \quad (2.91)$$

where $\tilde{h}_i[m] \sim \mathcal{CN}(0, 2\delta)$ is a proper complex Gaussian random variable with variance δ in the real and imaginary dimensions. Since the training sequence $\mathbf{X}[m]$ is known and has the length P , we can determine 2δ by computing the $\text{var}(\tilde{h}_i[m])$ as

$$\begin{aligned} \text{var}(\tilde{h}_i[m]) &= \frac{N_0}{\sum_{i=1}^P |x_i|^2} = \frac{N_0}{\text{PE}[|X|^2]} = \frac{N_0}{\text{PE}[|X_I + \text{j}X_Q|^2]} \\ &= \frac{N_0}{2P\mathcal{E}_s} \end{aligned} \quad (2.92)$$

2.7.3 Asymptotic SNR Analysis

We can suppress the block/symbol indices and consider the scalar observation at receive node i as

$$U_i = h_i X + W_i \quad (2.93)$$

where $X = X_I + jX_Q$ is drawn from an M^2 -QAM constellation with $E[|X_{I/Q}|^2] = \mathcal{E}_s$. Just like before, for our asymptotic analysis, we will assume signal energy $\mathcal{E}_s = \mathcal{E}_s^{(1)}/N$, i.e., the transmit power scales as $1/N$, where $\mathcal{E}_s^{(1)}$ is the per-symbol transmit energy with one receiver. We also assume $P = NP^{(1)}$, i.e., the training signal length scales with N , where $P^{(1)}$ is the training signal length with one receiver. Under this assumption, note that $P\mathcal{E}_s$ is a constant. Since N_0 is also fixed, the variance of channel estimation errors is constant.

2.7.3.1 Ideal Receive Beamforming: Perfect Channel Estimation

The output of ideal receive beamformer at node i is realized by using unquantized observations U_j and is defined as

$$Y_{bf} \equiv Y_i = \sum_{j \in \mathcal{P}} \sqrt{\rho_i} U_j = \alpha \sum_{j \in \mathcal{P}} |h_j| U_j \quad (2.94)$$

where $\rho_i = \frac{|h_i|^2 2\mathcal{E}_s}{N_0}$ and $\alpha = \sqrt{\frac{2\mathcal{E}_s}{N_0}}$ and \mathcal{P} is the set of nodes that are participating in hard decision exchanges since not all the receiving nodes participate in exchange due to poor received signal.

For the ideal receive beamformer, we have the vector observation

$$\mathbf{U} = \mathbf{h}X + \mathbf{W}. \quad (2.95)$$

Assuming no channel estimation error, the ideal receive beamformer output is given as

$$Y_{bf} = \mathbf{h}^H \mathbf{U} = \mathbf{h}^H \mathbf{h}X + \mathbf{h}^H \mathbf{W}. \quad (2.96)$$

The SNR of ideal receive beamforming (conditioned on the channel realizations) can be computed as

$$\begin{aligned}
\text{SNR}_{bf} &= \frac{(\mathbb{E}\{\mathbf{h}^H \mathbf{h}X + \mathbf{h}^H \mathbf{W} | X\})^2}{\text{var}\{\mathbf{h}^H \mathbf{h}X + \mathbf{h}^H \mathbf{W} | X\}} \\
&= \frac{\|\mathbf{h}\|^4 2\mathcal{E}_s}{\mathbf{h}^H \mathbb{E}\{\mathbf{W}\mathbf{W}^H\} \mathbf{h}} \\
&= \frac{\|\mathbf{h}\|^2 2\mathcal{E}_s}{N_0}.
\end{aligned} \tag{2.97}$$

If we further assume an i.i.d. Rayleigh fading channel such that $h_i \sim \mathcal{CN}(0, 2\lambda)$, then asymptotically we have $\lim_{N \rightarrow \infty} \frac{\|\mathbf{h}\|^2}{N} = 2\lambda$. The asymptotic SNR is then

$$\text{SNR}_{bf} \rightarrow \frac{4N\lambda\mathcal{E}_s}{N_0} = \frac{4\lambda\mathcal{E}_s^{(1)}}{N_0}. \tag{2.98}$$

2.7.3.2 Ideal Receive Beamforming: Noisy Channel Estimation

Now we consider ideal receive beamforming with channel estimates of the form

$$\hat{\mathbf{h}} = \mathbf{h} + \tilde{\mathbf{h}} \tag{2.99}$$

where $\tilde{\mathbf{h}} \sim \mathcal{CN}(0, 2\delta\mathbf{I})$. The ideal receive beamformer output with channel estimation error is given as

$$\begin{aligned}
Y_{bfe} &= \hat{\mathbf{h}}^H \mathbf{U} = \hat{\mathbf{h}}^H (\mathbf{h}X + \mathbf{W}) \\
&= (\mathbf{h} + \tilde{\mathbf{h}})^H (\mathbf{h}X + \mathbf{W}) \\
&= \mathbf{h}^H (\mathbf{h}X + \mathbf{W}) + \tilde{\mathbf{h}}^H (\mathbf{h}X + \mathbf{W}) \\
&= Y_{bf} + \tilde{Y}_{bf}.
\end{aligned} \tag{2.100}$$

Then, the SNR of ideal receive beamforming with channel estimation error (conditioned on the channel realizations) can be computed as

$$\text{SNR}_{bfe} = \frac{(\mathbb{E}\{Y_{bf} + \tilde{\mathbf{h}}^H (\mathbf{h}X + \mathbf{W}) | X\})^2}{\text{var}\{Y_{bf} + \tilde{\mathbf{h}}^H (\mathbf{h}X + \mathbf{W}) | X\}}. \tag{2.101}$$

Note that $\tilde{\mathbf{h}}$ is independent of \mathbf{h} and X . Since the channel estimates were generated from different observations than the ones used in the SNR calculations, $\tilde{\mathbf{h}}$ is also independent of \mathbf{W} . Hence,

$$\begin{aligned} \mathbb{E} \left\{ Y_{bf} + \tilde{\mathbf{h}}^H (\mathbf{h}X + \mathbf{W}) \mid X \right\} &= \mathbb{E} \{ Y_{bf} \mid X \} \\ &= \|\mathbf{h}\|^2 \sqrt{2\mathcal{E}_s} \end{aligned} \quad (2.102)$$

and the numerator of this expression is unchanged from the case with no channel estimation error. As for the denominator, since Y_{bf} and \tilde{Y}_{bf} are independent, we have

$$\begin{aligned} \text{var} \left\{ Y_{bf} + \tilde{Y}_{bf} \mid X \right\} &= \text{var} \{ Y_{bf} \mid X \} \\ &+ \text{var} \left\{ \tilde{\mathbf{h}}^H (\mathbf{h}X + \mathbf{W}) \mid X \right\} \\ &= \|\mathbf{h}\|^2 N_0 + \text{var} \left\{ \tilde{\mathbf{h}}^H (\mathbf{h}X + \mathbf{W}) \mid X \right\} \end{aligned} \quad (2.103)$$

We can compute the second term as

$$\begin{aligned} \text{var} \left\{ \tilde{\mathbf{h}}^H (\mathbf{h}X + \mathbf{W}) \mid X \right\} &= \mathbb{E} \left\{ \tilde{\mathbf{h}}^H (\mathbf{h}X + \mathbf{W}) \right. \\ &\times \left. (\mathbf{h}X + \mathbf{W})^H \tilde{\mathbf{h}} \mid X \right\} - \left| \mathbb{E} \left\{ \tilde{\mathbf{h}}^H (\mathbf{h}X + \mathbf{W}) \mid X \right\} \right|^2 \\ &= \mathbb{E} \left\{ \tilde{\mathbf{h}}^H (\mathbf{h}X + \mathbf{W}) \times (\mathbf{h}X + \mathbf{W})^H \tilde{\mathbf{h}} \mid X \right\} \end{aligned} \quad (2.104)$$

where the second equality follows from the fact that $\tilde{\mathbf{h}}$ is zero mean and independent of the other terms in the expectation. We can further compute

$$\begin{aligned} \text{var} \left\{ \tilde{\mathbf{h}}^H (\mathbf{h}X + \mathbf{W}) \mid X \right\} &= 2\mathcal{E}_s \mathbb{E} \left\{ \tilde{\mathbf{h}}^H \mathbf{h} \mathbf{h}^H \tilde{\mathbf{h}} \mid X \right\} \\ &+ \mathbb{E} \left\{ \tilde{\mathbf{h}}^H \mathbf{W} \mathbf{W}^H \tilde{\mathbf{h}} \mid X \right\} \\ &= 2\mathcal{E}_s \mathbf{h}^H \mathbb{E} \left\{ \tilde{\mathbf{h}} \tilde{\mathbf{h}}^H \mid X \right\} \mathbf{h} + \mathbb{E} \left\{ \tilde{\mathbf{h}}^H \mathbf{W} \mathbf{W}^H \tilde{\mathbf{h}} \mid X \right\} \\ &= 2\mathcal{E}_s \|\mathbf{h}\|^2 2\delta + \mathbb{E} \left\{ \tilde{\mathbf{h}}^H \mathbf{W} \mathbf{W}^H \tilde{\mathbf{h}} \mid X \right\} \\ &= \frac{\|\mathbf{h}\|^2 N_0}{P} + \mathbb{E} \left\{ \tilde{\mathbf{h}}^H \mathbf{W} \mathbf{W}^H \tilde{\mathbf{h}} \mid X \right\} \end{aligned} \quad (2.105)$$

The final expectation can be solved with iterated expectations since $\tilde{\mathbf{h}}$ and \mathbf{W} are independent. We can write

$$\begin{aligned}
\mathbb{E} \left\{ \tilde{\mathbf{h}}^H \mathbf{W} \mathbf{W}^H \tilde{\mathbf{h}} \mid X \right\} &= \mathbb{E} \left\{ \tilde{\mathbf{h}}^H \mathbb{E} \left\{ \mathbf{W} \mathbf{W}^H \mid X, \tilde{\mathbf{h}} \right\} \tilde{\mathbf{h}} \mid X \right\} \\
&= \mathbb{E} \left\{ \tilde{\mathbf{h}}^H (N_0 \mathbf{I}) \tilde{\mathbf{h}} \mid X \right\} \\
&= N_0 \mathbb{E} \left\{ \tilde{\mathbf{h}}^H \tilde{\mathbf{h}} \mid X \right\} = N_0 N 2\delta \\
&= \frac{N_0^2 N}{2P\mathcal{E}_s}. \tag{2.106}
\end{aligned}$$

Putting it all together, we have

$$\begin{aligned}
\text{var} \left\{ Y_{bf} + \tilde{\mathbf{h}}^H (\mathbf{h}X + \mathbf{W}) \mid X \right\} &= \\
\|\mathbf{h}\|^2 N_0 + \frac{\|\mathbf{h}\|^2 N_0}{P} + \frac{N_0^2 N}{2P\mathcal{E}_s}. \tag{2.107}
\end{aligned}$$

and hence

$$\text{SNR}_{bfe} = \frac{\|\mathbf{h}\|^2 2\mathcal{E}_s}{N_0 + \frac{N_0}{P} + \frac{N_0^2 N}{2\|\mathbf{h}\|^2 P\mathcal{E}_s}}. \tag{2.108}$$

Asymptotically, since P grows proportionally with N and $P\mathcal{E}_s$ is fixed, the middle term in the denominator vanishes. So for large N with vanishing per-node SNR we can write

$$\text{SNR}_{bfe} \rightarrow \frac{\|\mathbf{h}\|^2 2\mathcal{E}_s}{N_0 + \frac{N_0^2 N}{2\|\mathbf{h}\|^2 P\mathcal{E}_s}}. \tag{2.109}$$

Moreover, since $\lim_{N \rightarrow \infty} \frac{\|\mathbf{h}\|^2}{N} = 2\lambda$, $\mathcal{E}_s = \frac{\mathcal{E}_s^{(1)}}{N}$, and $P = NP^{(1)}$, it can be easily obtained that

$$\text{SNR}_{bfe} \rightarrow \frac{4\lambda\mathcal{E}_s^{(1)}}{N_0 \left(1 + \frac{N_0}{4\lambda P^{(1)}\mathcal{E}_s^{(1)}} \right)}. \tag{2.110}$$

The results in (2.97) and (2.109) allow us to compute the penalty of channel estimation error in an ideal receive beamformer as $N \rightarrow \infty$ as

$$\mathcal{P}_{bf} = \frac{\text{SNR}_{bf}}{\text{SNR}_{bfe}} \rightarrow 1 + \frac{N_0}{4\lambda P^{(1)}\mathcal{E}_s^{(1)}}. \tag{2.111}$$

2.7.3.3 Pseudo-Beamforming: Perfect Channel Estimation

Pseudo-beamforming is a simple but sub-optimal combining technique where (2.94) is performed on the *hard decisions* from each node. In networks with M^2 -QAM modulation, the pseudo-beamformer combiner output is a combination of in-phase and quadrature components of hard decisions and it is expressed as below

$$\begin{aligned} Y_{pbf} \equiv Y_i &= \sum_{j \in \mathcal{P}} \sqrt{\rho_i} V_j = \alpha \sum_{j \in \mathcal{P}} |h_j| V_j \\ &= \alpha \sum_{j \in \mathcal{P}} |h_j| (\text{Re}(V_j) + j \text{Im}(V_j)) \end{aligned} \quad (2.112)$$

where $\text{Re}(V_j), \text{Im}(V_j) \in \mathcal{X}$ for all j and are conditionally independent given the transmitted symbol.

The asymptotic SNR of pseudo-beamforming for various modulation formats was analyzed in [46]. The proof for obtaining mean and variance of in-phase or quadrature component of M^2 -QAM hard decisions using the transition probabilities is stated in the following.

Proof: An M^2 -QAM constellation has real-valued alphabet containing M symbols for each of its in-phase (I) and quadrature (Q) components given as $\mathcal{X}_{I/Q} = \{x_1, x_2, \dots, x_M\} = \{-(M-1)a, \dots, -a, a, \dots, (M-1)a\}$ where a is just a constant used for scaling the symbols to satisfy the energy constraint $E[X_{I/Q}^2] = \mathcal{E}_s$. Now we can compute the conditional mean of hard decisions for I or Q component at the receive node j as $E[\text{Re}(V_j)|X = x_\ell] = \sum_{m=1}^M x_m p_{m,\ell}$, where $p_{m,\ell}$ is the transition probability and is defined as $p_{m,\ell} := \text{Prob}(\text{decide } V_j = x_m | X = x_\ell)$. If we assume the standard hard decision regions for M^2 -QAM and an AWGN channel with magnitude $|h_j|$ and noise variance of $N_0/2$, we can express the transition probabilities for $m \in \{2, \dots, M-1\}$ as

$$p_{m,\ell} = Q((2|\ell - m| - 1)\rho_j) - Q((2|\ell - m| + 1)\rho_j) \quad (2.113)$$

and for $m \in \{1, M\}$ as

$$p_{m,\ell} = Q((2|\ell - m| - 1)\rho_j) \quad (2.114)$$

for $\ell \in \{1, \dots, M\}$ where $\rho_j^2 := \frac{|h_j|^2 a^2}{N_0/2}$ and $Q(x) := \int_x^\infty \frac{1}{\sqrt{2\pi}} e^{-t^2/2} dt$ is the tail probability of standard Gaussian density. In the low per-node SNR regime of interest, $\rho_j \rightarrow 0$ and the arguments of the Q-functions would be small. For small arguments we can approximate the Q-functions as

$$Q(x) = \frac{1}{2} - \int_0^x \frac{1}{\sqrt{2\pi}} e^{-t^2/2} dt \approx \frac{1}{2} - \frac{x}{\sqrt{2\pi}}. \quad (2.115)$$

Therefore for low per-node SNR regime with small ρ_j and using the facts that $x_m = -x_{M-m+1}$ for $m \in \{1, \dots, M\}$, and $|\ell - 1| - |\ell - M| = 2\ell - M - 1$ since always $M \geq \ell$ and $\ell \geq 1$, so $|\ell - 1| = \ell - 1$ and $|\ell - M| = M - \ell$ and therefore $x_\ell = (2\ell - M - 1)a$ for $\ell \in \{1, \dots, M\}$, we can drive the conditional mean of the hard decisions as follow.

$$\begin{aligned} \mathbb{E}[\text{Re}(V_j)|X = x_\ell] &\approx \left(\frac{1}{2} - \frac{(2|\ell - 1| - 1)\rho_j}{\sqrt{2\pi}} \right) x_1 \\ &+ \sum_{m=2}^{M-1} \frac{2\rho_j}{\sqrt{2\pi}} x_m + \left(\frac{1}{2} - \frac{(2|\ell - M| - 1)\rho_j}{\sqrt{2\pi}} \right) x_M \\ &= \left(\frac{2(2\ell - M - 1)\rho_j}{\sqrt{2\pi}} \right) x_M \\ &= \left(\frac{2(M - 1)\rho_j}{\sqrt{2\pi}} \right) x_\ell \end{aligned} \quad (2.116)$$

For computing the variance of hard decisions we use the fact that $x_1^2 = (M - 1)^2 a^2$ and all the terms with ρ_j or ρ_j^2 are discarded since the $\rho_j \rightarrow 0$ in a low per-node SNR regime. Therefore, the variance of hard decisions would be calculated as

$$\begin{aligned} \text{var}[\text{Re}(V_j)|X = x_\ell] &= \mathbb{E}[\text{Re}(V_j)^2|X = x_\ell] - (\mathbb{E}[\text{Re}(V_j)|X = x_\ell])^2 \\ &\approx 2 \left(\frac{1}{2} - \frac{(2|\ell - 1| - 1)\rho_j}{\sqrt{2\pi}} \right) x_1^2 \\ &+ 2 \sum_{m=2}^{M/2-1} \frac{2\rho_j}{\sqrt{2\pi}} x_m^2 - \left(\frac{2(M - 1)\rho_j}{\sqrt{2\pi}} \right)^2 x_\ell^2 \\ &\approx 2(M - 1)^2 a^2 \end{aligned} \quad (2.117)$$

Following the same procedures for M -PAM, we derive the conditional mean and variance of hard decisions for M^2 -QAM. First, we derive the conditional mean of M^2 -QAM hard decisions for in-phase and quadrature components as

$$\mathbb{E}[\text{Re}(V_j)|X = x_\ell] = \mathbb{E}[\text{Im}(V_j)|X = x_\ell] = \left(\frac{2(M-1)\rho_j}{\sqrt{2\pi}} \right) x_\ell \quad (2.118)$$

since the statistics of in-phase and quadrature components are the same. Second, the conditional variance of M^2 -QAM hard decisions in the low per-node SNR regime can be calculated as

$$\text{var}[\text{Re}(V_j)|X = x_\ell] = \text{var}[\text{Im}(V_j)|X = x_\ell] \approx 2(M-1)^2 a^2 \quad (2.119)$$

The only difference here with the M -PAM is a 2 multiplier which is the result of having $X = X_I + jX_Q$ in M^2 -QAM. These results allow us to compute the conditional mean and variance of the pseudo-beamformer output with M^2 -QAM hard decisions. The conditional mean can be computed as

$$\begin{aligned} \mathbb{E}[Y_{pbf}|X = x_\ell] &= \alpha \sum_{j \in \mathcal{P}} |h_j| \mathbb{E}[\text{Re}(V_j)|X = x_\ell] + j \alpha \sum_{j \in \mathcal{P}} |h_j| \mathbb{E}[\text{Im}(V_j)|X = x_\ell] \\ &= \alpha \sum_{j \in \mathcal{P}} |h_j| \mathbb{E}[\text{Re}(V_j)|X = x_\ell] (1 + j) \\ &= \alpha \sum_{j \in \mathcal{P}} |h_j| \left(\frac{2(M-1)\rho_j}{\sqrt{2\pi}} \right) x_\ell (1 + j) \end{aligned} \quad (2.120)$$

by replacing the ρ_j from $\rho_j^2 := \frac{|h_j|^2 a^2}{N_0/2}$ we have

$$\begin{aligned} \mathbb{E}[Y_{pbf}|X = x_\ell] &= \alpha \sum_{j \in \mathcal{P}} \left(\frac{2(M-1)|h_j|^2 a}{\sqrt{2\pi N_0/2}} \right) x_\ell (1 + j) \\ &= \frac{\alpha 2(M-1)a x_\ell}{\sqrt{\pi N_0}} (1 + j) \sum_{j \in \mathcal{P}} |h_j|^2 \end{aligned} \quad (2.121)$$

using the fact that $\sum_{j \in \mathcal{P}} |h_j|^2 = \|h\|^2$, we get

$$\mathbb{E}[Y_{pbf}|X = x_\ell] = \frac{2\alpha(M-1)a\|h\|^2}{\sqrt{\pi N_0}} x_\ell (1 + j) \quad (2.122)$$

Similarly, the conditional variance of the pseudo-beamformer output with M^2 -QAM hard decisions in the low per-node SNR regime can be computed as

$$\begin{aligned}
\text{var}[Y_{pbf}|X = x_\ell] &= \text{var} \left[\alpha \sum_{j \in \mathcal{P}} |h_j| \text{Re}(V_j) \middle| X = x_\ell \right] + \text{var} \left[\alpha \sum_{j \in \mathcal{P}} |h_j| \text{Im}(V_j) \middle| X = x_\ell \right] \\
&= 2\alpha^2 \sum_{j \in \mathcal{P}} |h_j|^2 \text{var}[\text{Re}(V_j)|X = x_\ell] \\
&= 2\alpha^2 \sum_{j \in \mathcal{P}} |h_j|^2 (M-1)^2 a^2 \\
&= 2\alpha^2 (M-1)^2 a^2 \sum_{j \in \mathcal{P}} |h_j|^2
\end{aligned} \tag{2.123}$$

It follows from the fact that $\text{var}(x + jy) = \text{var}(x) + \text{var}(y)$. Therefore we would have

$$\text{var}[Y_{pbf}|X = x_\ell] = 2\alpha^2 (M-1)^2 a^2 \|h\|^2 \tag{2.124}$$

Now we can calculate the SNR_{pbf} as

$$\begin{aligned}
\text{SNR}_{pbf} &= \frac{|\text{E}[Y_{pbf}|X = x_\ell]|^2}{\text{var}[Y_{pbf}|X = x_\ell]} \\
&= \frac{4\alpha^2 (M-1)^2 a^2 \|h\|^4 |x_\ell|^2 |1 + j|^2}{2\alpha^2 (M-1)^2 a^2 \|h\|^2 \pi N_0}
\end{aligned} \tag{2.125}$$

By replacing the $|x_\ell|^2 = 2\mathcal{E}_s$ and using the facts that $\lim_{N \rightarrow \infty} \frac{\|h\|^2}{N} = 2\lambda$ and $\mathcal{E}_s = \frac{\mathcal{E}_s^{(1)}}{N}$ we would have

$$\text{SNR}_{pbf} \rightarrow \frac{2\|h\|^2 2\mathcal{E}_s 2}{\pi N_0} = \frac{8\lambda \mathcal{E}_s^{(1)}}{\pi N_0} \tag{2.126}$$

Therefore, with M^2 -QAM and for all M , we have

$$\text{SNR}_{pbf}^{M^2\text{-QAM}} \approx \frac{2}{\pi} \text{SNR}_{bf}^{M^2\text{-QAM}} \tag{2.127}$$

2.7.3.4 Pseudo-Beamforming: Noisy Channel Estimation

To model the effect of channel estimation error on the decision variable at an individual receiver, we first define the perfect and noisy channel estimate, respectively,

as follow

$$\begin{aligned} h_j &= |h_j|e^{j\theta} \\ \hat{h}_j &= |\hat{h}_j|e^{j\hat{\theta}} \end{aligned} \quad (2.128)$$

we also have $\hat{h} = h + \tilde{h}$, where $\tilde{h} \sim \mathcal{CN}(0, 2\delta)$ is the channel estimation error. To compute the conditional mean and variance of the pseudo-beamformer output with noisy channel estimation and computing the SNR afterwards, we have to compute the conditional mean and variance of the hard decisions for M^2 -QAM modulation. For this purpose, we first have to express the decision variable of the receivers for cases with and without perfect channel estimation. For the case with perfect channel estimation, decision variable would be as follow

$$\begin{aligned} U_j &= \frac{1}{h_j}(h_j X + W_j) \\ &= X + \frac{W_j}{h_j} \end{aligned} \quad (2.129)$$

and with estimation error it would be as

$$\begin{aligned} U_{j_e} &= \frac{1}{\hat{h}_j}(h_j X + W_j) \\ &= \frac{h_j}{\hat{h}_j} X + \frac{W_j}{\hat{h}_j} \end{aligned} \quad (2.130)$$

where $y_j = h_j X + W_j$ is the received signal at the receiver, and U_j is the decision variable obtained by compensation of channel effect on the received signal, based on the estimation of channel by the receiver. In order to find the transition probabilities we have to calculate the mean and variance of the decision variable at the receiver. For the case that has no channel estimation error we can obtain the mean as

$$\begin{aligned} \mathbb{E}[U_j|X = x_\ell] &= \mathbb{E}\left[X + \frac{W_j}{h_j} \middle| X = x_\ell\right] \\ &= X + \frac{1}{h_j} \mathbb{E}[W_j|X = x_\ell] = X \end{aligned} \quad (2.131)$$

where we used the fact that W_j and h_j are independent and $E[W_j] = 0$. For variance calculation we would have

$$\begin{aligned}\text{var}[U_j|X = x_\ell] &= \text{var}\left[X + \frac{W_j}{h_j} \middle| X = x_\ell\right] \\ &= \frac{1}{|h_j|^2} \text{var}[W_j|X = x_\ell] = \frac{N_0}{2|h_j|^2}\end{aligned}\quad (2.132)$$

since X is independent of W_j and h_j , and the channel h_j is considered constant during transmission time-slot. Using the equations (2.131) and (2.132) we can obtain the transition probabilities of $p_{m,\ell} := \text{Prob}(\text{decide } V_j = x_m | X = x_\ell)$ for M^2 -QAM modulation as stated in [46] as follow

$$\begin{aligned}p_{m,\ell} &= Q\left(\frac{(2|\ell - m| - 1)a}{\sqrt{\frac{N_0}{2|h_j|^2}}}\right) - Q\left(\frac{(2|\ell - m| + 1)a}{\sqrt{\frac{N_0}{2|h_j|^2}}}\right) \\ &= Q((2|\ell - m| - 1)\rho_j) - Q((2|\ell - m| + 1)\rho_j)\end{aligned}\quad (2.133)$$

where $\rho_j = \frac{|h_j|a}{\sqrt{N_0/2}}$ is the signal to noise ratio at the receiver j . Here the transmitted signal is $X = x_\ell = 2\ell - M - 1$ and the detected signal is assumed to be $V_j = x_m = 2m - M - 1$.

Now, if we consider channel estimation error at the receiver, the mean of decision variable would be obtained by following terms

$$\begin{aligned}E[U_{je}|X = x_\ell] &= E\left[\frac{h_j}{\hat{h}_j}X + \frac{W_j}{\hat{h}_j} \middle| X = x_\ell\right] \\ &= h_j X E\left[\frac{1}{\hat{h}_j} \middle| X = x_\ell\right].\end{aligned}\quad (2.134)$$

In order to obtain the $E[\frac{1}{\hat{h}_j} | X = x_\ell]$, we have to use the following equation about the mean of inverse of random variable

$$E\left[\frac{1}{X}\right] = \frac{1}{E[X]} + \frac{\text{var}[X]}{E[X]^3}.\quad (2.135)$$

Therefore, by applying the above method in (2.134) we get

$$E[U_{je}|X = x_\ell] = h_j X \left(\frac{1}{E[\hat{h}_j]} + \frac{\text{var}[\hat{h}_j]}{E[\hat{h}_j]^3} \right),\quad (2.136)$$

where the mean and variance of channel estimation \hat{h}_j is

$$\mathbb{E}[\hat{h}_j] = \mathbb{E}[h_j] + \mathbb{E}[\tilde{h}_j] = h_j \quad (2.137)$$

$$\text{var}[\hat{h}_j] = \text{var}[h_j] + \text{var}[\tilde{h}_j] = 2\delta. \quad (2.138)$$

By replacing (2.137) and (2.138) in equation (2.136) we would have

$$\mathbb{E}[U_{je}|X = x_\ell] = X \left(1 + \frac{2\delta}{|h_j|^2} \right). \quad (2.139)$$

Since phase of the received signal in M -PAM modulation (as in in-phase or quadrature part of M^2 -QAM) does not have effect in final decision and on error probability calculation, as stated here [50], we can use h and $|h|$ interchangeably.

We now have to calculate the variance of decision variable in order to be able to obtain the transition probabilities when there is channel estimation error. To obtain variance we have to calculate

$$\begin{aligned} \text{var}[U_{je}|X = x_\ell] &= \text{var}\left[\frac{h_j}{\hat{h}_j}X + \frac{W_j}{\hat{h}_j}|X = x_\ell\right] \\ &= |h_j|^2|X|^2\text{var}\left[\frac{1}{\hat{h}_j}|X = x_\ell\right] + \text{var}\left[\frac{W_j}{\hat{h}_j}|X = x_\ell\right] \\ &= |h_j|^2|X|^2\text{var}\left[\frac{1}{\hat{h}_j}|X = x_\ell\right] + \frac{N_0}{2}\mathbb{E}\left[\frac{1}{|\hat{h}_j|^2}|X = x_\ell\right]. \end{aligned} \quad (2.140)$$

Now we have to obtain the $\text{var}\left[\frac{1}{\hat{h}_j}\right]$ and $\mathbb{E}\left[\frac{1}{\hat{h}_j^2}\right]$ to be able to calculate the variance of decision variable. To do so, we use the equation below to obtain the variance of the inverse of a random variable

$$\text{var}\left[\frac{1}{X}\right] = \frac{\text{var}[X]}{\mathbb{E}[X]^4}. \quad (2.141)$$

We also have to calculate the mean and variance of the square of channel estimation

$$\mathbb{E}[\hat{h}_j^2] = \mathbb{E}[h_j^2 + \tilde{h}_j^2 + 2h_j\tilde{h}_j] = |h_j|^2 + 2\delta. \quad (2.142)$$

$$\text{var}[\hat{h}_j^2] = \text{var}[h_j^2 + \tilde{h}_j^2 + 2h_j\tilde{h}_j] = \mathbb{E}[|\tilde{h}_j|^4] - 4\delta^2 + 8|h_j|^2\delta. \quad (2.143)$$

Using the equations in (2.135, 2.141, 2.142 and 2.143) and replacing them in (2.140) we get

$$\text{var}[U_{je}|X = x_\ell] = |X|^2 \frac{2\delta}{|h_j|^2} + \frac{N_0}{2} \left(\frac{1}{|h_j|^2 + 2\delta} + \frac{\text{E}[|\tilde{h}_j|^4] - 4\delta^2 + 8|h_j|^2\delta}{(|h_j|^2 + 2\delta)^3} \right). \quad (2.144)$$

By having mean and variance of decision variable with channel estimation error we can obtain the transition probabilities as

$$p_{m,\ell} = Q \left(\frac{(2|\ell - m| - 1)a \left(1 + \frac{2\delta}{|h_j|^2}\right)}{\sqrt{|X|^2 \frac{2\delta}{|h_j|^2} + \frac{N_0}{2} \left(\frac{1}{|h_j|^2 + 2\delta} + \frac{\text{E}[|\tilde{h}_j|^4] - 4\delta^2 + 8|h_j|^2\delta}{(|h_j|^2 + 2\delta)^3} \right)}} \right) - Q \left(\frac{(2|\ell - m| + 1)a \left(1 + \frac{2\delta}{|h_j|^2}\right)}{\sqrt{|X|^2 \frac{2\delta}{|h_j|^2} + \frac{N_0}{2} \left(\frac{1}{|h_j|^2 + 2\delta} + \frac{\text{E}[|\tilde{h}_j|^4] - 4\delta^2 + 8|h_j|^2\delta}{(|h_j|^2 + 2\delta)^3} \right)}} \right), \quad (2.145)$$

which in this equation we can replace the $|X^2|$ with $2\mathcal{E}_s$. Now by having the transition probabilities we can compute the mean and variance of hard decisions at the receiver. Before that, to make the calculation simpler we define the signal to noise ratio at the receiver j in case of having channel estimation error $\hat{\rho}_j$ as

$$\hat{\rho}_j = \frac{a \left(1 + \frac{2\delta}{|h_j|^2}\right)}{\sqrt{2\mathcal{E}_s \frac{2\delta}{|h_j|^2} + \frac{N_0}{2} \left(\frac{1}{|h_j|^2 + 2\delta} + \frac{\text{E}[|\tilde{h}_j|^4] - 4\delta^2 + 8|h_j|^2\delta}{(|h_j|^2 + 2\delta)^3} \right)}}. \quad (2.146)$$

We also can replace the variance of channel estimation error 2δ with $\frac{N_0}{P\mathcal{E}_s}$. Using the same proof as in case with perfect channel estimation, we can get the mean and variance of hard decisions as

$$\text{E}[\text{Re}(V_j)|X = x_\ell] \approx \left(\frac{2(M-1)\hat{\rho}_j}{\sqrt{2\pi}} \right) x_\ell \quad (2.147)$$

$$\text{var}[\text{Re}(V_j)|X = x_\ell] \approx 2(M-1)^2 a^2, \quad (2.148)$$

To obtain the SNR at the receiver with channel estimation error, first we have to obtain the mean and variance of pseudo-beamformer combiner output as stated in

(2.112), but this time we have to use the magnitude of channel estimation with error.

$$\begin{aligned} Y_{pbfe} \equiv Y_i &= \sum_{j \in \mathcal{P}} \sqrt{\rho_i} V_j = \alpha \sum_{j \in \mathcal{P}} |\hat{h}_j| V_j \\ &= \alpha \sum_{j \in \mathcal{P}} |\hat{h}_j| (\text{Re}(V_j) + j \text{Im}(V_j)). \end{aligned} \quad (2.149)$$

We then can compute the mean and variance of pseudo-beamformer output just like the ones in (2.120 and 2.123) but this time we have magnitude of channel estimation error and corresponding SNR at the receiver. So, the mean can be calculated as

$$\mathbb{E}[Y_{pbfe}|X = x_\ell] = \alpha \sum_{j \in \mathcal{P}} |\hat{h}_j| \left(\frac{2(M-1)\hat{\rho}_j}{\sqrt{2\pi}} \right) x_\ell (1 + j), \quad (2.150)$$

and variance as

$$\text{var}[Y_{pbfe}|X = x_\ell] = 2\alpha^2(M-1)^2 a^2 \sum_{j \in \mathcal{P}} |\hat{h}_j|^2. \quad (2.151)$$

However, due to complexity of mathematical proof of these equations, we use analytical solutions to calculate the SNR for large number of receivers and in low per-node SNR regime. So, as the result we have the SNR_{pbfe} as

$$\begin{aligned} \text{SNR}_{pbfe} &= \frac{|\mathbb{E}[Y_{pbfe}|X = x_\ell]|^2}{\text{var}[Y_{pbfe}|X = x_\ell]} \\ &= \frac{4\alpha^2(M-1)^2 a^2 |x_\ell|^2 |1 + j|^2 \sum_{j \in \mathcal{P}} |\hat{h}_j| \frac{\hat{\rho}_j}{a}}{2\alpha^2(M-1)^2 a^2 \pi N_0 \sum_{j \in \mathcal{P}} |\hat{h}_j|^2} \\ &= \frac{4|x_\ell|^2 \sum_{j \in \mathcal{P}} |\hat{h}_j| \frac{\hat{\rho}_j}{a}}{\pi N_0 \sum_{j \in \mathcal{P}} |\hat{h}_j|^2} \end{aligned} \quad (2.152)$$

By replacing the $|x_\ell|^2 = 2\mathcal{E}_s$ and using the facts that $\lim_{N \rightarrow \infty} \frac{\|\mathbf{h}\|^2}{N} = 2\lambda$, $\mathcal{E}_s = \frac{\mathcal{E}_s^{(1)}}{N}$, $P = P^{(1)}N$ and $2\delta = \frac{N_0}{P\mathcal{E}_s}$ we would have

$$\text{SNR}_{pbfe} \rightarrow \frac{8\lambda \mathcal{E}_s^{(1)}}{\pi N_0 \left(1 + \frac{N_0}{4\lambda P^{(1)} \mathcal{E}_s^{(1)}}\right)} \quad (2.153)$$

Therefore, with M^2 -QAM and for all M , we have

$$\text{SNR}_{pbfe}^{M^2\text{-QAM}} \approx \frac{2}{\pi} \text{SNR}_{bfe}^{M^2\text{-QAM}} \quad (2.154)$$

Using the results in (2.126) and (2.153) we can compute the penalty of channel estimation error in an pseudo-beamforming as $N \rightarrow \infty$ as

$$\mathcal{P}_{pbf} = \frac{\text{SNR}_{pbf}}{\text{SNR}_{pbf e}} \rightarrow 1 + \frac{N_0}{4\lambda P^{(1)} \mathcal{E}_s^{(1)}}. \quad (2.155)$$

2.7.4 Numerical Results

The simulation results of this section are presented here. In this simulation a 16-QAM modulation is chosen for the forward link between single transmitter and the receive cluster. The number of receive nodes inside the cluster are $N = [10 \ 20 \ 40 \ 80 \ 160 \ 320 \ 640 \ 1280 \ 2560 \ 5120 \ 7680]$. The number of iterations for each channel/noise realization is chosen to be 1000 and the per-symbol transmit energy with one receiver $\mathcal{E}_s^{(1)} = 10$ and training signal length with one receiver $P^{(1)} = 1$. The magnitude of each symbol is $a = \sqrt{2}$ and the number of payload symbols per block is $Q = 100$. The total noise power $N_0 = 15$ and channel variance in real and imaginary dimension is $\lambda = 2$.

Figure 2.5 shows the comparison of the SNRs between ideal receive beamforming and pseudo-beamforming each with and without channel estimation error. The results from Figure 2.5 confirms our proofs that the ratio of the SNRs between ideal receive beamforming and pseudo-beamforming in both case of perfect and noisy channel estimation are equal to $\frac{2}{\pi}$ and the SNR in each case converges to the calculated limit for large N.

Figure 2.6 shows the comparison of the penalties between the ideal and pseudo beamformer. It can be seen that, the penalty term in both cases converges to the same number since the SNR ratios in each case, as shown in equation (2.43) for an ideal beamformer and (2.89) for a pseudo beamformer are the same.

Figure 2.7 shows the mean and variance of the hard decisions when there is channel estimation error. The results from the figure show that, the calculated mean of the hard decisions closely follows the numerical results as the number of N gets large.

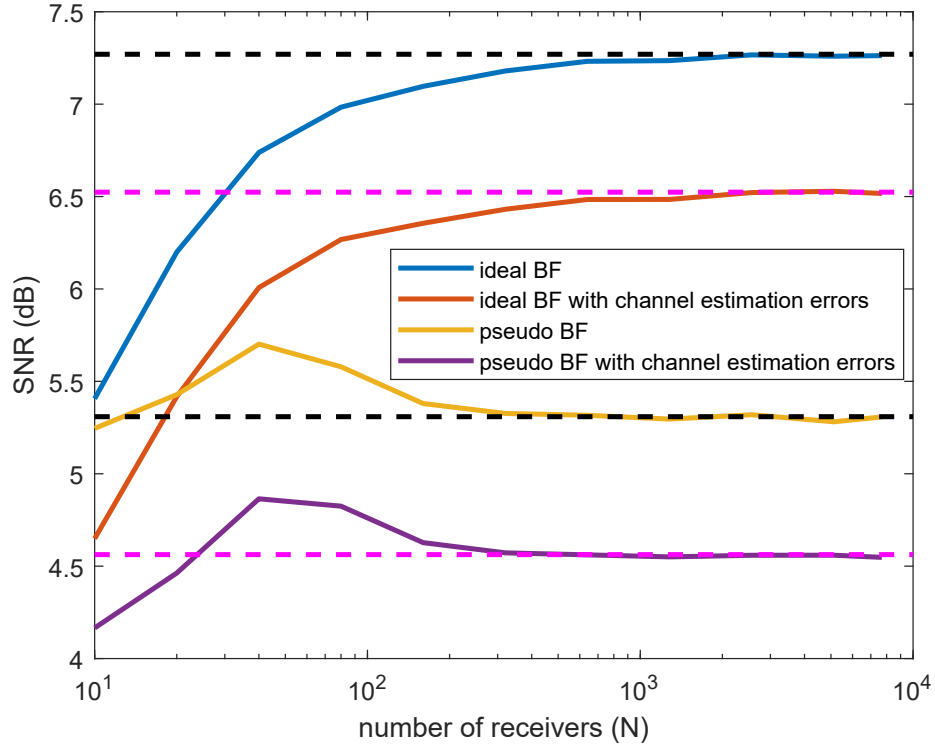


Figure 2.5: Comparison of the SNRs between ideal receive beamforming and pseudo-beamforming with and without channel estimation error in 16-QAM modulation. The dotted lines are the calculated SNRs for large N in each scenario.

Also, the variance of the hard decisions approaches to the upper bound obtained from the theoretical results for large N .

2.7.5 Conclusion

Like previous section with M -PSK modulation, in this section we used theoretical calculations, asymptotic analysis and numerical results from simulation, to obtain and characterize the effect of imperfect channel estimation in a distributed reception system this time with M^2 -QAM modulation. Using theoretical computations, we derived closed-form expressions for the SNR of both ideal receive beamforming and pseudo-beamforming. As it was expected, the results of our analysis show that chan-

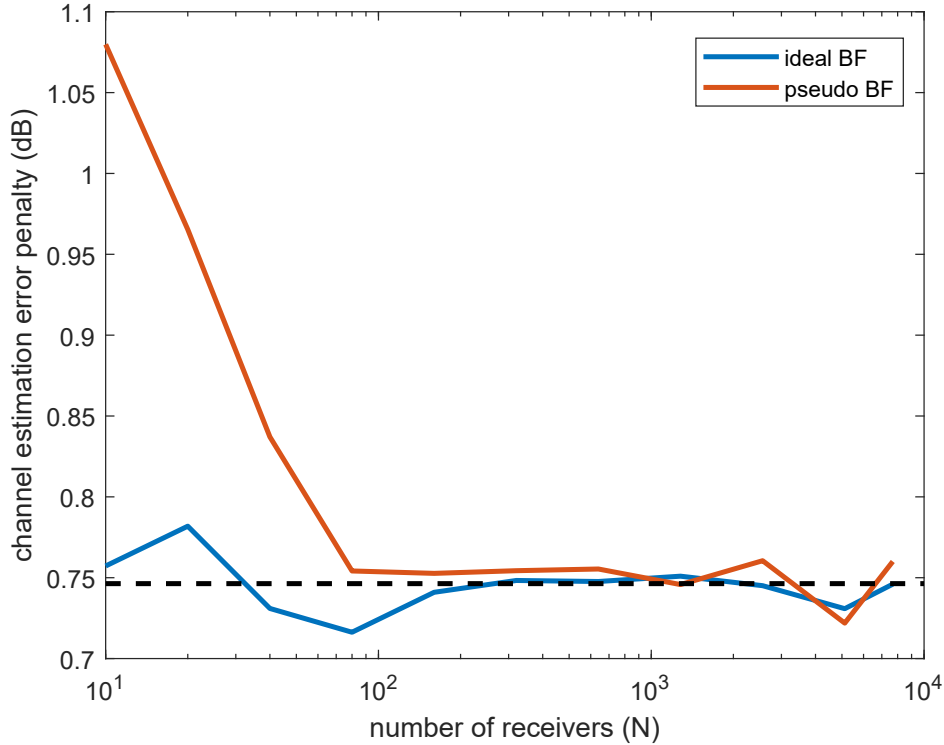


Figure 2.6: Comparison of the penalties between the ideal and pseudo beamformer in 16-QAM modulation.

nel estimation error in 16-QAM modulation degrades the performance of distributed reception with both ideal and pseudo-beamforming techniques by almost 0.75 dB compared to 1.38 dB in QPSK modulation. Just like the previous case with M -PSK modulation, the SNR ratio between ideal receive beamforming and pseudo-beamforming does not depend on the amount of channel estimation error and are identical to the SNR ratios with no channel estimation error. So, our analysis shows, channel estimation error causes the same amounts of performance degradation in ideal beamforming and pseudo-beamforming systems despite the fact that the channel estimation errors manifests themselves quite differently in both systems. Also, simulation results confirmed our calculations for the mean and variance of hard decisions with channel estimation error, and also our results for the penalty term in both ideal and pseudo-

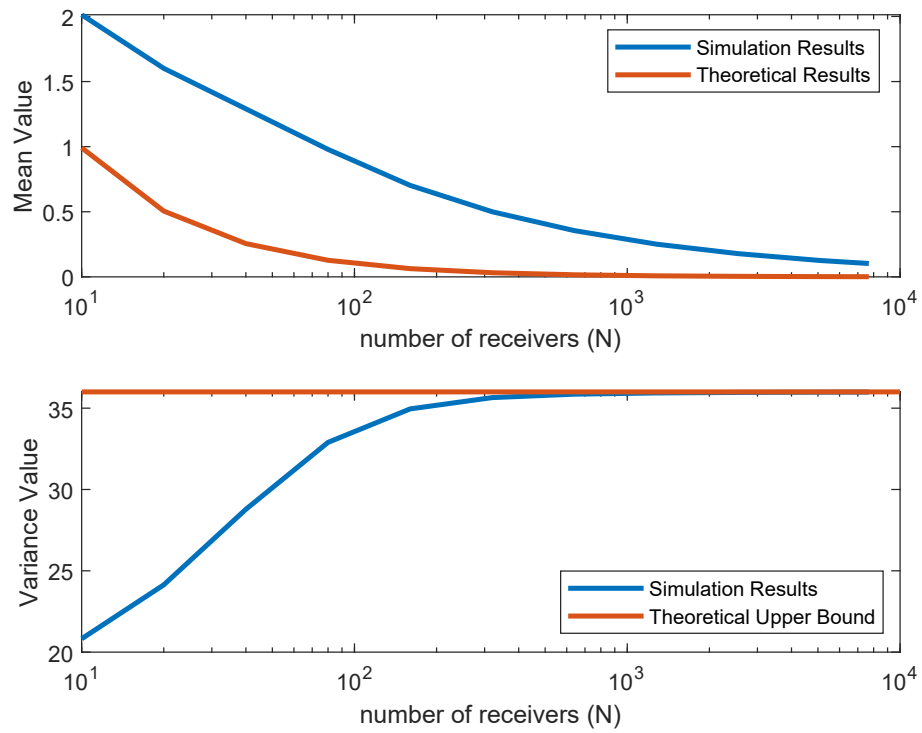


Figure 2.7: Mean and variance of the hard decisions when there is channel estimation error in 16-QAM modulation.

beamforming techniques.

Chapter 3

Oscillator Modeling For Improved Phase Synchronization

3.1 Introduction

Characterization and modeling of clock oscillator stability is important for many applications requiring an accurate time and/or frequency reference. This chapter focuses on the application area of cooperative communication protocols [51–54], in which two or more sources transmit simultaneously in a single sub-channel. A key challenge is maintaining synchronization between transmitters to pico-second accuracy, which in turn requires characterizing the stability of the independent frequency references for each transmitter.

Oscillator stability has been traditionally characterized by the Allan variance and multistate stochastic models [55–57] which were originally developed for high precision, high cost sources such as atomic clocks. Knowledge of model parameters allows development of tracking and prediction techniques (e.g. based on the Kalman filter) which enable accurate prediction of and compensation for oscillator drift.

Difficulty arises in applying these techniques to low cost, moderate precision crystal oscillators used in applications such as software-defined radio (SDR), as significant

deviations in measured phase noise from the prediction of models in [56, 57] are observed for some oscillators. For the novel contributions of this work, we present measured phase noise data for a range of crystal oscillators, propose an alternative phase noise modeling strategy, and show improved phase tracking and prediction performance resulting from the proposed model.

3.2 Background

In this section a general definition of cooperative communication and how these types of networks work is given along with an example of phase realignment of transmitters. Also, the phase noise of the software-defined radio output is shown and analyzed.

3.2.1 Cooperative communication

In cooperative communication protocols, two or more sources transmit simultaneously in the same sub-channel [51–54].

Figure 3.1 shows a conceptual view of the beamforming principle, in which the individual transmitter carrier waveform phases are adjusted to arrive in-phase at the receive antenna. Compared to orthogonal transmit cooperation, these protocols offer the potential for improved power efficiency since carrier signals from each source arrive in phase and constructively combine at the intended destination. The key challenge to realizing these benefits is maintaining strict synchronization between transmitters: Phase offset must be less than a fraction of the carrier waveform, of order picoseconds for commonly used SDR frequencies.

Figure 3.2 from [52] shows the need for continuously updated phase realignment. This figure shows beamforming gain in a three-source system over time, with a gain of 0 dB corresponding to incoherent transmission and a theoretical maximum gain of 10 dB. At time $t = 0$ the oscillators are synchronized and gain of 10 dB is briefly observed,

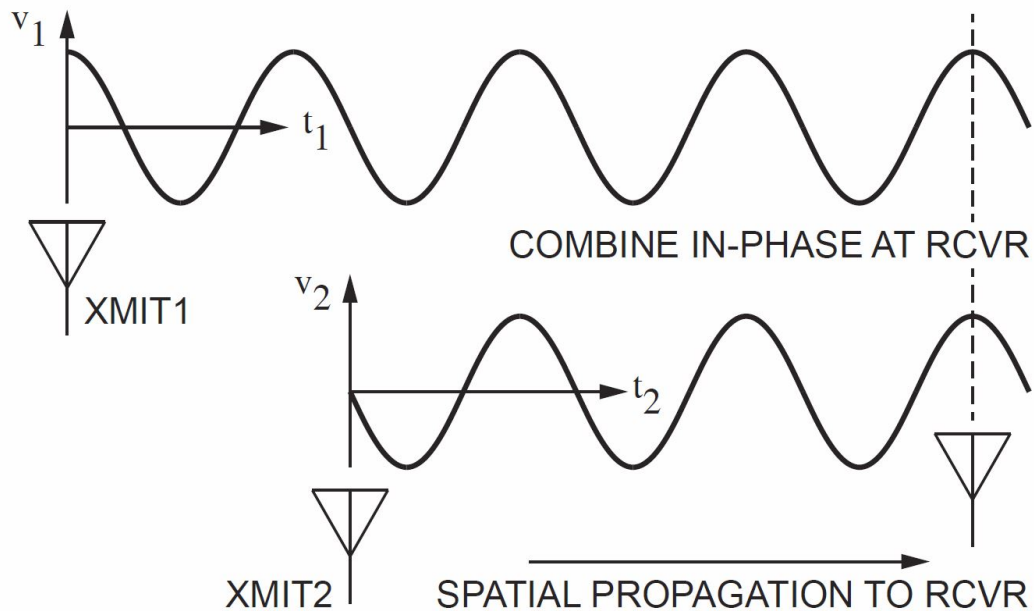


Figure 3.1: Conceptual beamforming.

but gain quickly drops near zero in less than 10 ms as the source oscillator phases drift out of phase alignment. Interrupting channel usage for phase measurement and realignment on a millisecond time scale would detract significantly from the achievable system data rate, adding an unacceptable overhead in data transmission.

To extend the amount of time available between necessary phase realignments, phase error prediction is also used. At $t = 50$ ms the oscillator phases are realigned, and based on the observed oscillator behavior, the phase error drift of each source oscillator is predicted and partially canceled. Due to unpredictable random drift, the observed beamforming gain decreases over time, in this case to approximately 9 dB by the next resynchronization at $t = 100$ ms. With prediction, the allowable time between phase realignment is extended to 50 ms in this example.

The following section describes sources of phase noise and oscillator drift for SDRs used in cooperative communication.

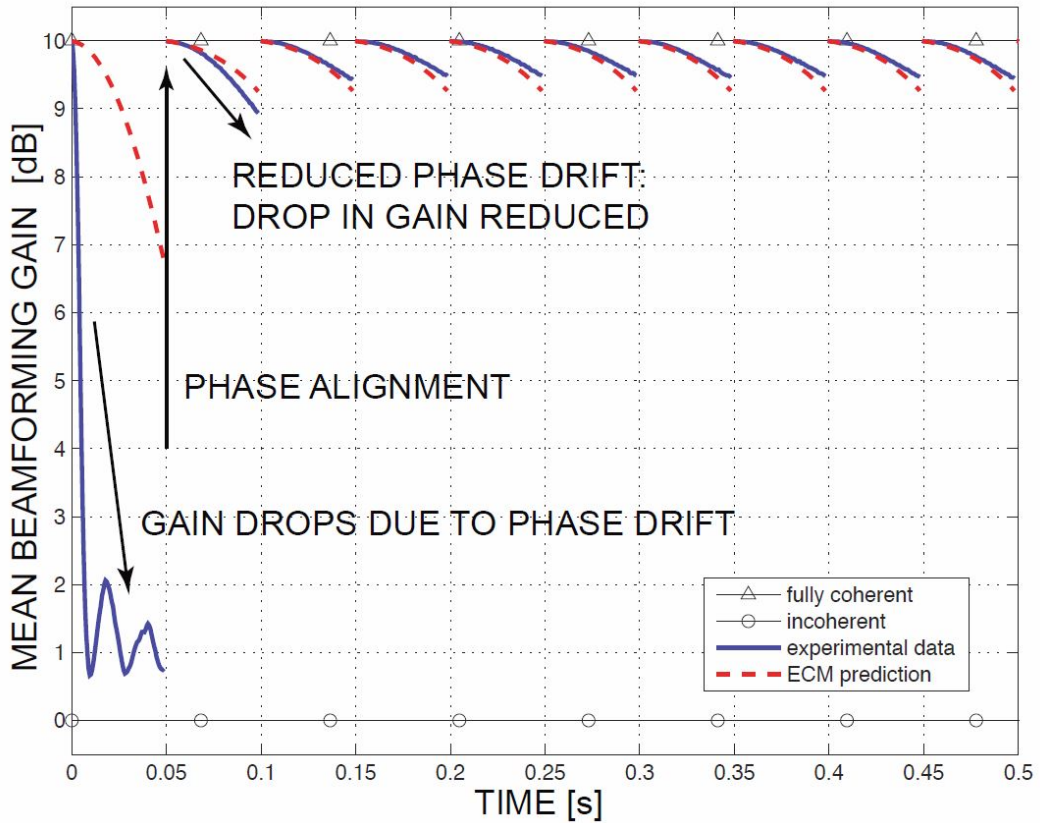


Figure 3.2: Need for clock resynchronization.

3.2.2 SDR output phase noise

Figure 3.3 shows a simplified block diagram of a software-defined radio as implemented in the USRP-2 [58] platform. Precise frequency reference is required for both the baseband digital-to-analog converter (DAC) functions (400 MS/s clock DAC-CLK) and the local oscillator (LO) synthesizer which upconverts the I/Q baseband data signals for transmitting at RF. In [58] the frequency reference is provided by a temperature compensated crystal oscillator (TCXO), which will influence the spectral characteristics of the RF output.

Figure 3.4 shows the measured phase noise of the USRP output when producing a continuous unmodulated 900MHz carrier. (All measurements in this work were

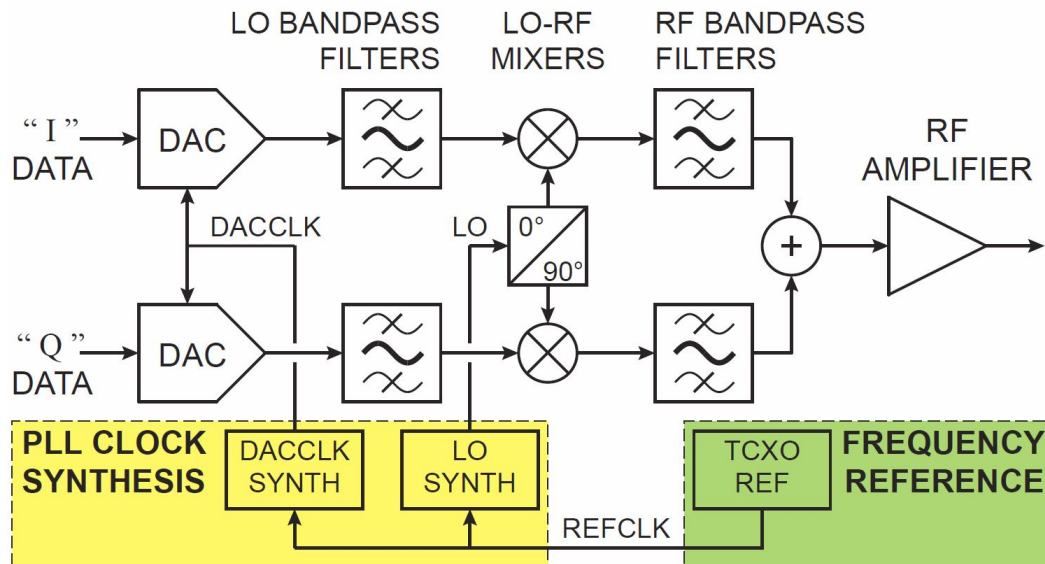


Figure 3.3: SDR simplified block diagram.

performed using the Keysight E5052B Signal Source Analyzer [59]). As described in [60,61], the output phase noise is a combination of contributions from the reference oscillator (green highlight) and the phase-locked loop (PLL) synthesizer (yellow). At offset frequencies above ≈ 10 kHz, noise power is dominated by the PLL synthesizers voltage-controlled oscillator (VCO) phase noise as well as spurs due to DAC quantization noise and nonlinearity. For synchronization purposes, we are concerned with oscillator drift at time scales of $\approx 100 \mu\text{s}$ and longer, which is determined by noise power at offset frequencies below 10 kHz. At offset frequencies < 10 kHz performance is dominated by the REF source, and shows two regions with

- -40 dB/decade slope corresponding to a $1/f^4$ noise power law for offset frequencies $f < 100$ Hz, and
- -20 dB/decade slope corresponding to a $1/f^2$ noise power law for offset frequencies $100 \text{ Hz} < f < 10 \text{ kHz}$.

The $1/f^4$ and $1/f^2$ noise power laws follow from a simple model for oscillator

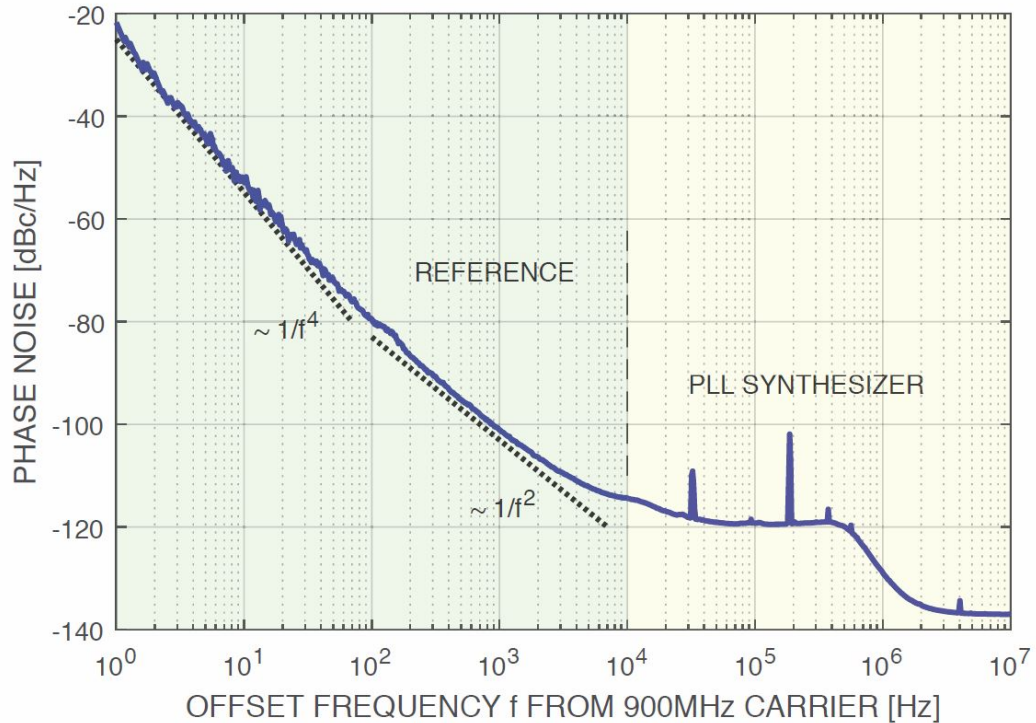


Figure 3.4: Measured phase noise of USRP carrier output.

phase noise, which will be briefly reviewed in the following section.

3.3 Oscillator Noise Modeling

In this section the two-state oscillator phase noise model would be described in details and the role of oscillator model in phase prediction is shown.

3.3.1 Two-state oscillator phase noise model

In [56], the output of a sinusoidal oscillator is modeled as

$$u(t) = U_0 \sin(2\pi\nu_0 t + \varphi(t)) \quad (3.1)$$

in which ν_0 is the nominal frequency, $\varphi(t)$ is an error term due to oscillator phase noise, and U_0 is the oscillator amplitude. Any effects due to variation in U_0 are assumed to be negligible since the analysis considers phase noise only; for this reason the analysis also applies to non-sinusoidal oscillators such as the frequency reference used in [58].

In (3.1) the error $\varphi(t)$ has units of radians of phase. This error can be expressed in terms of time error $x(t)$ by normalizing to the nominal radian frequency

$$x(t) = \frac{\varphi(t)}{2\pi\nu_0} \quad (3.2)$$

with which (3.1) becomes

$$u(t) = U_0 \sin 2\pi\nu_0(t + x(t)) \quad (3.3)$$

In [56] it is shown that the output noise process can be modeled by a simplified two-state system shown in graphical form in Figure 3.5 and expressed mathematically as

$$x(t) = x_1(t) = \int_0^t (x_2(t) + \xi_1(t))dt \quad (3.4)$$

$$x_2(t) = \int_0^t \xi_2(t)dt \quad (3.5)$$

in which $\xi_1(t)$ and $\xi_2(t)$ are noise processes. As a time error, x_1 has units of seconds [s]; due to the time derivative to \dot{x}_1 , x_2 and $\xi_1(t)$ are dimensionless. Similarly, the units of $\xi_2(t)$ are [s⁻¹].

Expressing the system of Figure 3.5 in state space form gives:

$$\underbrace{\begin{bmatrix} \dot{x}_1 \\ \dot{x}_2 \end{bmatrix}}_{\dot{X}} = \underbrace{\begin{bmatrix} 0 & 1 \\ 0 & 0 \end{bmatrix}}_A \underbrace{\begin{bmatrix} x_1 \\ x_2 \end{bmatrix}}_{X(t)} + \underbrace{\begin{bmatrix} \xi_1 \\ \xi_2 \end{bmatrix}}_{\xi(t)} \quad (3.6)$$

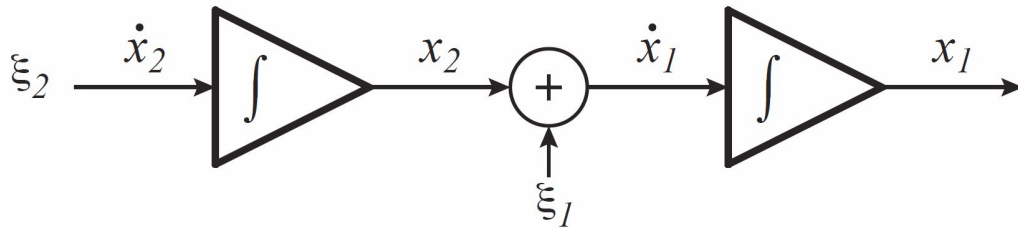


Figure 3.5: 2-state clock noise model.

As in [56], we model the process noise terms $\xi_1(t)$ and $\xi_2(t)$ as zero mean independent Gaussian random processes. Since these processes are independent, the autocorrelation is

$$\mathbf{R}_{\xi,\xi}(\tau) = \mathbf{E} [\xi(t)\xi^T(t + \tau)] = \underbrace{\begin{bmatrix} q_1 & 0 \\ 0 & q_2 \end{bmatrix}}_{\mathbf{Q}} \delta(\tau) \quad (3.7)$$

where $\delta(\tau)$ is the Dirac delta function.

From (3.4) and (3.5) with the noise model of (3.6), we expect the power spectral density to exhibit a $1/f^2$ region corresponding to a Wiener process from the integration of $\xi_1(t)$, and a $1/f^4$ region corresponding to the integration of $x_2(t)$, which is itself a Wiener process as the integral of $\xi_2(t)$. Table 3.1 lists all reference sources evaluated for this work. As an example, measured data from CS4 at a frequency of $\nu_0 = 40\text{MHz}$ in Figure 3.6 shows a phase noise plot $\mathcal{L}(f)$ with approximate $1/f^4$ and $1/f^2$ characteristics until reaching the noise floor of the measurement.

In accordance with [55] we can model the single-sided spectral density of phase fluctuations as

$$S_{\Phi}(f) = 2\mathcal{L}(f) = \frac{h_{-2}\nu_0^2}{f^4} + \frac{h_0\nu_0^2}{f^2} \quad (3.8)$$

with best-fit values to the measured $\mathcal{L}(f)$ for parameters h_{-2} and h_0 as shown in Figure 3.6. Note that there are also $1/f$ and $1/f^3$ regions corresponding to flicker

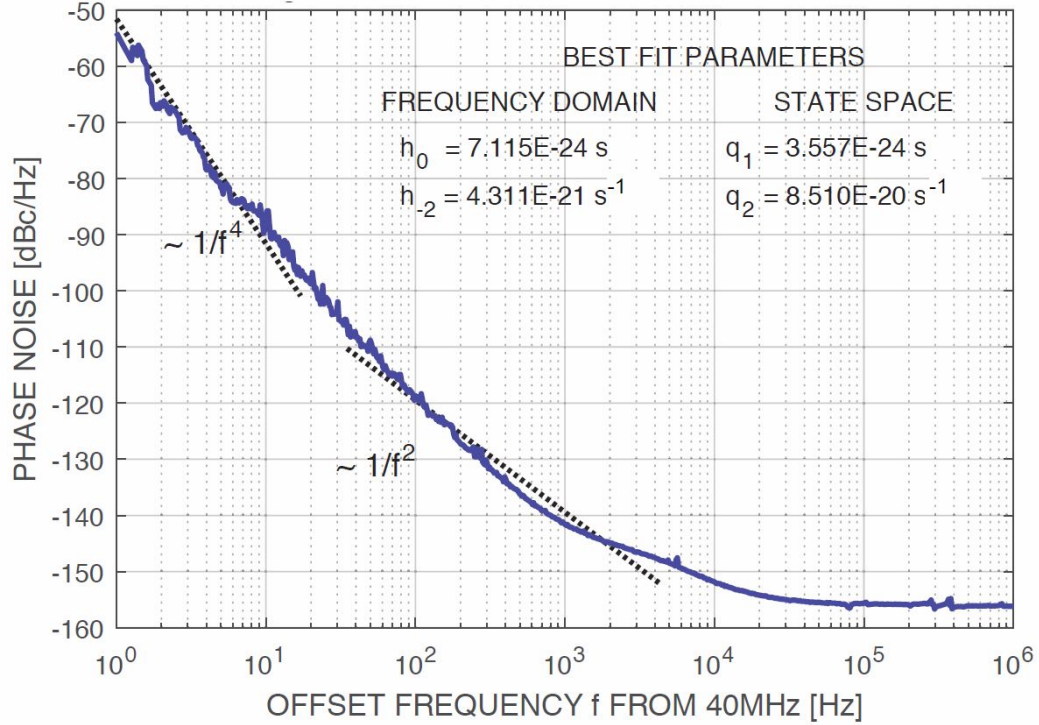


Figure 3.6: Measured phase noise for oscillator CS4 with 2-state model fit.

($1/f$) and integrated flicker ($1/f^3$) noise respectively. For simplicity these models were not incorporated in this work, but could be taken into account for a more accurate description of phase noise.

To fully describe the system of Figure 3.5, we need numerical values for q_1 and q_2 which describe the random processes. In [56, 57] these are obtained from the Allan variance $\sigma_y^2(\tau)$, a commonly used measurement for extremely stable clock sources [55]. For the two-state model of Figure 3.5, [56, 57] shows that the Allan variance will take the form

$$\sigma_y^2(\tau) = \frac{q_1}{\tau} + \frac{q_2\tau}{3} \quad (3.9)$$

The Allan variance (time domain) can be related to the phase noise (frequency

Table 3.1: Clock sources evaluated in this work

Source	Type	Brand	ν_0 [MHz]
CS1	VCXO	A	40
CS2	VCXO	A	100
CS3	XO	B	80
CS4	XO	B	40
CS5	OCXO	C	40
CS6	TCXO	C	40
CS7	XO	D	40
CS8	TCXO	E	100
CS9	VCXO	F	40

Key to Oscillator Type

XO	Crystal Oscillator
TCXO	Temperature Compensated XO
OCXO	Oven Controlled XO
VCXO	Voltage Controlled XO

domain) using expressions in [55]. For the two state noise model, [55] gives a form of

$$\sigma_y^2(\tau) = \frac{h_0}{2\tau} + \frac{2\pi^2 h_{-2}\tau}{3} \quad (3.10)$$

Equating coefficients in (3.9) and (3.10) gives

$$q_1 = \frac{h_0}{2} \quad q_2 = 2\pi^2 h_{-2} \quad (3.11)$$

Figure 3.6 shows the best-fit parameters for the two-state model given the measured noise performance.

3.3.2 Role of oscillator model in phase prediction

One value of the oscillator noise model is its role in determining a filter for prediction of oscillator phase error over time. Although the noise sources ξ_1 and ξ_2 are uncorrelated white noise sources, the integration in the model of Figure 3.5 imposes a correlation in the output error $x(t)$ that can be utilized in predicting future evolution of oscillator error.

In [52] it is shown that optimal minimum mean squared error (MSE) phase tracking and prediction can be achieved with a Kalman filter derived from the state-space model of the phase noise process. Since the Kalman filter operates in discrete time on measured samples of oscillator phase error, the continuous time model of (3.6) is converted to a discrete time model subject to the time interval between relative phase error measurements.

It is important to note that the size of the Kalman gain matrix is set by the number of states in the oscillator noise model. The results in Figure 3.2 were obtained using a 2×2 Kalman gain matrix resulting from the two-state noise model described in section 3.3.1.

3.4 Three-state Oscillator Model

In this section a three-state model for better prediction of oscillator’s phase noise performance is introduced. For this reason, we first investigated the phase noise performance of some low-cost oscillators which are suitable for use as frequency reference in an SDR. Then after proposing the new three-state model, the parameters for PLL in those oscillators are determined.

3.4.1 Survey of crystal oscillators

To investigate the applicability of the two-state model, phase noise performance was measured for a range of low-cost crystal oscillators suitable for use as the frequency reference in an SDR application. The oscillators tested are given in Table 3.1 and measured characteristics are shown in Figure 3.7. For offset frequencies below ≈ 100 Hz, all of the plots show behavior consistent with the two-state model. At higher offset frequencies, however, oscillators CS7 and CS8 show additional noise power beyond what could be predicted by a two-state model. Since tracking and prediction behavior in the cooperative communication application can rely on offset frequencies

up to ≈ 10 kHz, it is important to modify the two-state model to model the extra noise power and allow development of an appropriate Kalman filter.

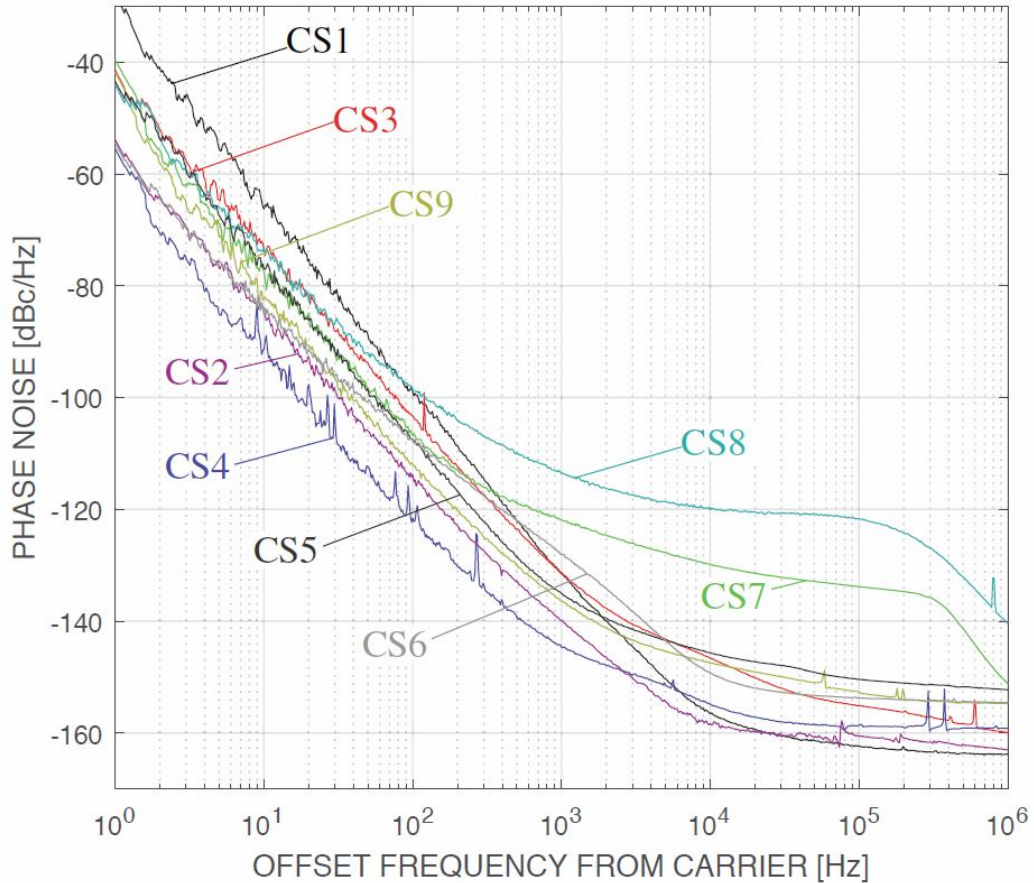


Figure 3.7: Summary of phase noise measurements.

3.4.2 Development of three-state model

The shape of excess noise power in the phase noise plots for oscillators CS7 and CS8 is similar to the phase noise of the synthesized SDR output shown in Figure 3.4. Indeed, the approach we will take in modeling the system for oscillators CS7 and CS8 is to assume that a phase-locked loop synthesizer is used to develop the output clock frequency. From the characteristics of extra noise power in CS7 and

CS8, such as low pass filter behavior and $-20 \frac{dB}{dec}$ slope, it can be inferred that, the new model should have an extra part performing as a low pass filter with one-pole transfer function system. Therefore, addition of this one pole or state to the two-state model, suggests that a three-state model should be able to better predict this extra noise power existing in these two oscillators phase noise plots. Figure 3.8 shows the proposed three-state model, with the previous two-state clock model as the input to a PLL synthesizer [60].

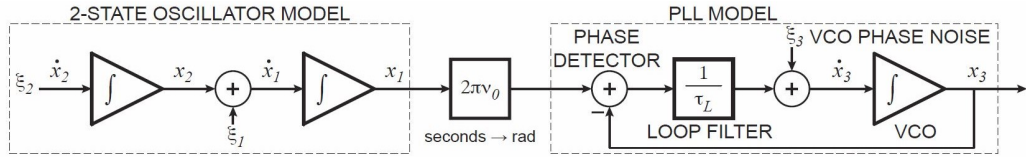


Figure 3.8: Three-state model for phase noise of source with PLL synthesizer.

Since the controlled variable in a PLL is phase, the output state x_1 must be multiplied by $2\pi\nu_0$ to convert the time variable x_1 in seconds to an equivalent phase in radians at the PLL input. The voltage controlled oscillator (VCO) is represented with an integrator, since phase is the integral of frequency. Two parameters characterize the VCO for purposes of state space modeling:

- For consistency with the noise representation in the 2-state oscillator model, VCO phase noise is modeled as a white noise input $\xi_3(t)$ with units rad/s.
- The loop bandwidth of the PLL response is determined by time constant τ_L .

The block diagram for clock multiplication PLL synthesis as described in [60] usually shows a divide-by-N in the PLL feedback path, to accomplish the frequency multiplication by N from input to output. In this case the effect of $1/N$ in the feedback is reflected in scaling of τ_L and other signal sources in the block diagram.

Expressing the system of Figure 3.8 in state space form gives:

$$\underbrace{\begin{bmatrix} \dot{x}_1 \\ \dot{x}_2 \\ \dot{x}_3 \end{bmatrix}}_{\dot{X}} = \underbrace{\begin{bmatrix} 0 & 1 & 0 \\ 0 & 0 & 0 \\ \frac{2\pi\nu_0}{\tau_L} & 0 & \frac{-1}{\tau_L} \end{bmatrix}}_A \underbrace{\begin{bmatrix} x_1 \\ x_2 \\ x_3 \end{bmatrix}}_{X(t)} + \underbrace{\begin{bmatrix} \xi_1 \\ \xi_2 \\ \xi_3 \end{bmatrix}}_{\xi(t)} \quad (3.12)$$

with output x_3 now in units of radians of phase.

3.4.3 Determining PLL parameters

As in [56], we model the new process noise term $\xi_3(t)$ as a zero mean independent Gaussian random process; now the \mathbf{Q} matrix in the autocorrelation of (3.7) is

$$\mathbf{Q} = \begin{bmatrix} q_1 & 0 & 0 \\ 0 & q_2 & 0 \\ 0 & 0 & q_3 \end{bmatrix} \quad (3.13)$$

The new model parameters q_3 and τ_L can be determined from the phase noise plot. From Figure 3.8 the transfer function from ξ_3 to x_3 is

$$x_3 = \left(\frac{\tau_L}{1 + s\tau_L} \xi_3 \right) \quad (3.14)$$

Since ξ_3 is a white noise source, we expect from (3.14) to see a lowpass characteristic in the output phase noise due to ξ_3 , which is observed in the measured phase noise of Figure 3.9.

To account for the lowpass phase noise power spectral density, we add a lowpass term to (3.8)

$$S_\Phi(f) = 2\mathcal{L}(f) = \frac{h_{-2}\nu_0^2}{f^4} + \frac{h_0\nu_0^2}{f^2} + \frac{h_\nu}{1 + (f/f_L)^2} \quad (3.15)$$

For q_3 describing the variance of ξ_3 , using the square of the magnitude of the transfer function in (3.14) and equating coefficients with (3.15) gives

$$\tau_L = \frac{1}{2\pi f_L} \quad q_3 = \frac{h_\nu}{\tau_L^2} \quad (3.16)$$

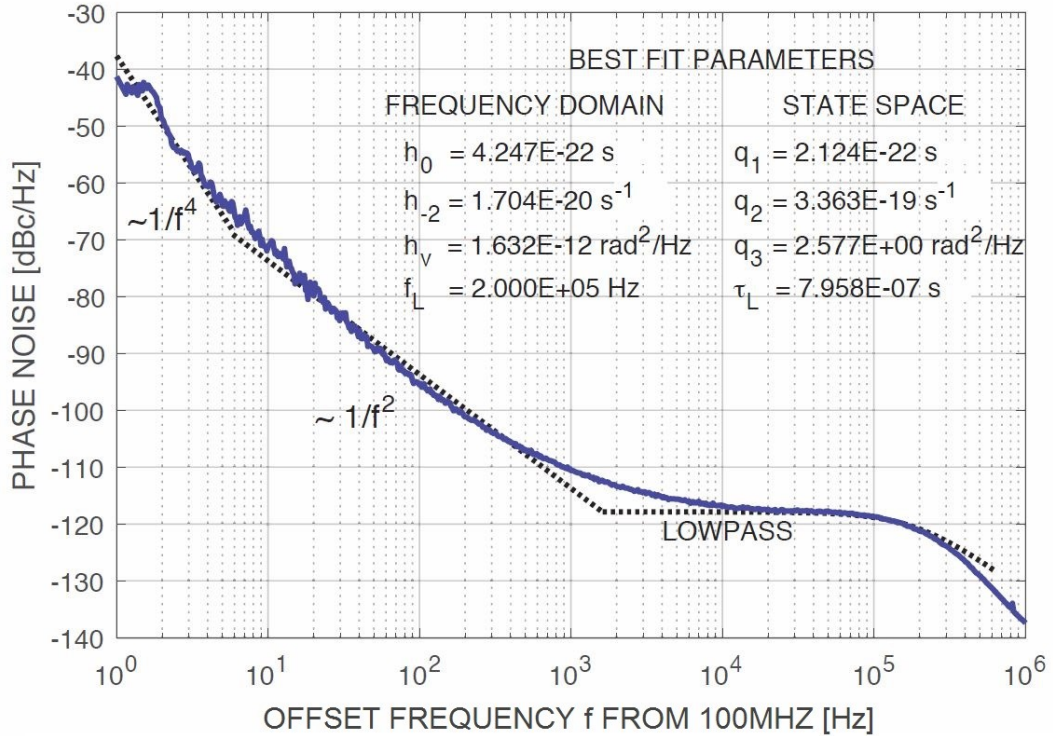


Figure 3.9: Measured phase noise for oscillator CS8 with 3-state model fit.

Figure 3.9 shows the best-fit parameters for the three-state model given the measured noise performance for oscillator CS8.

3.5 Measurement and Simulation results

To test the applicability of the three-state model, a Kalman filter was defined using (3.12) with parameters from Figure 3.9 for oscillator CS8. A Monte Carlo approach was used to generate simulated phase error waveforms with noise power as shown in Figure 3.9. Phase error was sampled at a 2 MHz rate to capture dynamics up to the 1 MHz offset frequency in Figure 3.9.

Figure 3.10 shows sample waveforms for a prediction time of $10 \mu\text{s}$. The three-state filter prediction (red) was compared to a two-state filter (blue) using only the q_1

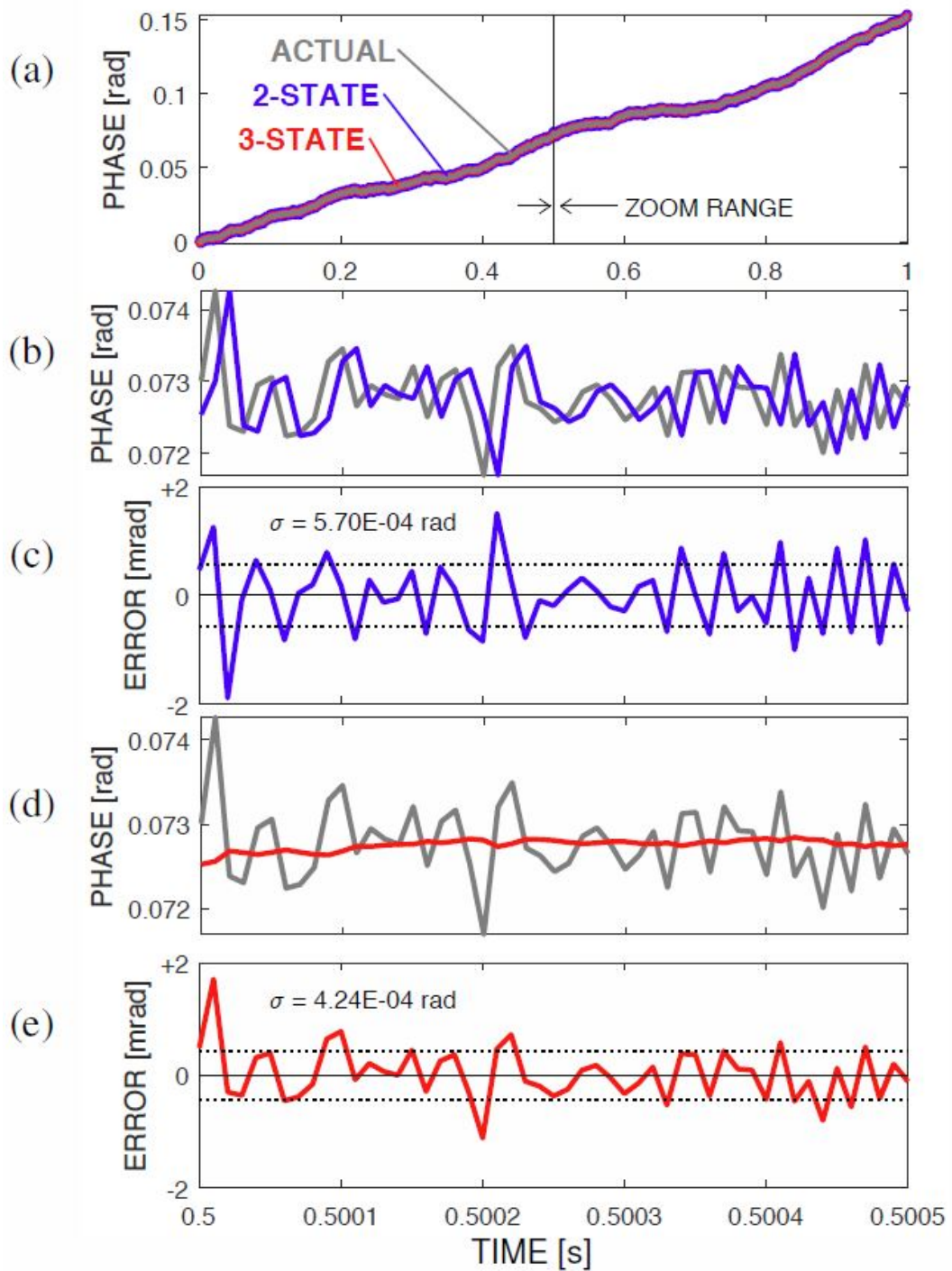


Figure 3.10: Prediction for oscillator CS8 with 2- and 3-state model fits.

and q_2 parameters corresponding to the low-offset-frequency region in Figure 3.9. To emphasize oscillator modeling, no measurement noise was included. Figure 3.10(a) shows the behavior of both filters relative to the actual phase error over a time scale of seconds. Both filters track the long term phase error closely, as expected since both filters share the two states corresponding to the low offset frequency ($1/f^4$ and $1/f^2$) phase noise asymptotes in Figure 3.9.

Figure 3.10(b) shows the prediction (blue) and actual phase (gray) for the two-state filter; prediction error is shown in Figure 3.10(c). Figure 3.10(d) and (e) show the prediction and error for the three-state filter; in the case of this particular waveform the MSE is improved by 2.9 dB over the two-state filter.

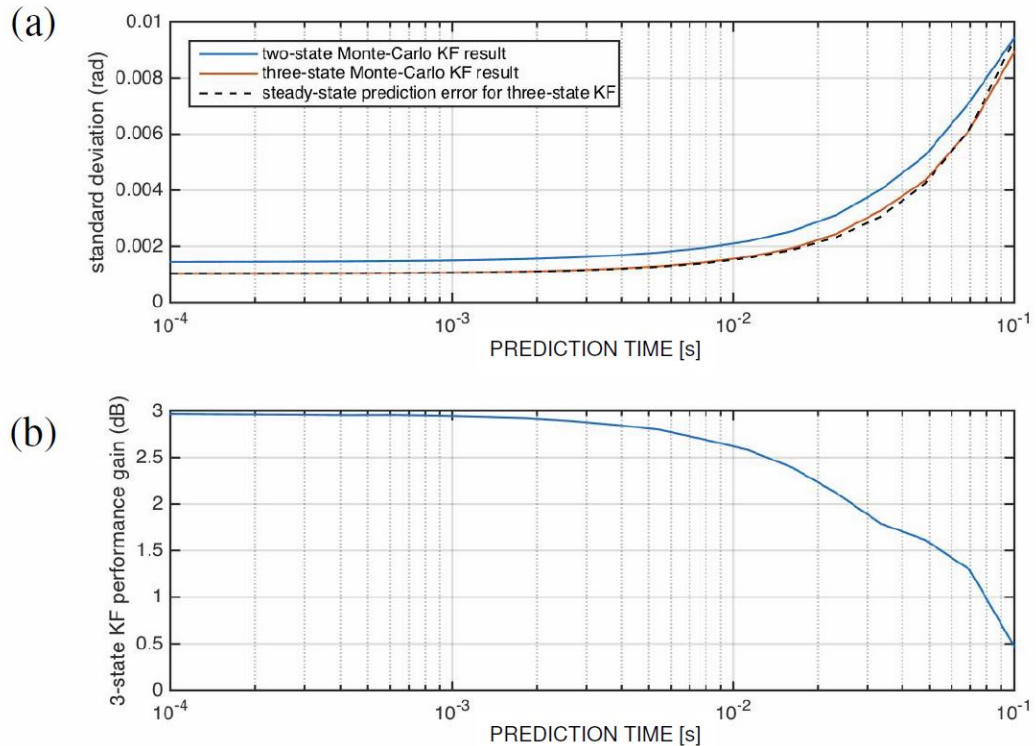


Figure 3.11: Relative performance, 2-state vs. 3-state model fit.

Figure 3.11(a) shows the standard deviation (averaged over the Monte Carlo ensemble) for both filters over a range of prediction times from 100 μ s to 100 ms. As

expected, error increases with prediction time, but at all times the three-state filter error is smaller. Figure 3.11(b) shows that the three-state filter advantage exceeds 2.5 dB for prediction times up to 10 ms; for longer prediction times the advantage is less pronounced as the performance of both predictors is degraded.

3.6 Conclusion

A survey of widely available, low-cost oscillators shows two distinct types of shape for the frequency domain characteristic of phase noise performance. For oscillators exhibiting a phase noise density similar to that of a PLL synthesizer architecture, the traditional two-state model yields suboptimal performance in phase tracking and prediction. The proposed three-state model is shown to provide up to 3 dB improvement in MSE of prediction.

Chapter 4

Wireless Power Transfer With Simultaneous Distributed Beamforming Using One-bit Feedback

In this chapter three different rules are introduced to make the maximum possible power delivery to a cluster of receive nodes in a distributed reception scenario. These three rules are, Unanimous, Majority and Summation rules. The Unanimous rule updates the transmitters' phases if all the receive nodes receive higher power than the previous time slot. While, the phase update happens in the Majority rule if more than half of the nodes are shown improvement in their received power. The third one or Summation rule updates the transmitters' phases if sum of the received power by all the nodes has improved compared to the previous time slot. Performance of these proposed rules are measured and compared against each other and it is shown that among these three, the Summation rule has a better performance of about 1.45 dB and 0.23 dB over Unanimous and Majority rules respectively. Also, the problem of

maximizing the received weighted sum power is introduced and a solution for that is given.

4.1 Introduction

A wireless transmission system with multiple transmitters and receivers as illustrated in Figure 4.1 is considered here. This system includes N number of distant transmitters which send their signals to a receive cluster with M number of receivers. Each node in the cluster measures the power or the Received Signal Strength (RSS) of the received signal and compares that to the previous received RSS and determines if the received power has increased or not. These decisions are then exchanged over a wireless local area network between the nodes inside the cluster using the methods in [32, 46, 47, 49] and based on one of the proposed rules in this paper a final decision is made and the result is sent back to the transmitters through a one-bit feedback which they use to adjust their phases and enhance their beamforming.

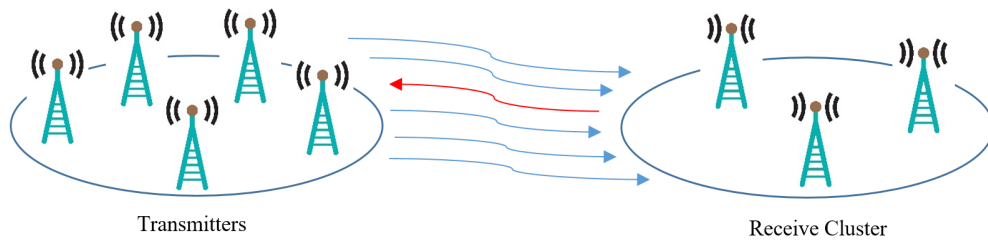


Figure 4.1: A wireless transmission system with multiple receivers and one-bit feedback

Wireless power transfer is one of the topics that is gaining more attention in the recent years especially by rapid expansion of mobile and wearable devices and also wireless sensor networks which they all have one problem in common and that is their limited power resources and the need to be recharged frequently using a power supply

and usually by wire. Most of these application consists of one or more transmitters with multiple antennas and only one receiver, so most of the research done in this area are focused on single receiver networks. For example in [62] a new channel training algorithm has been proposed to achieve optimal design of transmit signals in networks with multiple transmitters and single receiver. In [63] distributed adaptation by transmitters have been used to achieve phase alignment using only one-bit feedback from the receiver indicating if the received power has increased or decreased, where then, the transmitters update their phases by a small random amount after receiving the feedback at each iteration. This paper uses the method described in this work and also [64] by assuming multiple receivers and proposes three different decision rules to decide if the received power has been improved or declined at the receive cluster. There are a number of other papers that have studied the concept of having multiple receivers but they have used a different approaches which mostly consists of channel state information (CSI) calculation and decision making in the transmitter side. A channel learning method using an optimization technique called analytic center cutting plane method (ACCPM) that only requires one-bit feedback from each receiver has been proposed in [65,66]. Four protocols have been introduced for wireless sensor networks with multiple mobile chargers by [67] which are distributed and use limited information about the network. From these four, two of them use distributed, limited knowledge coordination and the other two perform centralized, global network knowledge coordination and charging.

The main contribution of this paper is that, three new simple rules for decision making about the received power in the receive cluster are proposed and since these rules are simple and fast to perform they do not require too much processing power and energy from the nodes and they can be implemented at the receiver side. Also, the final decision about the received power level is sent back with a single one-bit feedback signal, transmitted by the receive node which has the highest received power.

The rest of this chapter is organized as follows. Section 4.2 describes the system

model that is used here and defines the transmitted signal, channel characteristics and received signal strength or power at the receivers. In Section 4.3 the problem of maximizing received power is explained and in Section 4.4 the solution to this problem is discussed. Section 4.5 talks about proposed decision making models and how they work and how feedback generation and phase update process are done. In Section 4.7 the results of simulation of implementing these rules in the corresponding defined scenario is presented and in Section 4.8 the conclusions are stated.

4.2 System Model

We assume there are N number of distant transmitters each with single antenna. The channel between each transmitter and receiver is assumed to be complex Gaussian and is fixed for all iterations but it is a different value for each transmitter. At the receiver side, we have M number of receivers in a receive cluster which is assumed to be fully connected using a reliable wireless or wired local area network. The channel between each transmitter and receiver is defined as below,

$$h_{n,m} \sim \mathcal{CN}(0, 1) \quad (4.1)$$

Where $h_{n,m}$ with $n \in \{1, \dots, N\}$ and $m \in \{1, \dots, M\}$ is the channel between transmitting node n and receiving node m . Magnitudes of these channels, $a_{n,m}$ are normalized and their phases are shown with $\phi_{n,m}$.

At the beginning of transmission each transmitting node picks a random phase from a uniform distribution between $[-\pi, \pi]$ and uses this phase to send the signal to the receiver over the channel. The transmitted signal is

$$x_{n,k} = e^{j\theta_{n,k}} \quad (4.2)$$

Where $\theta_{n,k}$ is the phase of the n th transmitter at time slot k . Also, it is assumed that the magnitude of transmitted signal is one. All the nodes inside the receive

cluster receive these signals and then their RSS are measured at each node locally. The received signal at each node in the receive cluster is

$$y_{m,k} = \sum_{n=1}^N h_{n,m} x_{n,k} = \sum_{n=1}^N a_{n,m} e^{j(\theta_{n,k} + \phi_{n,m})} \quad (4.3)$$

and the received power at each node is defined by

$$\mathcal{P}_{m,k} = |y_{m,k}|^2 \quad (4.4)$$

These measured values are then shared among all the nodes and based on one of the decision rules introduced in 4.5, it is decided if the received power has increased inside the cluster or not. If it is increased a one-bit feedback of one is sent to the transmitters otherwise a zero would be sent as the feedback. For each of these rules, it is assumed that, the feedback bit is transmitted by the node that has received the highest power in that time slot.

4.3 Problem Setup

In this section we discuss the basic problem setup for simultaneous distributed beamforming and then we provide some 3 transmitter results. Let N and M correspond to the number of transmitters and receivers, respectively. We assume we have single-path channels from each transmitter to each receiver. Let the path length in meters from transmitter n to receiver m be denoted as $d_{n,m}$. Then the time of flight from transmitter n to receiver m is $\tau_{n,m} = d_{n,m}/c$, where c is the speed of light. Assuming far field conditions hold such that we can use Friis' equation with isotropic antennas, we can write the gain of the channel from transmitter n to receiver m as

$$a_{n,m} = \frac{\lambda}{4\pi d_{n,m}}, \quad (4.5)$$

where $\lambda = c/f_c$ is the wavelength at carrier frequency f_c . Hence, the impulse response of the channel from transmitter n to receiver m can be written as

$$\begin{aligned} g_{n,m} &= a_{n,m}\delta(t - \tau_{n,m}) \\ &= \frac{\lambda}{4\pi d_{n,m}}\delta(t - \tau_{n,m}). \end{aligned} \quad (4.6)$$

Suppose transmitter n transmits a constant complex baseband signal given as $x_n(t) \equiv e^{j\theta_n}$ on carrier frequency f_c . Then the baseband received signal at receiver m from transmitter n can be written as

$$r_{n,m} = a_{n,m}e^{j(\theta_n - \omega_c\tau_{n,m})}, \quad (4.7)$$

where $\omega_c = 2\pi f_c$. Hence, the complex baseband channel can be written as $h_{n,m} = a_{n,m}e^{-j\phi_{n,m}}$ where $\phi_{n,m} = \omega_c\tau_{n,m}$.

The transmitters adjust their phases θ_n to achieve a particular beam pattern. The power of the received signal at receiver m can be written as

$$\rho_m = \left| \sum_{n=1}^N h_{n,m}e^{j\theta_n} \right|^2. \quad (4.8)$$

If we assign a positive weight w_m to receiver m , we can define the weighted sum received power as

$$\begin{aligned} \Gamma &= \sum_{m=1}^M w_m \rho_m \\ &= \sum_{m=1}^M w_m \left| \sum_{n=1}^N h_{n,m}e^{j\theta_n} \right|^2. \end{aligned} \quad (4.9)$$

Given any weighting $\{w_1, \dots, w_M\}$ and channels $\{h_{1,1}, \dots, h_{N,M}\}$, we can formulate an optimization problem to maximize the weighted sum received power as

$$\Gamma^* = \max_{\{\theta_1, \dots, \theta_N\}} \Gamma. \quad (4.10)$$

This, of course, will not have a unique solution for two reasons:

- Adding or subtracting the same phase from all θ_n does not affect (4.8). Hence, we can factor out θ_1 and consider only the phase differences with respect to θ_1 . To do this, define

$$\Delta_n = \theta_n - \theta_1. \quad (4.11)$$

Of course, $\Delta_1 = 0$. Then we can rewrite (4.8) as

$$\rho_m = \left| \sum_{n=1}^N h_{n,m} e^{j\Delta_n} \right|^2. \quad (4.12)$$

This means that the optimization problem can be reduced by one parameter and can be rewritten as

$$\Gamma^* = \max_{\{\Delta_2, \dots, \Delta_N\}} \Gamma, \quad (4.13)$$

with

$$\Gamma = \sum_{m=1}^M w_m \left| \sum_{n=1}^N h_{n,m} e^{j\Delta_n} \right|^2. \quad (4.14)$$

- Adding or subtracting multiples of 2π from any of the phase difference terms Δ_n results in the same solution. Hence, it makes sense to constrain the search to $-\pi < \Delta_n \leq \pi$ for all $n = 2, \dots, N$. Remember $\Delta_1 = 0$.

4.4 Problem Solution

The problem setup that we have is as follow and the goal is to maximize the received weighted sum power Γ ,

$$\Gamma = \sum_{m=1}^M w_m \left| \sum_{n=1}^N h_{n,m} e^{j\Delta_n} \right|^2. \quad (4.15)$$

where we wanted to find a Γ^* such that,

$$\Gamma^* = \max_{\{\Delta_2, \dots, \Delta_N\}} \Gamma \quad (4.16)$$

where $-\pi \leq \Delta_n \leq \pi$ for $n = 2, \dots, N$ and $\Delta_1 = 0$.

We can rewrite the Γ as following and consider it as a multivariate problem,

$$\Gamma = \sum_{m=1}^M w_m \left| \underbrace{h_{1,m}e^{j\Delta_1} + h_{2,m}e^{j\Delta_2} + \dots + h_{N,m}e^{j\Delta_N}}_{K_m} \right|^2. \quad (4.17)$$

since we know that $h_{n,m} = a_{n,m}e^{-j\phi_{n,m}}$, then we can write K_m as,

$$K_m = a_{1,m}e^{j(-\phi_{1,m}+\Delta_1)} + a_{2,m}e^{j(-\phi_{2,m}+\Delta_2)} + \dots + a_{N,m}e^{j(-\phi_{N,m}+\Delta_N)}. \quad (4.18)$$

If we want to maximize the Γ with respect to a desired Δ_n for example for $n = k$, we have to take the derivative of Γ with respect to Δ_k and set it equal to zero while assuming the other Δ_n with $n \neq k$ are constant. For this reason we can rewrite K_m as follow,

$$\begin{aligned} K_m &= \left(\overbrace{a_{1,m} \cos(-\phi_{1,m} + \Delta_1) + \dots + a_{N,m} \cos(-\phi_{N,m} + \Delta_N)}^{A_m, \text{ for all } n \neq k} + a_{k,m} \cos(-\phi_{k,m} + \Delta_k) \right) \\ &+ j \left(\overbrace{a_{1,m} \sin(-\phi_{1,m} + \Delta_1) + \dots + a_{N,m} \sin(-\phi_{N,m} + \Delta_N)}^{B_m, \text{ for all } n \neq k} + a_{k,m} \sin(-\phi_{k,m} + \Delta_k) \right) \\ &= K_{r,k,m} + jK_{i,k,m}. \end{aligned} \quad (4.19)$$

where

$$K_r = A_m + a_{k,m} \cos(-\phi_{k,m} + \Delta_k). \quad (4.20)$$

$$K_i = B_m + a_{k,m} \sin(-\phi_{k,m} + \Delta_k). \quad (4.21)$$

So, then we would have,

$$\frac{\partial \Gamma}{\partial \Delta_k} = \sum_{m=1}^M w_m \frac{\partial}{\partial \Delta_k} |K_m|^2. \quad (4.22)$$

Which results in,

$$\frac{\partial}{\partial \Delta_k} |K_m|^2 = \frac{\partial}{\partial \Delta_k} (K_r^2 + K_i^2) = 2K_r \frac{\partial K_r}{\partial \Delta_k} + 2K_i \frac{\partial K_i}{\partial \Delta_k}. \quad (4.23)$$

Therefore,

$$\begin{aligned}
\frac{\partial}{\partial \Delta_k} |K_m|^2 &= -2K_r a_{k,m} \sin(-\phi_{k,m} + \Delta_k) + 2K_i a_{k,m} \cos(-\phi_{k,m} + \Delta_k) \\
&= -2A_m a_{k,m} \sin(-\phi_{k,m} + \Delta_k) - 2a_{k,m}^2 \sin(-\phi_{k,m} + \Delta_k) \cos(-\phi_{k,m} + \Delta_k) \\
&\quad + 2B_m a_{k,m} \cos(-\phi_{k,m} + \Delta_k) + 2a_{k,m}^2 \cos(-\phi_{k,m} + \Delta_k) \sin(-\phi_{k,m} + \Delta_k) \\
&= -2A_m a_{k,m} \sin(-\phi_{k,m} + \Delta_k) + 2B_m a_{k,m} \cos(-\phi_{k,m} + \Delta_k).
\end{aligned} \tag{4.24}$$

Replacing the results from (4.24) into (4.22) we get,

$$\frac{\partial \Gamma}{\partial \Delta_k} = \sum_{m=1}^M w_m (-2A_m a_{k,m} \sin(-\phi_{k,m} + \Delta_k) + 2B_m a_{k,m} \cos(-\phi_{k,m} + \Delta_k)) = 0. \tag{4.25}$$

Which results in,

$$\sum_{m=1}^M w_m (A_m a_{k,m} \sin(-\phi_{k,m} + \Delta_k)) = \sum_{m=1}^M w_m (B_m a_{k,m} \cos(-\phi_{k,m} + \Delta_k)). \tag{4.26}$$

If we expand the term inside $\sin()$ and $\cos()$ functions we get,

$$\begin{aligned}
&\sum_{m=1}^M \overbrace{w_m A_m a_{k,m} \sin(-\phi_{k,m})}^{P_{A,k,m}} \cos(\Delta_k) + \sum_{m=1}^M \overbrace{w_m A_m a_{k,m} \cos(-\phi_{k,m})}^{Q_{A,k,m}} \sin(\Delta_k) \\
&= \sum_{m=1}^M \overbrace{w_m B_m a_{k,m} \cos(-\phi_{k,m})}^{P_{B,k,m}} \cos(\Delta_k) - \sum_{m=1}^M \overbrace{w_m B_m a_{k,m} \sin(-\phi_{k,m})}^{Q_{B,k,m}} \sin(\Delta_k)
\end{aligned} \tag{4.27}$$

After simplification we have,

$$\sum_{m=1}^M \overbrace{(P_{B,k,m} - P_{A,k,m})}^{P_{k,m}} \cos(\Delta_k) = \sum_{m=1}^M \overbrace{(Q_{A,k,m} + Q_{B,k,m})}^{Q_{k,m}} \sin(\Delta_k) \tag{4.28}$$

Therefore, the critical points for Γ function would be,

$$\tan(\Delta_k) = \frac{\sum_{m=1}^M P_{k,m}}{\sum_{m=1}^M Q_{k,m}} \quad \rightarrow \quad \Delta_k = \tan^{-1} \left(\frac{\sum_{m=1}^M P_{k,m}}{\sum_{m=1}^M Q_{k,m}} \right) \tag{4.29}$$

To find out the values of Δ_k s we have to replace the $P_{k,m}$ and $Q_{k,m}$ by their content as a function of Δ_n , so for $P_{k,m}$ we would have

$$\begin{aligned}
P_{k,m} &= P_{B,k,m} - P_{A,k,m} \\
&= w_m B_m a_{k,m} \cos(-\phi_{k,m}) - w_m A_m a_{k,m} \sin(-\phi_{k,m}) \\
&= w_m a_{k,m} (B_m \cos(-\phi_{k,m}) - A_m \sin(-\phi_{k,m}))
\end{aligned} \tag{4.30}$$

and for $Q_{k,m}$,

$$\begin{aligned}
Q_{k,m} &= Q_{A,k,m} + Q_{B,k,m} \\
&= w_m A_m a_{k,m} \cos(-\phi_{k,m}) + w_m B_m a_{k,m} \sin(-\phi_{k,m}) \\
&= w_m a_{k,m} (A_m \cos(-\phi_{k,m}) + B_m \sin(-\phi_{k,m}))
\end{aligned} \tag{4.31}$$

Now we have to replace the value for A_m and B_m from (4.19) into the (4.30) and (4.31). By doing so, for $P_{k,m}$ we get,

$$\begin{aligned}
P_{k,m} &= w_m a_{k,m} \left(\left(\sum_{\substack{n=1 \\ n \neq k}}^N a_{n,m} \sin(-\phi_{n,m} + \Delta_n) \right) \cos(-\phi_{k,m}) \right. \\
&\quad \left. - \left(\sum_{\substack{n=1 \\ n \neq k}}^N a_{n,m} \cos(-\phi_{n,m} + \Delta_n) \right) \sin(-\phi_{k,m}) \right) \\
&= w_m a_{k,m} \left(\sum_{\substack{n=1 \\ n \neq k}}^N a_{n,m} (\sin(-\phi_{n,m} + \Delta_n) \cos(-\phi_{k,m}) - \cos(-\phi_{n,m} + \Delta_n) \sin(-\phi_{k,m})) \right) \\
&= w_m a_{k,m} \left(\sum_{\substack{n=1 \\ n \neq k}}^N a_{n,m} \sin(-\phi_{n,m} + \phi_{k,m} + \Delta_n) \right)
\end{aligned} \tag{4.32}$$

and for $Q_{k,m}$ we get,

$$\begin{aligned}
Q_{k,m} &= w_m a_{k,m} \left(\left(\sum_{\substack{n=1 \\ n \neq k}}^N a_{n,m} \cos(-\phi_{n,m} + \Delta_n) \right) \cos(-\phi_{k,m}) \right. \\
&\quad \left. + \left(\sum_{\substack{n=1 \\ n \neq k}}^N a_{n,m} \sin(-\phi_{n,m} + \Delta_n) \right) \sin(-\phi_{k,m}) \right) \\
&= w_m a_{k,m} \left(\sum_{\substack{n=1 \\ n \neq k}}^N a_{n,m} (\cos(-\phi_{n,m} + \Delta_n) \cos(-\phi_{k,m}) + \sin(-\phi_{n,m} + \Delta_n) \sin(-\phi_{k,m})) \right) \\
&= w_m a_{k,m} \left(\sum_{\substack{n=1 \\ n \neq k}}^N a_{n,m} \cos(-\phi_{n,m} + \phi_{k,m} + \Delta_n) \right) \tag{4.33}
\end{aligned}$$

Therefore, by replacing (4.32) and (4.33) into (4.29), the Δ_k would be

$$\Delta_k = \tan^{-1} \left(\frac{\sum_{m=1}^M w_m a_{k,m} \left(\sum_{\substack{n=1 \\ n \neq k}}^N a_{n,m} \sin(-\phi_{n,m} + \phi_{k,m} + \Delta_n) \right)}{\sum_{m=1}^M w_m a_{k,m} \left(\sum_{\substack{n=1 \\ n \neq k}}^N a_{n,m} \cos(-\phi_{n,m} + \phi_{k,m} + \Delta_n) \right)} \right). \tag{4.34}$$

We can further simplify this solution by assuming that phases in the equation (4.14) are summed to zero so that the vectors are added together like a scalar and give the maximum summation. So, if we replace $h_{n,m} = a_{n,m} e^{-j\phi_{n,m}}$ in that equation, we would have

$$\Gamma = \sum_{m=1}^M w_m \left| \sum_{n=1}^N a_{n,m} e^{j(\Delta_n - \phi_{n,m})} \right|^2. \tag{4.35}$$

Now if we set the phases to zero we would have

$$\Delta_n = \phi_{n,m}. \tag{4.36}$$

By replacing the above result in (4.34) we get

$$\Delta_k = \tan^{-1} \left(\frac{\sum_{m=1}^M w_m a_{k,m} \left(\sum_{\substack{n=1 \\ n \neq k}}^N a_{n,m} \sin(\phi_{k,m}) \right)}{\sum_{m=1}^M w_m a_{k,m} \left(\sum_{\substack{n=1 \\ n \neq k}}^N a_{n,m} \cos(\phi_{k,m}) \right)} \right). \tag{4.37}$$

In the range of $-\pi \leq \Delta_k \leq \pi$, each Δ_k would have two answers which means Γ has two critical points where one is minimum and the other is maximum due to trigonometric structure of Γ . To find out the absolute maximum and minimum over all Δ_k s we have to form the Taylor expansion of the Γ and form the Hessian matrix. In this case the Hessian matrix would be a diagonal matrix since the second partial derivatives of the form $\frac{\partial^2 \Gamma}{\partial \Delta_i \partial \Delta_j} = 0$ for all $i \neq j$. So, to form the Hessian we get another derivative from (4.25) and then we would have,

$$\frac{\partial^2 \Gamma}{\partial \Delta_k^2} = \sum_{m=1}^M w_m (-2A_m a_{k,m} \cos(-\phi_{k,m} + \Delta_k) - 2B_m a_{k,m} \sin(-\phi_{k,m} + \Delta_k)). \quad (4.38)$$

The results from (4.38) forms the elements on the diagonal of Hessian matrix. Then, by replacing the values from (4.29) into the Hessian matrix we would be able to find out the absolute maximum and minimum of received weighted sum power.

For the special case of $N = 3$, we have only Δ_2 and Δ_3 to maximize since $\Delta_1 = 0$. To do so, we have to do two steps, the first one is to keep Δ_2 as constant and find the max and min of Δ_3 , and then the next step is to set Δ_3 as constant and solve for max and min of Δ_2 .

For the case that Δ_2 is kept constant ($\Delta_2 = 0$), the first and second derivative of weighted sum power with respect to Δ_3 are shown in the Figure 4.2. The points of zero crossing for the first derivative give us the points on Δ_3 axis at which the max and min happens, and the second derivative plot shows which one of these two are min and which one is the max.

For the case where Δ_3 is kept constant ($\Delta_3 = 0$), the result is shown in Figure 4.3. Comparing these two figures with the contour plots that we had for $N = 3$ (Figure 4.4), we find out that the obtained values for Δ_3 and Δ_2 (for respective constant Δ_2 and Δ_3), are consistent with the contour plot.

Based on the problem setup and the results, here we have a multivariate optimiza-

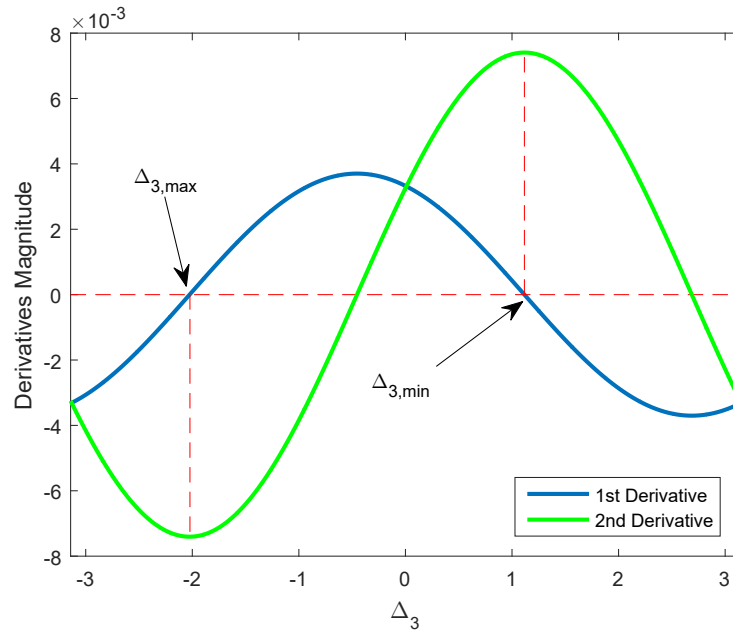


Figure 4.2: First and second derivative with respect to Δ_3 when $\Delta_2 = 0$.

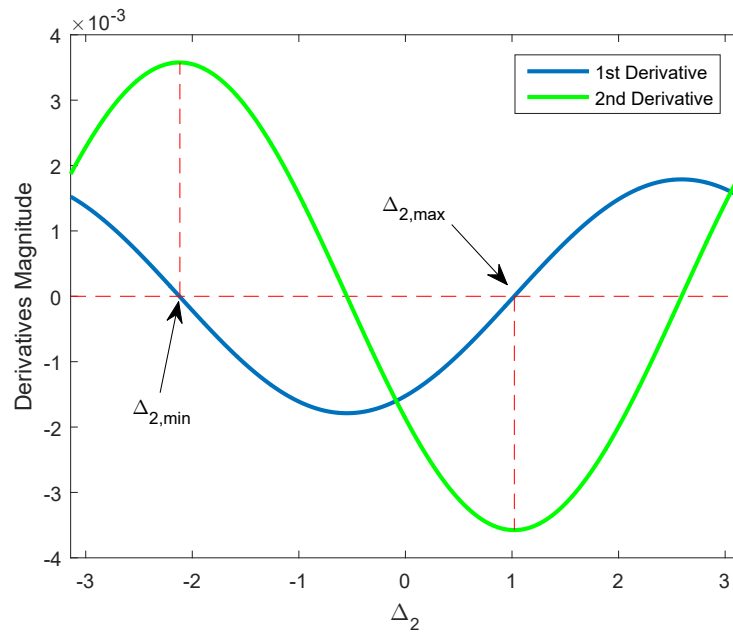


Figure 4.3: First and second derivative with respect to Δ_2 when $\Delta_3 = 0$.

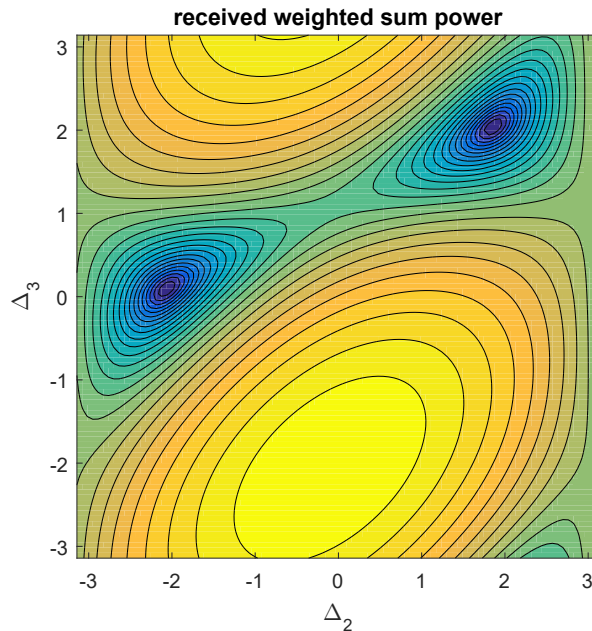


Figure 4.4: Contour plots of received weighted sum power vs Δ_3 and Δ_2 .

tion problem which is not convex since its second derivative is not always positive (or always negative) and it changes its sign, but the above calculations show that in the range of $[-\pi, \dots \pi]$, there are one minimum and one maximum for each variable in this problem.

4.5 Proposed Decision Making Methods

Based on the received one-bit feedbacks from receivers, three methods are introduced to help decision making in transmitters regarding when and how to update their phases. These methods are described in more details in the following sections. A one-bit feedback signal is sent as one if the received power in current iteration is higher than the previous one, and it is zero otherwise.

4.5.1 Unanimous Rule

This rule is defined as follow,

$$db = \begin{cases} 1, & \mathcal{P}_{m,k+1} > \mathcal{P}_{m,k}, \text{ for all } m \\ 0, & \text{Otherwise.} \end{cases} \quad (4.39)$$

Where db is the decision bit at the transmitters and $\mathcal{P}_{m,k}$ is the received power by receiver m at time k . In this rule, if all the received one-bit feedback signals from receivers are one, then the decision bit would be one and transmitters update their phases as described in (4.43), otherwise the phase are updated according to (4.44).

4.5.2 Majority Rule

If this rule is applied at transmitters, the decision bit would be one if majority of the received one-bit feedback signals are one, and it would be zero otherwise. We can define the rule as follow,

$$db = \begin{cases} 1, & \mathcal{P}_{m,k+1} > \mathcal{P}_{m,k}, \text{ for all } m \in \{1, \dots, m'\} \\ 0, & \text{Otherwise.} \end{cases} \quad (4.40)$$

Where $m' > \frac{M}{2}$ is the number of nodes that have an increase in their power.

4.5.3 Summation Rule

If this rule is in effect, receivers sent full feedback signals with the amount of power they have received, then at the transmitters these feedback signals are summed together and if the result is higher than the sum power from previous iteration, the decision bit at transmitter would be one, otherwise it would be zero.

$$db = \begin{cases} 1, & \sum_{m=1}^M \mathcal{P}_{m,k+1} > \sum_{m=1}^M \mathcal{P}_{m,k} \\ 0, & \text{Otherwise.} \end{cases} \quad (4.41)$$

4.6 Phase Update Procedure

At the beginning of transmission, all the transmitters pick up a random phase from a set of uniformly distributed phases over the range of $[-\pi, \pi]$.

$$\theta_{n,k} \sim \mathcal{U}[-\pi, \pi] \quad (4.42)$$

Using these phases a common signal is sent by transmitters through $N \times M$ complex Gaussian noiseless channels as defined in (4.1) with normalized magnitude. At the receive cluster, each node receives the signals from all the transmitting nodes and calculates the total received power, which is the sum of the power from each received signal at the place of that node. Then each node generates a one-bit feedback signal indicating if the received power has increased at the place of that node or not and these one-bit feedback signals are then sent to the transmitters. In the case of Summation rule, the whole received power as a full feedback is sent to transmitters from each node. It is assumed that the feedback signals would reach at all transmitters without any error. Afterward, based on what are the feedback signals the following procedure is performed to update the phase at each transmitter.

If based on the received feedback signals and the applicable rule, the decision bit is one, then all the phases would be updated by adding one small phase perturbation drawn from a uniformly distributed phases as described below,

$$\begin{aligned} \boldsymbol{\theta}_{k+1} &= \boldsymbol{\theta}_k + \boldsymbol{\delta}_k \\ \boldsymbol{\delta}_k &\sim \mathcal{U}[-\alpha\pi, \alpha\pi] \end{aligned} \quad (4.43)$$

Here $\boldsymbol{\delta}_k$ is the vector of generated phase perturbations at time slot k and $\alpha < 1$ is the scaling factor that determines how large or small should the perturbation be. With large values of α the convergence to the steady state power would be faster but it may cause the algorithm to stuck in a local maximum power rather than the global maximum achievable power. On the other hand, small values would cause the phase update process to take much longer time to approach the final value, so a proper

value should be selected for update process. This perturbation would be kept until a feedback of zero is received.

If the decision bit is determined to be zero, at the receive cluster, the nodes would replace their current power reading with the power from previous time slot. At the transmitters' side the phase from previous time slot would be updated with the current phase perturbation and then a new perturbation would be generated. Also, the phase from previous time slot would replace the current phase as described below,

$$\begin{aligned}
\boldsymbol{\theta}_{k+1} &= \boldsymbol{\theta}_{k-1} + \boldsymbol{\delta}_k \\
\boldsymbol{\delta}_{k+1} &= \boldsymbol{\delta}_{new} \\
\mathcal{P}_k &= \mathcal{P}_{k-1} \\
\boldsymbol{\theta}_k &= \boldsymbol{\theta}_{k-1}
\end{aligned} \tag{4.44}$$

After all the necessary updates have been done, a signal with the updated phase would be sent to the receivers and this process continues until the power reaches to a steady state level.

4.7 Simulation results

In this section the numerical results of the simulation for each proposed rule is presented. For the simulation we have assumed $N = 10$ transmitters and $M = 3$ receivers. The complex Gaussian channels are generated with zero mean ($\mu = 0$) and unit variance ($\sigma^2 = 1$). The initial phases of transmitters are selected from a uniformly distributed numbers between $-\pi$ and π . The scaling factor for phase perturbation distribution range is selected to be $\alpha = \frac{1}{50}$. For each rule the number of iterations is chosen to be 10,000. The position of the transmitters and receivers are assumed fixed.

The results for each rule are as follow. For these results to be comparable with each other, the random number generator has been seeded to a same number for each

rule's simulation.

4.7.1 Unanimous Rule Results

As can be seen from Figure 4.5 and also the contour plot of Figure 4.6, in Unanimous rule the received power at each node increases by each iteration and reaches to the maximum achievable power for that node based on the current channel conditions, and it is expected, since in this rule all the receive nodes should have an increase in their power for the feedback to be one. In the phase update process as it is expected, the phases do not converge to the same value since the channel for each transmitter differs from the others but phase of each transmitter converges to a final value that results in the best beamforming and maximum power at the receiver side. In this example, the maximum power is received by the first receiver and it equals 17.78 dB.

4.7.2 Majority Rule Results

In Majority rule, since the decision about the feedback is based on an increase in the majority of the nodes' power and not all of them, at each iteration, different set of receivers get the higher power and as a result the output power plot would be fluctuating a lot. To make the output for this rule suitable to read and compare, the received power is averaged over 10 monte-carlo iterations. Figure 4.7 shows these averaged power for each node in the receive cluster, and Figure 4.8 shows the contour plot of the received power. It can be seen that in this case it is possible to achieve higher levels of power compared to Unanimous rule but the received power is not reaching a constant value as it does in Unanimous rule. For the same reason, the phases at transmitters do not converge to a constant value and they also have fluctuation from one iteration to another. Here in this example, the maximum power is received by the third receiver and it equals ≈ 19 dB.

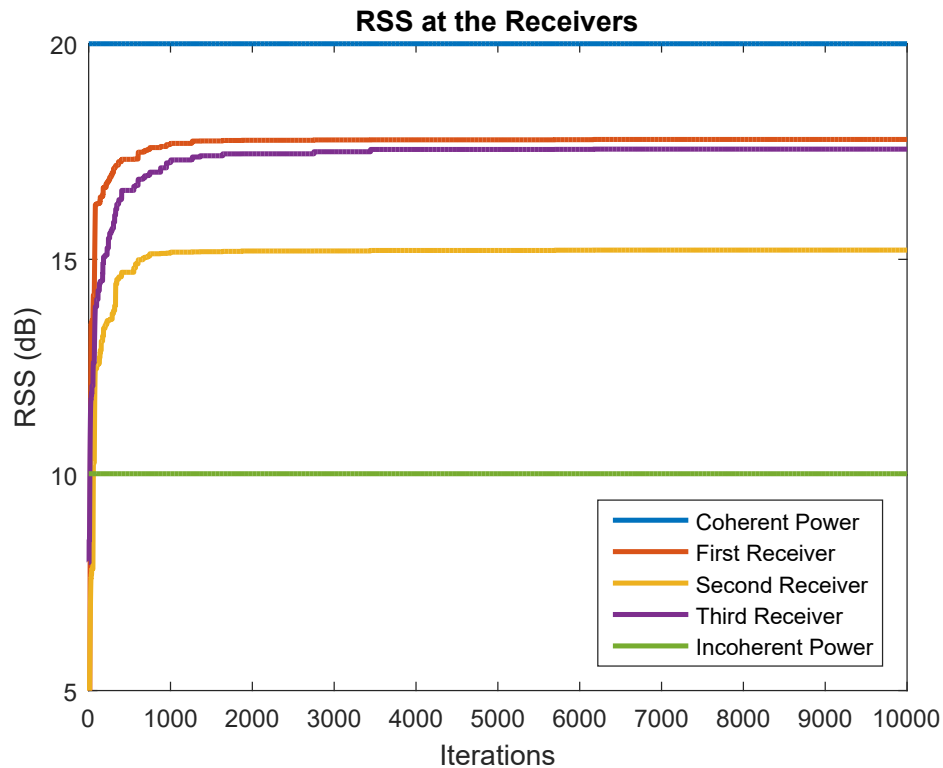


Figure 4.5: Received power at each node in Unanimous rule over iterations.

4.7.3 Summation Rule Results

Since in this rule the sum of all the received powers are considered, it is possible to receive a feedback of one while some of the nodes are experiencing loss of power and that is because the other nodes may have a large increase in their received power such that it compensates for the loss of the other nodes. As a result, we see that in Figure 4.9 some receivers show a decrease in their power while at the same time the other receivers have an increase in their power. Figure 4.10 shows the contour plot of the received power and it can be seen that the maximum power can be reached with this rule. Also, due to use of this method, it is possible that at some point the loss in some nodes become greater than the gain in the other nodes which will cause a zero feedback to be sent and consequently changes the transmitters' phase update

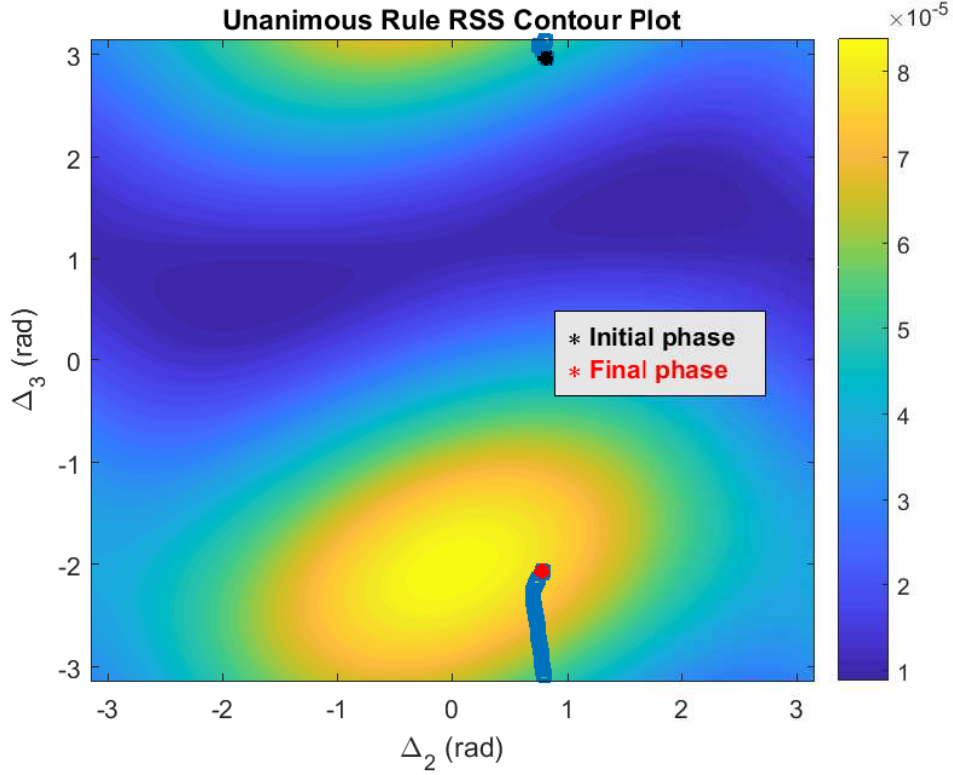


Figure 4.6: Contour plot of the received power in Unanimous rule over all transmitters phase difference iterations.

process. For the case of this simulation, the maximum power is received by the third receiver and it equals 19.23 dB.

4.7.4 Effect Of Scaling Factor α On Convergence

The value that is chosen for the scaling factor in phase perturbation can slow or expedite the convergence process or even causes divergence. To show the effect of this scaling factor α , a receiver in Summation rule is selected and the effect of changing the α is demonstrated on that particular receiver. For this purpose, a range of different values are selected for α and defined as below,

$$\alpha = \frac{1}{n}, \quad n = [10, 50, 100, 150, 200]. \quad (4.45)$$

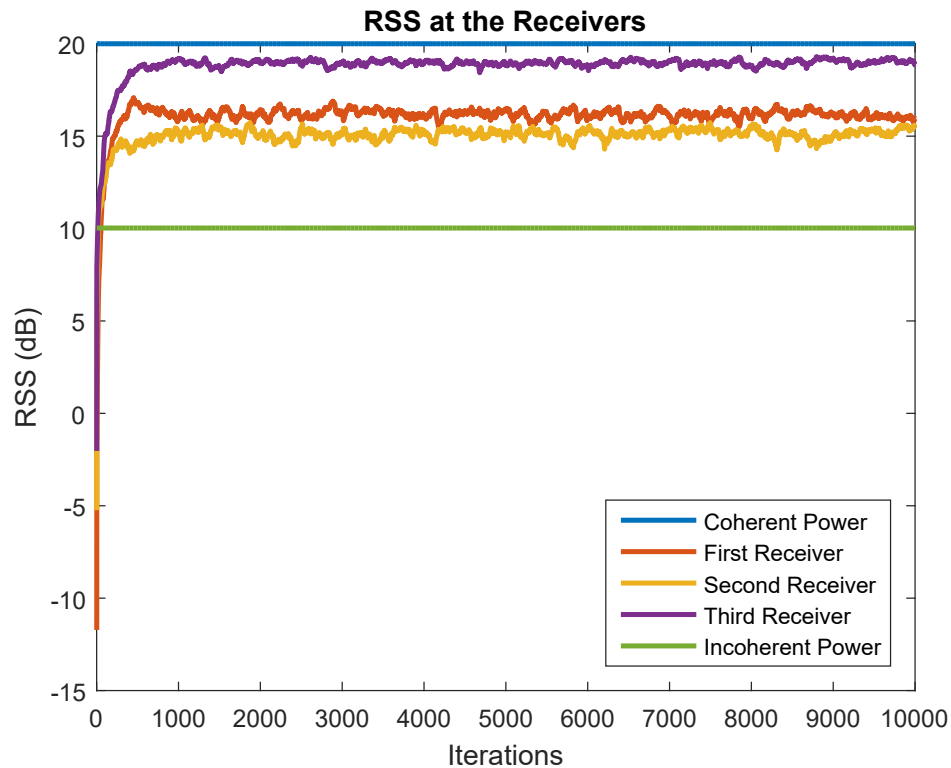


Figure 4.7: Received power at each node in Majority rule over iterations.

The result of implementing these scaling factors is depicted in Figure 4.11. As can be seen, when α gets smaller the convergence becomes slower, and at some point it will diverge.

4.7.5 Effect Of Sparsity On Convergence

When the carrier frequency of transmission gets large and wavelength of the signal gets smaller than the distance between receivers, the array becomes sparse and will cause Majority and Unanimous rules to stop updating before reaching to optimum power level, while Summation rule is still able to reach to the optimum power level. To show this effect, the carrier frequency have been increased to 1 GHz, and the results of having sparse array for each different rules are shown in Figures 4.12, 4.13

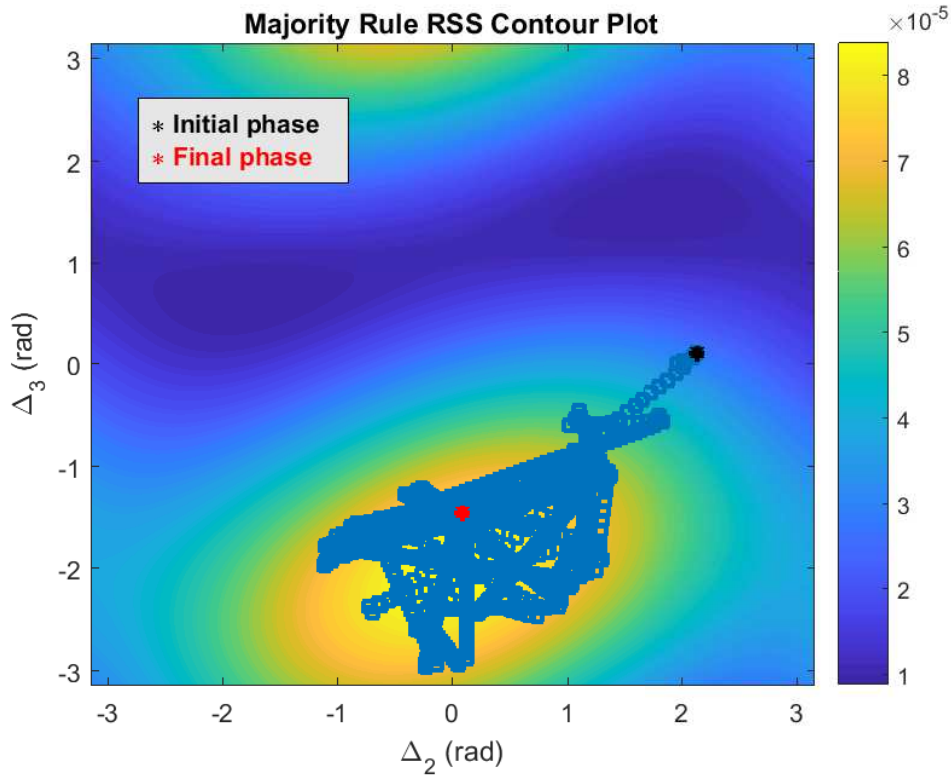


Figure 4.8: Contour plot of the received power in Majority rule over all transmitters phase difference iterations.

and 4.14.

4.8 Conclusion

In this chapter we proposed three different rules that can be applied in the receiver side and we compared their results and efficiencies. Due to their simplicity and easy implementation, they do not required too much processing power and energy from the receivers, and compared to other methods, in these proposed rules only a one-bit feedback signal is sent from each receiver in the receive cluster. As shown in the results, the Summation rule can achieve a higher received power compared with the other two rules which is about 1.45 dB and 0.23 dB over Unanimous and Majority

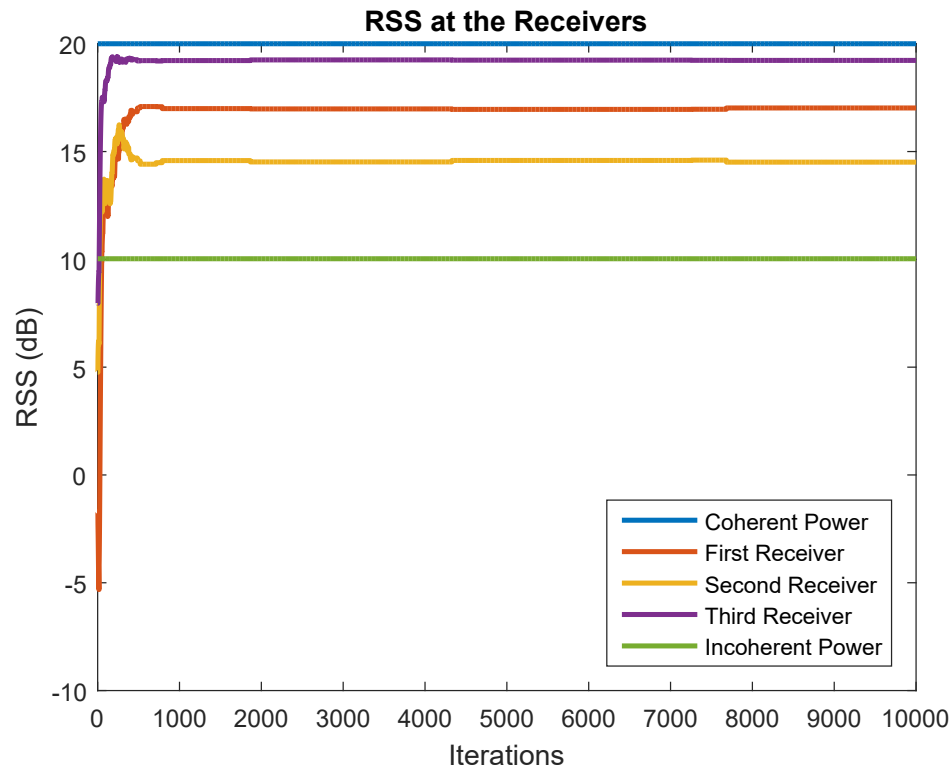


Figure 4.9: Received power at each node in Summation rule over iterations.

rules respectively. Also it converges to the maximum power faster than the other two rules. At the end, the effect of having different scaling factors on convergence speed and also the effect of having sparse array on the performance of each rule is investigated. The results show that the Summation rule is also more robust to sparsity compared to the two other rules.

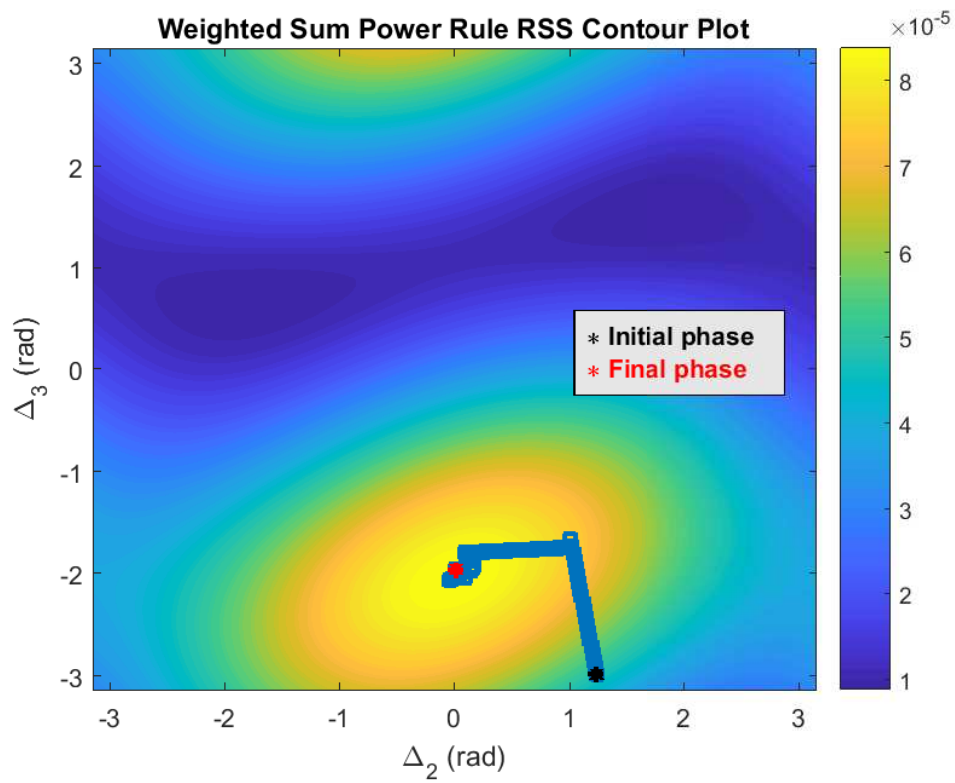


Figure 4.10: Contour plot of the received power in Summation rule over all transmitters phase difference iterations.

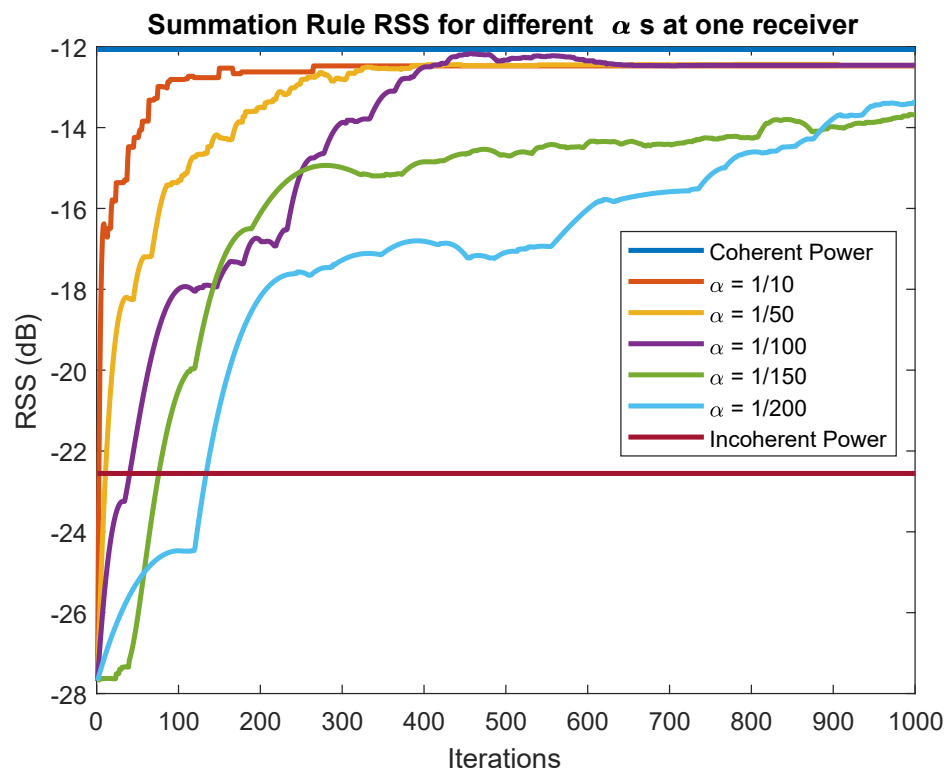


Figure 4.11: The effect of different scaling factors in received power for one of the receivers in Summation rule.

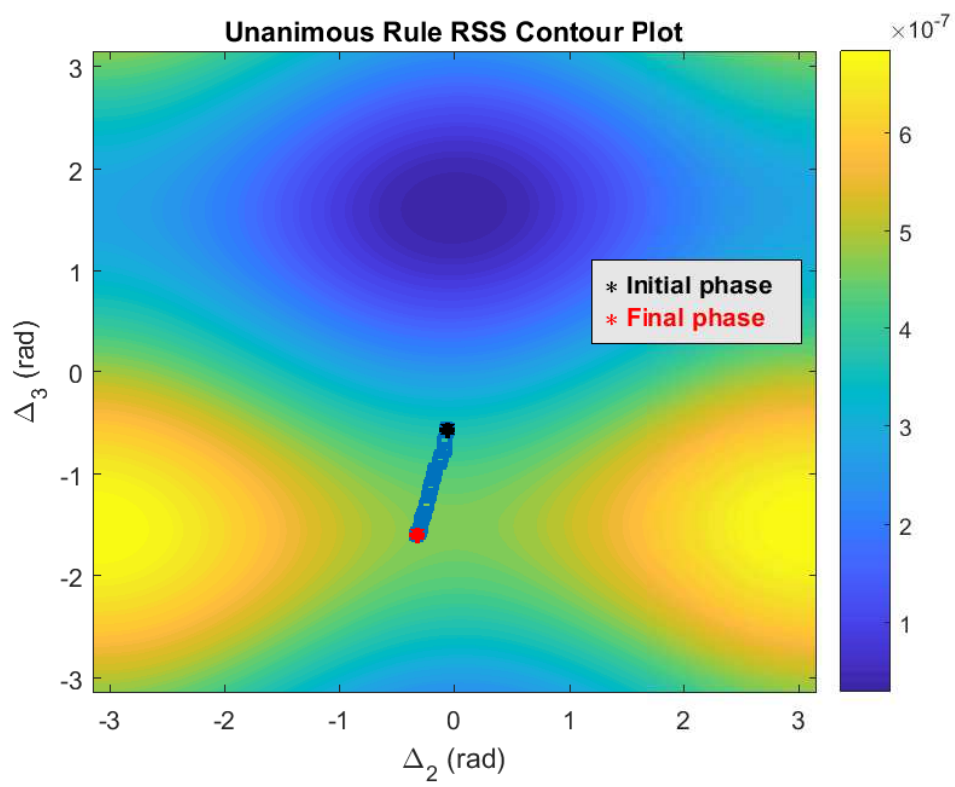


Figure 4.12: Contour of received power in Unanimous rule with sparse array.

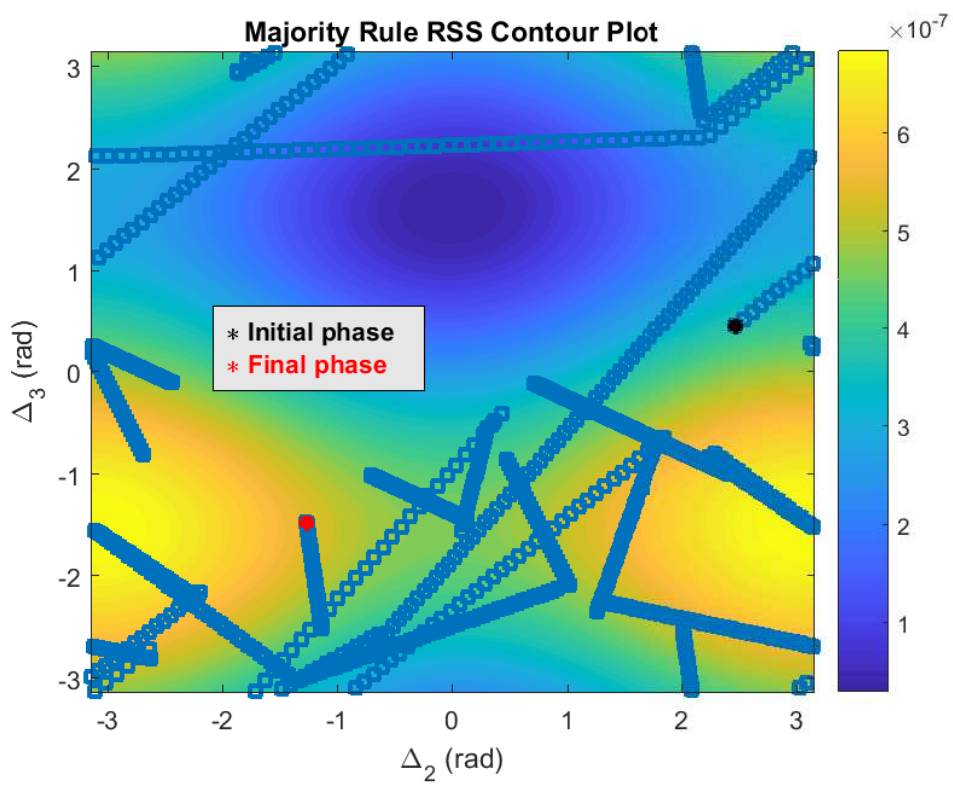


Figure 4.13: Contour of received power in Majority rule with sparse array.

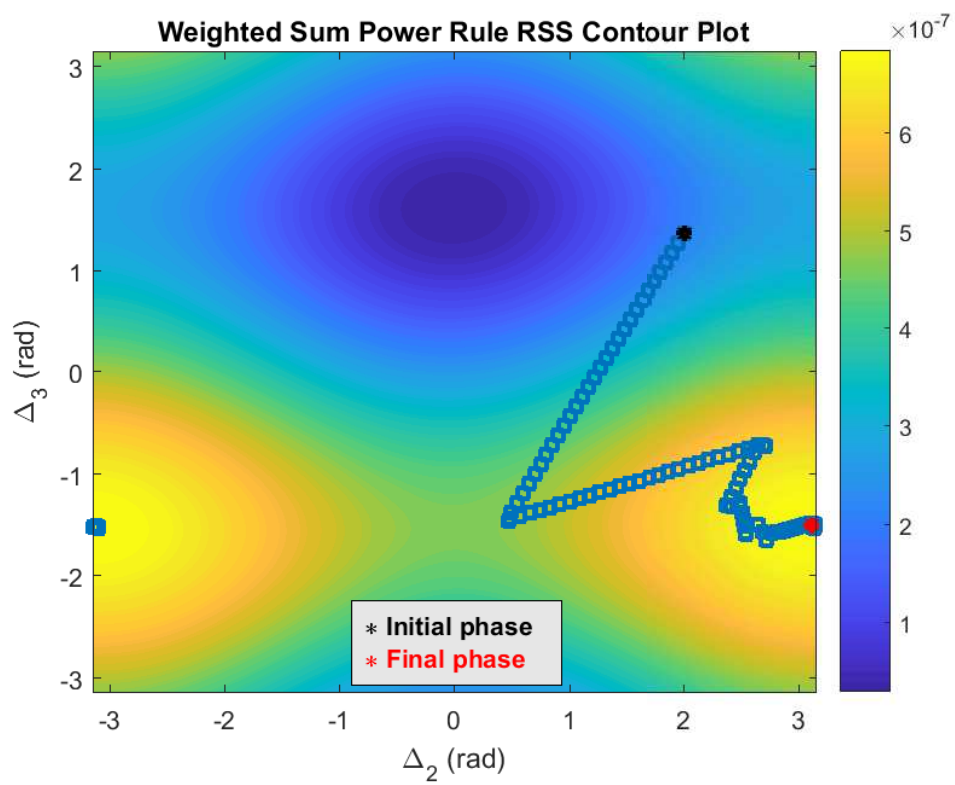


Figure 4.14: Contour of received power in Summation rule with sparse array.

Chapter 5

Summary and Future Work

5.1 Conclusions

In Chapter 2 we investigated the effect of channel estimation error on performance of distributed reception networks which using hard decisions to exchange information between receive nodes. In this process we assumed two different modulation schemes in transmission phase, M -PSK and M^2 -QAM. We showed that, in case of M -PSK the performance of the network with distributed reception with both ideal and pseudo-beamforming techniques reduces only by almost 1.38 dB when QPSK is used for example. In M^2 -QAM transmission this performance degradation is about 0.75 dB when 16-QAM is used, but the interesting outcome of our analysis in either of the cases is that, the SNR ratio between ideal receive beamforming and pseudo-beamforming does not depend on the amount of channel estimation error and are identical to the SNR ratios with no channel estimation error. So, our analysis shows, channel estimation error causes the same amounts of performance degradation in ideal beamforming and pseudo-beamforming systems despite the fact that the channel estimation errors manifests themselves quite differently in both systems.

In Chapter 3 a survey of widely available, low-cost oscillators have been performed which shows two distinct types of shape for the frequency domain characteristic of

phase noise performance. It has been shown that the traditional two-state model is not fully capable of doing a good phase tracking and prediction for oscillators exhibiting a phase noise density similar to that of a PLL synthesizer architecture. So, we introduced a three-state model which is capable of providing up to 3 *dB* improvement in MSE of prediction.

In Chapter 4 we analyzed the concept of wireless power transfer using one-bit feedback by doing convergence analysis on maximization of weighted sum power received at the receivers. Also, we proposed three different methods of decision making for phase correction at the transmitters based on the received one-bit feedback signals from receivers. And, at the end, the effect of sparsity in the network is investigated.

5.2 Future Work

One of the areas that can be investigated in the future in the topic of channel estimation error effect, is having multiple transmitters instead of one in the network and measuring the performance of the system and effect of additional transmitter on the overall system performance. In the topic of phase noise prediction of oscillators one interesting area would be the use of Artificial Intelligence and Machine Learning in the process of phase noise error estimation and prediction. As a suggestion in could thought as a time-series prediction using deep learning and neural networks. In wireless power transfer topic, it would be interesting to see how we can overcome the effect of sparsity as the transmission frequency increases, since the application of signals with higher frequencies are increasing and the use of networks with those set of frequencies are expected to increase in the future. Another possible area to investigate in this field, is the power compensation due to the loss of connection from one of the transmitters in the system, especially when the receivers have a minimum power constraint to remain operable.

Bibliography

- [1] J. Choi, D. J. Love, and T. P. Bidigare, “Coded distributed diversity: A novel distributed reception technique for wireless communication systems,” *IEEE Transactions on Signal Processing*, vol. 63, no. 5, pp. 1310–1321, March 2015.
- [2] “Coordinated multi-point operation for LTE physical layer aspects (release 11),” The 3rd Generation Partnership Project (3GPP), Sophia Antipolis, France, 3GPP TR 36.819 Std., Technical report (TR), 2011.
- [3] R. Irmer, H. Droste, P. Marsch, M. Grieger, G. Fettweis, S. Brueck, H. P. Mayer, L. Thiele, and V. Jungnickel, “Coordinated multipoint: Concepts, performance, and field trial results,” *IEEE Communications Magazine*, vol. 49, no. 2, pp. 102–111, February 2011.
- [4] D. Lee, H. Seo, B. Clerckx, E. Hardouin, D. Mazzarese, S. Nagata, and K. Sayana, “Coordinated multipoint transmission and reception in lte-advanced: deployment scenarios and operational challenges,” *IEEE Communications Magazine*, vol. 50, no. 2, pp. 148–155, February 2012.
- [5] M. Sawahashi, Y. Kishiyama, A. Morimoto, D. Nishikawa, and M. Tanno, “Coordinated multipoint transmission/reception techniques for LTE-advanced [coordinated and distributed MIMO],” *IEEE Wireless Communications*, vol. 17, no. 3, pp. 26–34, June 2010.
- [6] S. Brueck, L. Zhao, J. Giese, and M. A. Amin, “Centralized scheduling for

- joint transmission coordinated multi-point in lte-advanced,” in *2010 International ITG Workshop on Smart Antennas (WSA)*, Feb 2010, pp. 177–184.
- [7] L. Venturino, N. Prasad, and X. Wang, “Coordinated linear beamforming in downlink multi-cell wireless networks,” *IEEE Transactions on Wireless Communications*, vol. 9, no. 4, pp. 1451–1461, April 2010.
- [8] W. Yu, T. Kwon, and C. Shin, “Multicell coordination via joint scheduling, beamforming and power spectrum adaptation,” in *2011 Proceedings IEEE INFOCOM*, April 2011, pp. 2570–2578.
- [9] W. Roh and A. Paulraj, “Outage performance of the distributed antenna systems in a composite fading channel,” in *Proceedings IEEE 56th Vehicular Technology Conference*, vol. 3, 2002, pp. 1520–1524 vol.3.
- [10] W. Choi and J. G. Andrews, “Downlink performance and capacity of distributed antenna systems in a multicell environment,” *IEEE Transactions on Wireless Communications*, vol. 6, no. 1, pp. 69–73, Jan 2007.
- [11] J. Zhang and J. G. Andrews, “Distributed antenna systems with randomness,” *IEEE Transactions on Wireless Communications*, vol. 7, no. 9, pp. 3636–3646, September 2008.
- [12] A. M. Haimovich, R. S. Blum, and L. J. Cimini, “MIMO radar with widely separated antennas,” *IEEE Signal Processing Magazine*, vol. 25, no. 1, pp. 116–129, 2008.
- [13] Q. He, R. S. Blum, H. Godrich, and A. M. Haimovich, “Target velocity estimation and antenna placement for MIMO radar with widely separated antennas,” *IEEE Journal of Selected Topics in Signal Processing*, vol. 4, no. 1, pp. 79–100, Feb 2010.

- [14] M. Dianat, M. R. Taban, J. Dianat, and V. Sedighi, "Target localization using least squares estimation for MIMO radars with widely separated antennas," *IEEE Transactions on Aerospace and Electronic Systems*, vol. 49, no. 4, pp. 2730–2741, OCTOBER 2013.
- [15] I. Akyildiz, W. Su, Y. Sankarasubramaniam, and E. Cayirci, "Wireless sensor networks: a survey," *Computer Networks*, vol. 38, no. 4, pp. 393 – 422, 2002. [Online]. Available: <http://www.sciencedirect.com/science/article/pii/S1389128601003024>
- [16] I. F. Akyildiz, W. Su, Y. Sankarasubramaniam, and E. Cayirci, "A survey on sensor networks," *IEEE Communications Magazine*, vol. 40, no. 8, pp. 102–114, Aug 2002.
- [17] V. Mhatre and C. Rosenberg, "Design guidelines for wireless sensor networks: communication, clustering and aggregation," *Ad Hoc Networks*, vol. 2, no. 1, pp. 45 – 63, 2004. [Online]. Available: <http://www.sciencedirect.com/science/article/pii/S1570870503000477>
- [18] J. Yick, B. Mukherjee, and D. Ghosal, "Wireless sensor network survey," *Computer Networks*, vol. 52, no. 12, pp. 2292 – 2330, 2008. [Online]. Available: <http://www.sciencedirect.com/science/article/pii/S1389128608001254>
- [19] A. R. Hammons, J. R. Hampton, N. M. Merheb, and M. Cruz, "Cooperative MIMO field measurements for military uhf band in low-rise urban environment," in *2008 5th IEEE Sensor Array and Multichannel Signal Processing Workshop*, July 2008, pp. 122–126.
- [20] S. H. Lee, S. Lee, H. Song, and H. S. Lee, "Wireless sensor network design for tactical military applications : Remote large-scale environments," in *MILCOM 2009 - 2009 IEEE Military Communications Conference*, Oct 2009, pp. 1–7.

- [21] L. Atzori, A. Iera, and G. Morabito, “The internet of things: A survey,” *Computer Networks*, vol. 54, no. 15, pp. 2787 – 2805, 2010. [Online]. Available: <http://www.sciencedirect.com/science/article/pii/S1389128610001568>
- [22] J. Choi, D. J. Love, D. R. Brown, and M. Boutin, “Quantized distributed reception for MIMO wireless systems using spatial multiplexing,” *IEEE Transactions on Signal Processing*, vol. 63, no. 13, pp. 3537–3548, July 2015.
- [23] R. S. Blum, “Distributed detection for diversity reception of fading signals in noise,” *IEEE Transactions on Information Theory*, vol. 45, no. 1, pp. 158–164, Jan 1999.
- [24] P. K. Varshney, *Distributed Detection and Data Fusion*. USA, NY, New York: Springer, 1997.
- [25] A. Nayagam, J. M. Shea, and T. F. Wong, “Collaborative decoding in bandwidth-constrained environments,” *IEEE Journal on Selected Areas in Communications*, vol. 25, no. 2, pp. 434–446, February 2007.
- [26] A. Sanderovich, S. Shamai, Y. Steinberg, and G. Kramer, “Communication via decentralized processing,” *IEEE Transactions on Information Theory*, vol. 54, no. 7, pp. 3008–3023, July 2008.
- [27] R. Viswanathan and P. K. Varshney, “Distributed detection with multiple sensors i. fundamentals,” *Proceedings of the IEEE*, vol. 85, no. 1, pp. 54–63, Jan 1997.
- [28] A. Ribeiro and G. B. Giannakis, “Bandwidth-constrained distributed estimation for wireless sensor networks-part i: Gaussian case,” *IEEE Transactions on Signal Processing*, vol. 54, no. 3, pp. 1131–1143, March 2006.
- [29] —, “Bandwidth-constrained distributed estimation for wireless sensor networks-part ii: unknown probability density function,” *IEEE Transactions on Signal Processing*, vol. 54, no. 7, pp. 2784–2796, July 2006.

- [30] T.-Y. Wang, Y. S. Han, P. K. Varshney, and P.-N. Chen, “Distributed fault-tolerant classification in wireless sensor networks,” *IEEE Journal on Selected Areas in Communications*, vol. 23, no. 4, pp. 724–734, April 2005.
- [31] C. Yao, P. N. Chen, T. Y. Wang, Y. S. Han, and P. K. Varshney, “Performance analysis and code design for minimum hamming distance fusion in wireless sensor networks,” *IEEE Transactions on Information Theory*, vol. 53, no. 5, pp. 1716–1734, May 2007.
- [32] D. R. Brown, M. Ni, U. Madhow, and P. Bidigare, “Distributed reception with coarsely-quantized observation exchanges,” in *Information Sciences and Systems (CISS), 2013 47th Annual Conference on*, March 2013, pp. 1–6.
- [33] A. J. Viterbi, A. M. Viterbi, K. S. Gilhousen, and E. Zehavi, “Soft handoff extends cdma cell coverage and increases reverse link capacity,” *IEEE Journal on Selected Areas in Communications*, vol. 12, no. 8, pp. 1281–1288, Oct 1994.
- [34] G. Kramer, M. Gastpar, and P. Gupta, “Cooperative strategies and capacity theorems for relay networks,” *IEEE Transactions on Information Theory*, vol. 51, no. 9, pp. 3037–3063, Sept 2005.
- [35] E. Aktas, J. Evans, and S. Hanly, “Distributed decoding in a cellular multiple-access channel,” *IEEE Transactions on Wireless Communications*, vol. 7, no. 1, pp. 241–250, Jan 2008.
- [36] I. H. Wang and D. N. C. Tse, “Interference mitigation through limited receiver cooperation: Symmetric case,” in *Information Theory Workshop, 2009. ITW 2009. IEEE*, Oct 2009, pp. 579–583.
- [37] S. Yi, B. Azimi-Sadjadit, S. Kalyanaraman, and V. Subramanian, “Error control code combining techniques in cluster-based cooperative wireless networks,”

- in *Communications, 2005. ICC 2005. 2005 IEEE International Conference on*, vol. 5, May 2005, pp. 3510 – 3514 Vol. 5.
- [38] S. Yi, S. Kalyanaraman, B. Azimi-Sadjadi, and H. Shen, “Energy-efficient cluster-based cooperative fec in wireless networks,” *Wireless Networks*, vol. 15, no. 8, pp. 965–977, November 2009.
- [39] J. Choi and S. Choi, “Cooperative and distributed receiver processing based on message passing,” *Vehicular Technology, IEEE Transactions on*, vol. 60, no. 7, pp. 3066–3075, 2011.
- [40] T. Wong, X. Li, and J. Shea, “Distributed decoding of rectangular parity-check code,” *Electronics Letters*, vol. 38, no. 22, pp. 1364 – 1365, October 2002.
- [41] —, “Iterative decoding in a two-node distributed array,” in *MILCOM 2002. Proceedings*, vol. 2, October 2002, pp. 1320 – 1324 vol.2.
- [42] X. Li, T. Wong, and J. Shea, “Bit-interleaved rectangular parity-check coded modulation with iterative demodulation in a two-node distributed array,” in *Communications, 2003. ICC '03. IEEE International Conference on*, vol. 4, May 2003, pp. 2812 – 2816 vol.4.
- [43] A. Avudainayagam, J. Shea, T. Wong, and X. Li, “Reliability exchange schemes for iterative packet combining in distributed arrays,” in *Wireless Communications and Networking, 2003. WCNC 2003. 2003 IEEE*, vol. 2, March 2003, pp. 832 –837 vol.2.
- [44] A. Nayagam, J. Shea, and T. Wong, “Collaborative decoding in bandwidth-constrained environments,” *Selected Areas in Communications, IEEE Journal on*, vol. 25, no. 2, pp. 434 –446, February 2007.

- [45] X. Li, T. Wong, and J. Shea, “Performance analysis for collaborative decoding with least-reliable-bits exchange on awgn channels,” *Communications, IEEE Transactions on*, vol. 56, no. 1, pp. 58–69, January 2008.
- [46] D. Brown, U. Madhow, M. Ni, M. Rebholz, and P. Bidigare, “Distributed reception with hard decision exchanges,” *Wireless Communications, IEEE Transactions on*, vol. 13, no. 6, pp. 3406–3418, June 2014.
- [47] R. Wang, D. R. Brown, M. Ni, U. Madhow, and P. Bidigare, “Outage probability analysis of distributed reception with hard decision exchanges,” in *Signals, Systems and Computers, 2013 Asilomar Conference on*, Nov 2013, pp. 597–601.
- [48] M. GURSOY, “On the low-SNR capacity of phase-shift keying with hard-decision detection,” in *Information Theory, 2007. ISIT 2007. IEEE International Symposium on*, June 2007, pp. 166–170.
- [49] S. Razavi and D. R. Brown, “Characterizing the effect of channel estimation error on distributed reception with hard decision exchanges,” in *2016 25th International Conference on Computer Communication and Networks (ICCCN)*, Aug 2016, pp. 1–8.
- [50] A. Soysal, S. Ulukus, and C. Clancy, “Channel estimation and adaptive m-qam in cognitive radio links,” in *2008 IEEE International Conference on Communications*, May 2008, pp. 4043–4047.
- [51] D. R. Brown, G. B. Prince, and J. A. McNeill, “A method for carrier frequency and phase synchronization of two autonomous cooperative transmitters,” in *IEEE 6th Workshop on Signal Processing Advances in Wireless Communications, 2005.*, June 2005, pp. 260–264.
- [52] R. David, “Improving channel estimation and tracking performance in distributed MIMO communication systems.”

- [53] P. Bidigare, M. Oyarzyn, D. Raeman, D. Chang, D. Cousins, R. O'Donnell, C. Obranovich, and D. R. Brown, "Implementation and demonstration of receiver-coordinated distributed transmit beamforming across an ad-hoc radio network," in *2012 Conference Record of the Forty Sixth Asilomar Conference on Signals, Systems and Computers (ASILOMAR)*, Nov 2012, pp. 222–226.
- [54] F. Quitin, U. Madhow, M. M. U. Rahman, and R. Mudumbai, "Demonstrating distributed transmit beamforming with software-defined radios," in *2012 IEEE International Symposium on a World of Wireless, Mobile and Multimedia Networks (WoWMoM)*, June 2012, pp. 1–3.
- [55] "IEEE standard definitions of physical quantities for fundamental frequency and time metrology—random instabilities," *IEEE Std 1139-2008 (Revision of IEEE Std 1139-1999)*, pp. 1–50, Feb 2009.
- [56] L. Galleani, "A tutorial on the two-state model of the atomic clock noise," *Metrologia*, vol. 45, no. 6, p. S175, 2008. [Online]. Available: <http://stacks.iop.org/0026-1394/45/i=6/a=S23>
- [57] C. Zucca and P. Tavella, "The clock model and its relationship with the allan and related variances," *IEEE Transactions on Ultrasonics, Ferroelectrics, and Frequency Control*, vol. 52, no. 2, pp. 289–296, Feb 2005.
- [58] "USRP products," *E312* <http://www.ettus.com>, accessed, 2016.
- [59] "Keysight E5052B," *Signal Source Analyzer*.
- [60] J. A. McNeill and D. Ricketts, *The Designer's Guide to Jitter in Ring Oscillators*. Springer US, 2009.
- [61] J. A. McNeill, "A simple method for relating time- and frequency-domain measures of oscillator performance," in *2001 Southwest Symposium on Mixed-Signal Design (Cat. No.01EX475)*, 2001, pp. 7–12.

- [62] S. Lee and R. Zhang, “Distributed energy beamforming with one-bit feedback,” in *2016 IEEE Wireless Communications and Networking Conference*, April 2016, pp. 1–6.
- [63] R. Mudumbai, J. Hespanha, U. Madhow, and G. Barriac, “Distributed transmit beamforming using feedback control,” *IEEE Transactions on Information Theory*, vol. 56, no. 1, pp. 411–426, Jan 2010.
- [64] —, “Scalable feedback control for distributed beamforming in sensor networks,” in *Proceedings. International Symposium on Information Theory, 2005. ISIT 2005.*, Sept 2005, pp. 137–141.
- [65] J. Xu and R. Zhang, “Energy beamforming with one-bit feedback,” *IEEE Transactions on Signal Processing*, vol. 62, no. 20, pp. 5370–5381, Oct 2014.
- [66] —, “A general design framework for MIMO wireless energy transfer with limited feedback,” *IEEE Transactions on Signal Processing*, vol. 64, no. 10, pp. 2475–2488, May 2016.
- [67] A. Madhja, S. Nikolettseas, and T. P. Raptis, “Distributed wireless power transfer in sensor networks with multiple mobile chargers,” *Computer Networks*, vol. 80, pp. 89–108, 2015. [Online]. Available: <http://www.sciencedirect.com/science/article/pii/S1389128615000298>